UNIVERSITY OF OKLAHOMA

GRADUATE COLLEGE

A NEW MULTILATERATION OPTIMIZATION TECHNIQUE FOR AIR TRAFFIC MANAGEMENT AND SURVEILLANCE

A DISSERTATION

SUBMITTED TO THE GRADUATE FACULTY

in partial fulfillment of the requirements for the

degree of

Doctor of Philosophy

By

RONNIE BEASON
Norman, Oklahoma
2007

A NEW MULTILATERATION OPTIMIZATION TECHNIQUE FOR AIR TRAFFIC MANAGEMENT AND SURVEILLANCE

A DISSERTATION APPROVED FOR THE
SCHOOL OF ELECTRICAL AND COMPUTER ENGINEERING

BY

Dr. John E. Fagan, Chair

Dr. James Sluss, Jr.

Dr. Monte Tull

Dr. Samuel C. Lee

Dr. Hillel Kumin

ACKNOWLEDGEMENTS

My wife, Carla, shouldn’t have had to learn to read my face and try to decide whether or not to ‘ask’, but she was forced to. I was not very good at forgetting a bad day at the office, especially when I was “this close” to a major breakthrough – or so I thought time and time again over a period of several years. Too many times over the years I was less than pleasant to be around as a result of my dedication to this project. She, along with my three daughters, Rachel, Lauren and Rylee have put up with more nonsense from me than they deserve, and I love each of them very much.

I would like to express thanks to my committee, and a heartfelt appreciation to Dr. John Fagan. Many students have tried to properly acknowledge him, knowing it’s impossible to describe the actual impact that he has had on their lives. In an effort to avoid every cliché in the book to describe his effect on my life, I simply say thanks.

Fellow students have contributed significant amounts of time helping build, deploy and operate my system while providing enough personality to make it quite enjoyable. Specifically, Nick Cannon, Jonathan Harkness and John Dyer gave me many hours of their time and it is greatly appreciated. I would also like to thank Chad Davis and Chad Sherrell for their assistance.

I would not have been allowed to pursue this goal of mine without cooperation from the sales management team at National Instruments, and I would like to express my appreciation to them. Additionally, Andy Hinde (product support engineer at NI) was instrumental in lending technical support.

TABLE OF CONTENTS

LIST OF TABLES

LIST OF ILLUSTRATIONS

ABSTRACT

Multilateration is a new technology based on a proven concept which has recently become the focus of the air traffic surveillance community. However, the technology has yet to become an accepted method of air traffic surveillance based on its susceptibility to failure and the unpredictability of its reported data. These failures due to singularities that exist in the coverage area render certain zones within the network as ‘no coverage available’. In addition, all multilateration systems in existence today require line of sight connectivity from sensor to sensor throughout the network due to a dependence on a local reference transmitter for time synchronization.

In this dissertation a new methodology is presented which actively removes the singularities with a model of software-based rotational geometry. This new algorithm provides a new adaptive geometric optimization technique which reduces the effects of measurement error present in all multilateration systems.

Through the implementation of a GPS-based timing technology in a passive monitoring solution (Mode A/C), complete autonomy is achieved and the dependency on the local transmitter has been eliminated. This methodology allows for installations which do not have line of sight connectivity from sensor to sensor across the network.

As a result of this new methodology, the theoretical benefits of multilateration are realized without the shortcomings of existing systems. These contributions include a passive monitoring solution which delivers better accuracy, faster update rates and lower cost than the performance of primary and secondary surveillance radar. This solution produces a safer and more efficient method of air traffic surveillance.

CHAPTER 1

Introduction

Today's higher volume in air traffic is driving the need for the modernization of Air Traffic Control (ATC) surveillance technology. Radar has served as the primary tool for air traffic controllers for over a half century, but increased volume in air travel has placed a demand for more efficient use of our airways. The main radar components (Primary Surveillance Radar and Secondary Surveillance Radar) are not only based on an old technology, but they are also extremely expensive to install and maintain. The accuracy and resolution they provide are not capable of meeting the demands for the future of air traffic control. Newer technologies are being sought to not only manage more aircraft in smaller spaces, but also to increase and ensure safety to air travelers. Some of the most prominent technologies under consideration for modernizing air traffic surveillance include Mode S Secondary Surveillance Radar[1], Automatic Dependent Surveillance-Broadcast (ADS-B) [2], and Multilateration [3,4].

Multilateration is one of the technologies that is being sought as a solution to monitoring air traffic with the promise of more efficient update rates and more accurate position measurements than radar delivers today. It is a technology that has existed for many years as a means for locating objects at unknown positions. Its use is well documented in cases of locating objects by sensing the arrival times of their acoustic emissions. Examples include tracking whales via a network of hydrophones in the ocean, or tracking gun shots in high crime areas by monitoring a network of microphones.

However, only with recent (late 20^{th} century) advances in technology has it become an economically feasible technology for locating objects based on detecting their radio frequency broadcasts. Advances in timing synchronization and new instrumentation technology provide some of the basic components necessary to implement such a system. However, the technology has yet to become an accepted method of air traffic surveillance based on its susceptibility to failure and the unpredictability of its reported data.

Complications due to non-ideal measurement systems can cause divergences (or singularities) to be observed by these systems. The mathematical solutions which compute position locations are very sensitive to measurement error. This factor combined with poor geometrical configurations of the sensor network is capable of dictating operational limitations that outweigh the benefits of the technology.

This dissertation presents new algorithms and methodologies for the implementation of a new multilateration system design which addresses many of the shortcomings that exist in today's technology. A research proof of concept implementing new hardware and software models will be presented along with the experimental results of the new proof of concept methodology. The contributions of research in this dissertation are as follows:

- Autonomous operation - realization of multilateration system without the dependence on a reference transmitter
- New methodology of software-defined rotational geometry to identify and filter mathematical divergences (singularities) which plague fixed geometry systems
- Passive solution for tracking aircraft (listen only)

- Complete timing solution based on GPS technology

As a result of the implementation of this new multilateration methodology, air traffic control is made more efficient with increased accuracy and better update rates than radar. Other benefits include much lower installation and maintenance costs, and the technology does not put additional requirements on aircraft avionics.

1.1 Chapter Overview

Chapter 2 – Air Traffic Control Surveillance Technologies

- Brief history of air traffic control technology
- Analysis of existing technology for monitoring air traffic
- Comparison of strengths and weaknesses of each technology that is in use or being considered for use in monitoring air traffic

Chapter 3 – Conceptualization of System - An Overview

- High level overview of the research concept
- Background research on the method of Time Difference of Arrival (TDOA) and the theory behind its use in multilateration systems
- The ECEF and ENU coordinate systems used for this research
- An overview of the architecture of the research proof of concept

Chapter 4 – System Development Architecture

- Design of the RF sensor and the Central Processing Station

- Hardware and software development for signal conditioning and digital signal processing solutions

<u>Chapter 5 – Experimental Results</u>

- Experimental objective and configuration
- Experimental results with error analysis

<u>Chapter 6 – Conclusion and Future Work</u>

- Conclusions based on experimental results and error analysis
- Recommendations for future work

CHAPTER 2

Air Traffic Control Surveillance Technologies

2.1 Introduction

Surveillance plays a critical role in Air Traffic Control (ATC). The ability to accurately determine the location of all aircraft occupying a given airspace has direct influence on the maximum separation distances required between aircraft. This has a direct relationship with the efficiency in which a given airspace may be utilized.

In areas without electronic surveillance, where ATC is reliant on pilots to verbally report their position, aircraft have to be separated by relatively large distances to account for the uncertainty in the estimated position and the timeliness of the information.

Conversely, in terminal areas where accurate surveillance systems are used and the aircraft positions are updated more frequently, the airspace can be used more efficiently to safely accommodate a higher density of aircraft. It also allows aircraft vectoring for efficiency, capacity and safety reasons. New technologies are sought to further increase the capacity in which a given airspace can be utilized. As uncertainty of position and identity of terminal area aircraft are reduced, so are the maximum separation distances necessary to sustain safe, efficient air traffic [5].

The most common technologies that are used in ATC are primary radar and secondary radar (with and without Mode S). The combination of primary and secondary radar, ADS-B, and recently multilateration has emerged as technologies that could improve surveillance in many ways. Each will be discussed in the following sections.

2.2 Radar

Radar is a technology which detects the range and bearing of an aircraft based upon the difference in time between transmission of pulses to the aircraft and the receipt of energy from the aircraft. The technology requires a large rotating antenna and associated machinery and support electronics. The technology was first implemented in a role for detecting aircraft just prior to World War II and proceeded to become ATC's core component for controlling air space, and today covers nearly 90% of the United States.

Airport Surveillance Radar (ASR-11) is an integrated primary and secondary radar system being deployed at terminal air traffic control sites. It consists of two integrated electronic subsystems: primary surveillance radar (PSR) and secondary surveillance radar (SSR). PSR is the high energy transmission of electromagnetic waves that 'paints' the object of interest and measures the transit time of energy to reflect, or backscatter back to the receiver. From this measurement, range and azimuth are provided. SSR then uses a much lower power transmission to interrogate the aircraft's transponder to request its IDENT (Mode A) or altitude (Mode C). When operating properly, the combination of the two (PSR and SSR) are capable of identifying and locating aircraft in the terminal area. This system experiences performance degradation with distant targets due to loss of signal return. Resolution is also decreased due to the width of the beam at great distances. SSR has a three degree beam width, which, at thirty miles becomes a quarter-mile area of coverage, thus limiting resolution to nearly 1500 feet.

Figure 2. 1- Primary and Secondary Surveillance Radar [6].

ASR-11 is an aging technology which consumes significant electrical power (25 kW) and a considerable amount of infrastructure in the form of towers and rotating machinery. Significant costs accompany the installation of a radar system with a typical installation time requiring several months. In addition, the maintenance and support life cycle costs are extremely high. Figure 2.1 is an illustration of an ASR-11 installation which includes both PSR and SSR.

2.2.1 Primary Surveillance Radar (PSR)

Primary Surveillance Radar uses a continually rotating antenna mounted on a tower to transmit electromagnetic waves that reflect, or backscatter, from the surface of aircraft up to sixty miles from the radar installation. The radar system measures the time required for a radar echo to return and the direction of the signal. From this, the system can then measure the distance of the aircraft from the radar antenna and the bearing (direction) of the aircraft in relation to the antenna. PSR operating without the assistance of SSR does not provide the identity or the altitude of the aircraft. Unlike SSR, however, PSR does operate without a dependency of equipment on the aircraft.

PSR installations are optimally located on high ground as direct line of sight is required in order to ‘paint’ an aircraft. A typical system requires a number of racks of equipment in an air-conditioned shelter. PSR operates in the range of 2700 to 2900 MHz with a transmitter which generates a peak effective power of 25 kW [7]. Enormous amounts of power must be radiated to ensure returns from the target. This is especially true if long range is desired.

Because of the small amount of energy returned to the receiver, returns may easily be disrupted due to signal attenuation/disruption attributed to inclement weather such as heavy rain and snow. Other sources of weak or false returns include ground clutter such as buildings and vehicles. Changes of target attitude or even birds can also affect the return to a radar system. Any of these false returns can plague radar's effectiveness.

Strengths of PSR

- Does not require a transponder to be installed or operating on the aircraft that is being tracked
- Can provide weather channel output if display of weather is required
- Well suited for airport surface surveillance

Weaknesses of PSR

- High Cost of installation and maintenance
- Requires acquisition of real estate
- Size of radar site (unsightly tower)
- Does not provide identity of aircraft
- Does not provide altitude
- Low update rate (between 4 and 12 seconds)
- Can often report false targets (ground vehicles, weather, birds, etc.)
- Poor performance in presence of ground and weather clutter especially for flight tangential to the radar
- High transmitter power required for long range performance – interference and environmental concerns
- Poor azimuth resolution (resolution of multiple aircraft in close proximity)

2.2.2 *Secondary Surveillance Radar (SSR)*

Secondary Surveillance Radar is a component of the Air Traffic Control Radar Beacon System (ATCRBS). In most cases, SSR is co-located with a PSR, usually with the SSR mounted on top of the PSR antenna. (see Figure 2.1)

ATCRBS is a modification of the Identification Friend or Foe (IFF) equipment developed during World War II at the same time radar was coming into use. The problem was differentiating between Allied and Axis aircraft, and IFF was the answer. The equipment on board each Allied aircraft received the radar pulses and transmitted a secret code in reply. The system worked well and after the war the concept was adapted for air traffic control. Improvements were made, and in addition to identity (Mode A), pressure based altitude indication (Mode C) was incorporated into the system to comprise the system still in use today.

SSR systems consist of two main elements, a ground based interrogator/receiver and an aircraft transponder. The aircraft's transponder responds to interrogations from the ground station. This provides, in addition to range and bearing, identity and/or altitude information. Today all commercial and civilian aircraft are equipped with transponders which are responsible for transmitting pressure based altitude (Mode C) and IDENT squawk (Mode A) when interrogated by the SSR system.

The SSR's ground station emits pulses of RF (radio frequency) energy which serve as an interrogation signal to the aircraft via the directional beam of a rotating antenna at a frequency of 1030 MHz. When the antenna beam is pointing in the direction of an aircraft, the onboard transponder determines whether the interrogation is requesting a Mode C or Mode A reply. The transponder then responds by modulating the appropriate response at 1090 MHz (see Figure 2.2). From this reply signal the ground station equipment detects and measures the aircraft's range and bearing. SSR also decodes the aircraft's replies to determine its identity and/or flight level, and passes the data to radar displays at ATC. The use of an airborne transponder permits the transponder reply frequency to be different from the ground transmitter frequency, therefore avoiding the problems of clutter returns experienced by PSR. Much lower transmitter powers are required compared with PSR since only one-way path losses are involved. The presence of the transponder also enables the reply signal to be modulated so that the additional data of identity and flight level can be communicated by the aircraft. The obvious drawback is of course that SSR is dependent on the presence of the airborne transponder and the accuracy of its pressure-based altitude reading [8].

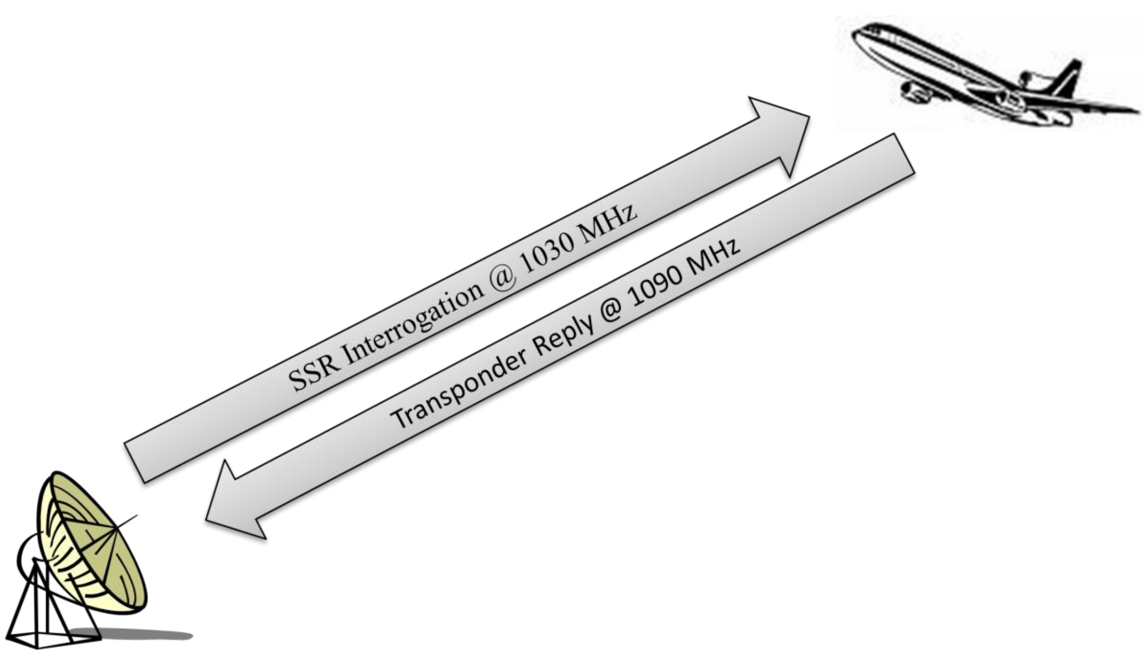

Figure 2. 2 - Secondary Surveillance Radar interrogation and reply.

Strengths of SSR

- Provides aircraft identity (Mode A)
- Provides aircraft altitude (Mode C)
- Provides good detection capability independent of clutter and weather

Weaknesses of SSR

- High Cost of installation and maintenance
- Requires optimum site with unobstructed view to aircraft
- Dependent on aircraft avionics (transponder)
- Altitude indication is dependent on the accuracy of on board sensor and limited to 100 foot resolution
- No error detection provided in IDENT and altitude broadcast
- Poor azimuth accuracy and resolution
- Sometimes reports false targets or position (reflections, multipath)
- Can sometimes confuse Mode A replies as Mode C and vice versa
- Cannot resolve multiple aircraft at the same location (garbled/mixed replies)

2.2.3 Mode S Secondary Surveillance Radar

Mode S is an improvement of Mode A/C. It contains all the functions of Mode A/C, and also allows selective addressing of targets by the use of unique 24 bit aircraft addresses, and a two-way data link between the ground station and the aircraft for the exchange of information. It provides the transponder the capability to report altitude with

25 foot resolution although the accuracy and resolution also depend on the altitude sensor systems on board the aircraft.

Mode S radars typically use monopulse techniques to measure the azimuth position of an aircraft and have large vertical aperture antennas, and hence, are less subject to multipath effects. In addition, they are able to discretely interrogate single aircraft transponders, and hence, can discriminate between two aircraft at the same geographical position.

A Mode S radar is backwards compatible with a conventional SSR Mode A/C radar, and the detection and processing of Mode A/C transponder replies is essentially identical. However, to achieve the benefits of Mode S, the aircraft must have Mode S capable transponders.

Strengths of Mode S SSR

- Altitude and identity are protected and the downlink is error free
- Can resolve two aircraft at the same location
- Provides 25 foot altitude instead of 100 foot common to Mode C

Weaknesses of Mode S SSR

- Requires optimum site with unobstructed view to aircraft
- Benefits apply only to the few Mode S equipped aircraft
- More complex to set up than SSR
- Greater dependence on aircraft avionics

- Some currently deployed Mode A/C transponders are not compliant with the standards and fail to respond to Mode S interrogations properly

2.3 Automatic Dependent Surveillance – Broadcast (ADS-B)

ADS-B is a system that uses transmissions from aircraft to provide geographical position, pressure altitude data, positional integrity measures, flight identity, 24-bit aircraft address, velocity and other data which have been determined by airborne sensors.

Typically, the airborne position sensor is a GPS receiver, or the GPS output of a Multi-Mode Receiver (MMR). This sensor must provide integrity data that indicates the containment bound on positional errors. The altitude sensor is typically the same barometric source used for SSR. Integrated GPS and inertial systems are also used. Currently inertial only sensors do not provide the required integrity data although these are likely to be provided in the future.

An ADS-B ground system uses a non-rotating antenna positioned within a coverage area, to receive messages transmitted by aircraft. Typically a simple pole (DME like) antenna can be used.

While ADS-B has the lowest cost and simplest use of all options to provide air-ground surveillance, the technology is not going to be mature for another decade. The FAA has issued a notice of proposed rulemaking (NPRM) that would require all aircraft flying at or above FL240 (Flight Level 24000 ft) to have "ADS-B out" performance capability by 2020 [9]. Even with this mandate, it will not benefit terminal areas where altitudes are below 24000 feet. The most significant weakness of ADS-B is that it requires ADS-B avionics including GPS in participating aircraft, and a very small percentage of aircraft are currently equipped. The majority of small aircraft will not be equipped which further weakens the system.

Strengths of ADS-B

- Simple ground station design without transmitter
- Very low ground station costs
- Higher update rate
- Higher performance velocity vector measured by avionics rather than that determined by positional data on the ground
- High accuracy and integrity
- Accuracy not dependent on range from ground station
- Can be easily deployed for temporary use due to size and cost

Weaknesses of ADS-B

- Complete dependence on aircraft avionics
- Currently low percentage of aircraft equipped with proper avionics
- FAA not expected to mandate ADS-B compliance until 2020
- Outages expected due to poor GPS geometry when satellites are out of service

2.4 Multilateration

Multilateration is a system that uses the existing infrastructure for secondary surveillance radar. This technology relies on signals from an aircraft's transponder (Mode

A/C or Mode S) being detected at a number of receiving stations to locate the aircraft in either two dimensions or three dimensions.

These systems use a technique known as Time Difference of Arrival (TDOA) to establish surfaces which represent constant differences in distance between the target and pairs of receiving stations. From these differences in signal arrival times, the system is capable of determining the position of the aircraft by plotting a solution based on the intersection of the surfaces.

Multilateration systems can be defined as either passive or active. Passive systems require only ground receivers. An active system requires ground receivers and at least

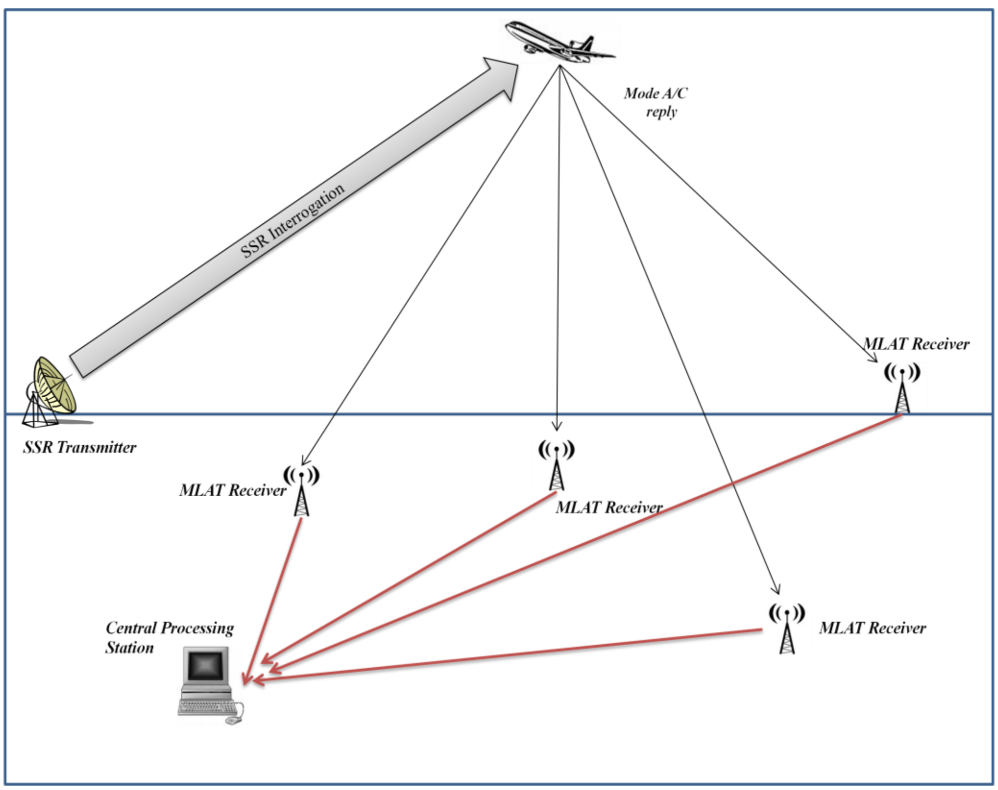

Figure 2. 3 - Multilateration system with four receivers (sensors).

one interrogator. Multiple interrogators may be required to meet coverage requirements. In most applications, multilateration systems are active and must interrogate aircraft to obtain altitude and identity data. Passive systems rely on nearby radar platforms to perform the interrogation.

The accuracy of a multilateration system is dependent on the geometry of the target in relation to the receiving stations, and the accuracy with which the system's sensors can determine the arrival time of the signal. RF signals travel at the speed of light (3×10^8 m/sec) which is approximately one ft/nanosecond. Therefore, timing accuracy of each sensor must be on the order of nanoseconds if position calculation accuracy at least comparable to other surveillance technologies is desired. This requirement produces a need for a local reference transmitter to be broadcast line of sight to each sensor in the network to work in conjunction with GPS-based timing instrumentation.

One requirement of multilateration systems is that the central processing station must be able to determine the time difference of arrival of signals from aircraft. This requires two major components - a communications infrastructure to provide real-time TDOA data and a method of synchronization of common timing devices across the network. The method of synchronization of multiple ground receivers is usually accomplished via:

- A reference transmitter visible to all receiver stations, or
- The transmission of received signals by wideband data link to the central processing station, or
- Use of common clock (GPS or other) to synchronize the reception of signals, or

- The combination of a local clock and a reference transmitter

Multilateration is mainly used for airport surface surveillance and terminal area surveillance. A minimum of three receivers are required for surface surveillance in two dimensions, and a minimum of four receivers must receive the transponder signal in order to determine a three-dimensional solution.

Multilateration systems are rarely used outside of surface surveillance because of their difficulties in discerning altitude and position ambiguities due to a number of reasons. Primarily, the existence of singularities inside the geometrical configuration of the sensors renders the accuracy and dependability of the systems useless in certain areas of the geometry. These singularities, or mathematical divergences, are artifacts of extremely sensitive solution equations and measurement error due to non-ideal conditions such as timing resolution, signal-to-noise problems and multipath.

Strengths of Multilateration

- Higher update rate than PSR and SSR
- Much lower cost than radar
- Allows communication of identity and altitude
- Provides good detection capability independent of clutter and weather
- Passive versions can use existing SSR interrogation infrastructure
- Small size and non-rotating antenna

Weaknesses of Multilateration

- Requires multiple sites

- Requires real-time communications infrastructure between sensors and central processing station
- Requires multiple sites with unobstructed view to aircraft.
- Existence of singularities within area of coverage
- Subject to error due to multipath

CHAPTER 3

Conceptualization of System – an Overview

3.1 Overview

Chapter 3 is a high level overview of a new and novel GPS-based multilateration system design which utilizes new algorithms and new technology to locate aircraft in three dimensions. Each component of the system will be discussed in detail in Chapter 4, including details of the architecture of the hardware and software models necessary for the implementation of the new system. Through the implementation of these new GPS-based multilateration algorithms described in the next two chapters, contributions to air traffic surveillance produce higher quality air traffic surveillance service:

- Autonomous operation (no Reference Transmitter required)
- Elimination of solution singularities caused by fixed geometry systems
- Increased accuracy over current primary surveillance radar
- Increased accuracy over secondary surveillance radar
- More frequent aircraft position updates than radar
- 3-dimensional solutions (eliminating dependency on altitude indicator on board each aircraft)
- Architecture that takes advantage of current infrastructure (interrogator/transponder)
- Elimination of False Replies Uncorrelated in Time (FRUIT)

Multilateration is a new technology which has recently become the research and development focus of the air traffic surveillance community. This is based on its yet unrealized promise of increased accuracy and increased update rates for tracking airborne vehicles as well as ground traffic at airports. While multilateration systems exist, their acceptance in the role of air traffic surveillance has not yet occurred due to a number of shortcomings which hamper their reliability.

The GPS-based multilateration algorithms that have been developed as part of this research project present a novel solution to most of the shortcomings of existing multilateration systems. The new methodology is centered around a unique algorithm for calculating the three-dimensional position of an aircraft by measuring the Time Difference of Arrival (TDOA) of the signal coming from its Mode A/C transponder. The methodology was developed using new technology to implement the already proven theory of TDOA.

3.2 TDOA/Multilateration Theory

Multilateration using TDOA is a proven concept for locating objects based on the Time Difference of Arrival of a signal emanating from the object whose location is sought. For instance, TDOA techniques are used to locate the position of cell phone users within a network of cell towers by performing the necessary measurements of signal arrival time at different locations and using the data to locate the emission of radio frequency (RF) signals from the cell phone [10]. Another common use of TDOA is in the location of acoustic emissions, such as gun shots in an urban area, by measuring the arrival time of sound waves using a series of microphones dispersed throughout a neighborhood [11]. Hydrophone networks in the ocean are used to locate whales by using this technique as well [12]. The method of TDOA to implement a system to locate acoustic emissions is not as likely to have the same difficulties as one which locates the source of an RF transmission. This is due to the measurement error that is much more difficult and costly to eliminate when trying to capture and timestamp a signal that is traveling at the speed of light as opposed to the speed of sound.

In any TDOA measurement system, a network of sensors (passive devices) must be deployed in an optimal geometry to produce the desired results. In the case of acoustic TDOA, these sensors take the form of microphones, and in the case of cell phone location, the network of sensors consists of a series of cell phone towers each containing the ability to timestamp signal arrival time. In the case presented in this research the sensors being used are unique software-defined spectrum analyzers/dataloggers capable of measuring the precise arrival time of the Mode A/C transponder reply from nearby aircraft. These RF sensors, working in concert with GPS-based timing devices, measure the time of arrival of the signal as well as decode the Mode A/C message being transmitted. Identifying a unique RF transmission and timestamping its arrival at the sensor are the two pieces of information necessary to formulate a TDOA solution

The methodology of TDOA in multilateration can be looked at as a reverse technique of the architecture currently being used in Global Positioning Systems (GPS). In a GPS the system utilizes synchronized transmitters (satellites) from different *known locations* whose signals are received at an *unknown location* (x, y, z) by the GPS receiver. Since the transmitters are synchronized, GPS uses the concept of Time of Arrival (TOA)

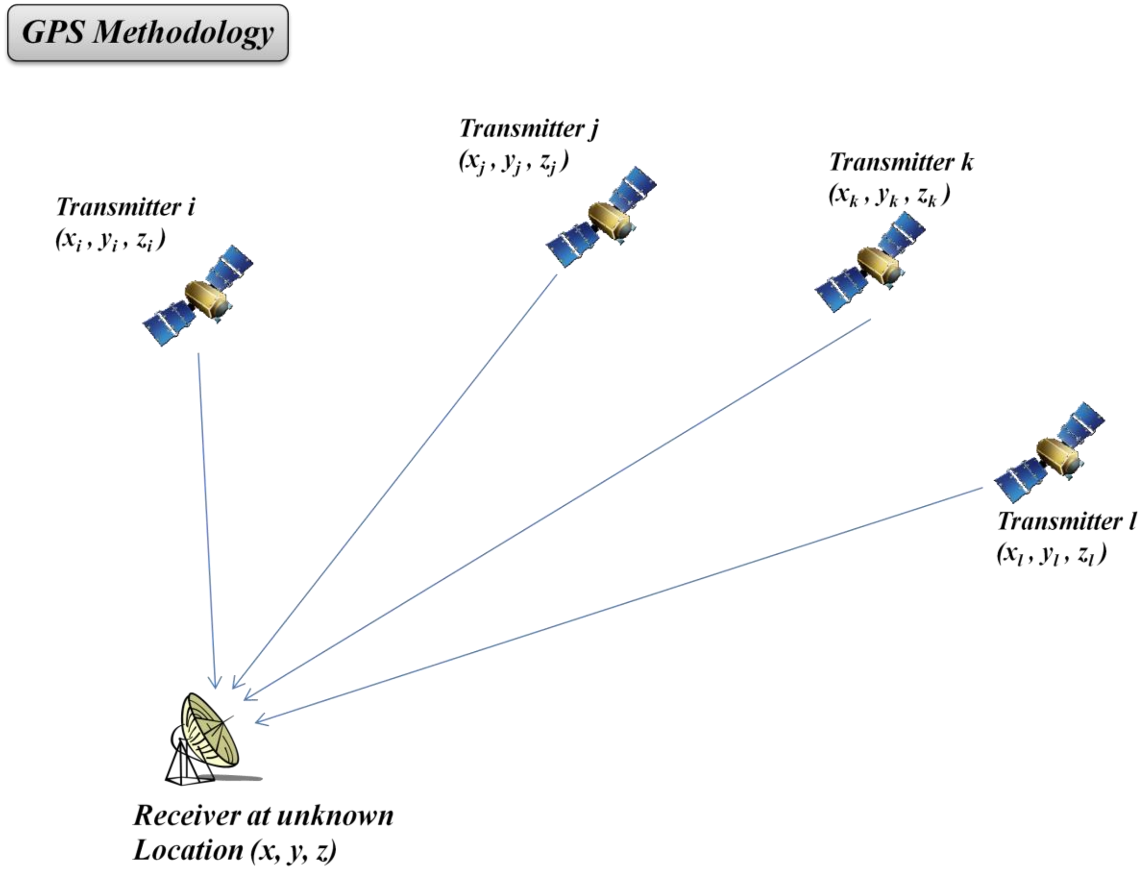

Figure 3. 1- GPS receiver at unknown location and constellation of satellites at known locations.

ranging to determine the unknown position. This concept entails measuring the time it takes for a signal transmitted by an emitter (the satellite) at a known location to reach the receiver.

This time interval, referred to as the signal propagation time, is then multiplied by the speed of the signal (speed of light) to obtain the emitter-to-receiver distance. By measuring the propagation time of the signal broadcast from multiple emitters at known locations, the receiver can determine its position [13]. Figure 3.1 illustrates this concept.

Likewise, in a multilateration system, four receivers which are synchronized by a common clock can then correlate the arrival time of a common signal which is emanating

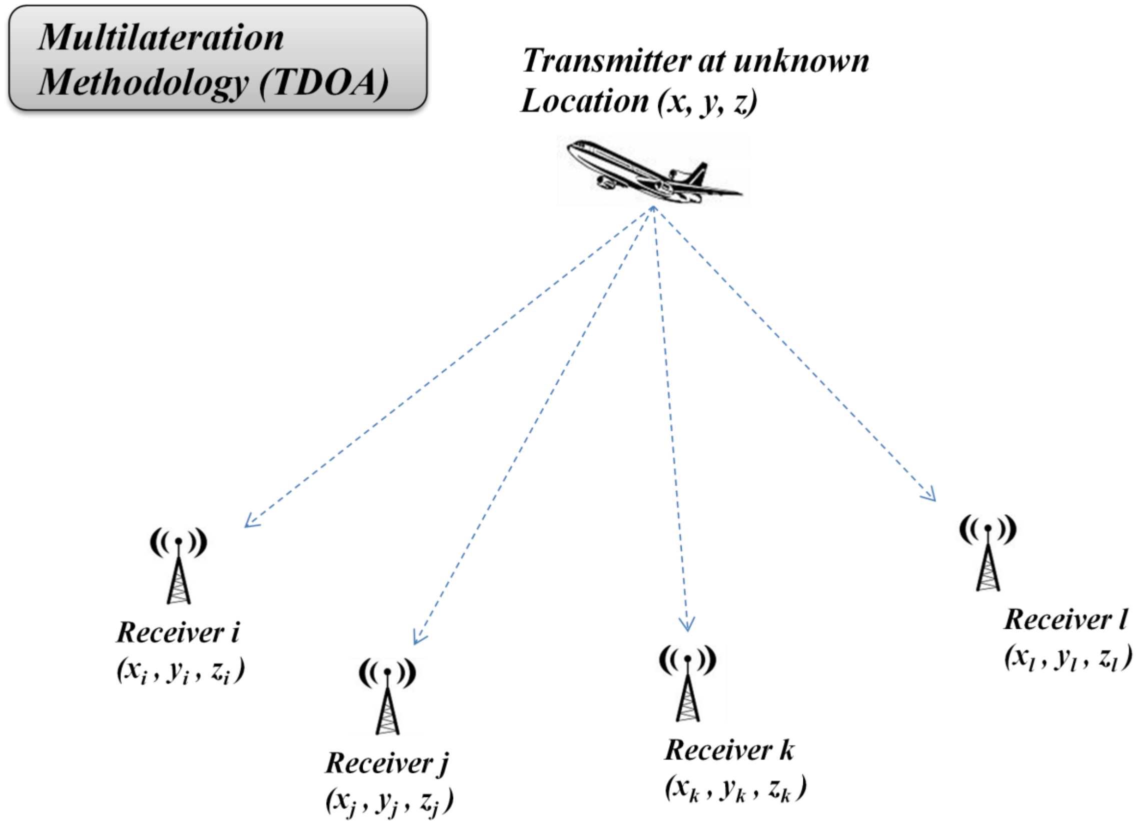

Figure 3. 2 - Multilateration system with four receivers at known locations locating a transmitter at an unknown location.

from an *unknown location (x, y, z)* from a mobile (such as an aircraft illustrated in Figure 3.2). Using TDOA data from the transponder signal acquired by a network of RF sensors, the position solution is computed providing the multilateration system's estimate of the aircraft location.

It is important to distinguish the difference between the TOA concept used in GPS systems and TDOA used in multilateration. In a TOA system, the time of transit of the signal is known simply by measuring the arrival time of the signal at the receiver because the time of transmission of the signal is known. In the case of multilateration, the transit time of the signal is not determined by simply capturing the arrival time of the signal because the time of transmission is an unknown.

The basis of the TDOA methodology is the equation for the distance between two points (x_1, y_1, z_1) and (x_2, y_2, z_2).

$$\boldsymbol{d = \sqrt{(x_i - x)^2 + (y_i - y)^2 + (z_i - z)^2}} \tag{3.1}$$

To remain consistent with standard notation for TDOA, *R* will be used to represent the distance, or *range*, from the unknown emitter location to the sensor at a known location. Now, if this equation is extended to indicate the distance between the position of an unknown emitter at (x, y, z) and a known location of a receiver *i* at (x_i, y_i, z_i), the equation takes on the form:

$$\boldsymbol{R_i = \sqrt{(x_i - x)^2 + (y_i - y)^2 + (z_i - z)^2}} \tag{3.2}$$

The range between the emitter (x, y, z) and the receiver (x_i, y_i, z_i) can also be represented by the multiplication of the travel time of the signal (τ_i) and the speed at which the signal is traveling (in this case the speed of light *c*). This *range equation* then takes on the form:

$$\boldsymbol{R_i = c\tau_i = c(t_i - t) = \sqrt{(x_i - x)^2 + (y_i - y)^2 + (z_i - z)^2}} \tag{3.3}$$

The travel time of the signal, τ_i (t_i - t) in this case, is unknown because the transmitter clock is not synchronized and the time at which the transmission originated (t) cannot be resolved. However, the arrival time of the signal (t_i) can be obtained with a sensor capable of accurately time stamping the arrival of RF signals. Using a network of four RF time stamping sensors at four known locations *i*, *j*, *k*, and *l*, the same relationship can be extended to represent the range from the emitter to each of the four sensors at known locations *i*, *j*, *k* and *l*.

$$\boldsymbol{R_j = c\tau_j = c(t_j - t) = \sqrt{(x_j - x)^2 + (y_j - y)^2 + (z_j - z)^2}} \tag{3.4}$$

$$\boldsymbol{R_k = c\tau_k = c(t_k - t) = \sqrt{(x_k - x)^2 + (y_k - y)^2 + (z_k - z)^2}} \tag{3.5}$$

$$\boldsymbol{R_l = c\tau_l = c(t_l - t) = \sqrt{(x_l - x)^2 + (y_l - y)^2 + (z_l - z)^2}} \tag{3.6}$$

Now, an equation can be generated using the range equation and looking at the range differences between a pair of sensors *i* and j:

$$\begin{aligned} \boldsymbol{R_{ij}} &= \boldsymbol{R_i - R_j} \\ &= \boldsymbol{\sqrt{(x_i - x)^2 + (y_i - y)^2 + (z_i - z)^2}} \\ &\qquad - \boldsymbol{\sqrt{(x_j - x)^2 + (y_j - y)^2 + (z_j - z)^2}} \end{aligned} \tag{3.7}$$

The range difference can now also be represented using the equations from above as seen in Equation 3.8:

$$\begin{aligned} \boldsymbol{R_{ij}} &= \boldsymbol{R_i - R_j = c(t_i - t) - c(t_j - t)} \\ &= \boldsymbol{c(t_i - t_j) = c \times TDOA_{ij}} \end{aligned} \tag{3.8}$$

Where $TDOA_{ij}$ is the *Time Difference of Arrival* $(t_i - t_j)$ of signals between locations *i* and *j*. The unknown time (t) drops out of the equation, and equating the different representations for the range difference R_{ij}, the following equation is derived containing only x, y and z as unknowns:

$$\boldsymbol{c \times TDOA_{ij}} = \sqrt{(\boldsymbol{x_i} - \boldsymbol{x})^2 + (\boldsymbol{y_i} - \boldsymbol{y})^2 + (\boldsymbol{z_i} - \boldsymbol{z})^2} - \sqrt{(\boldsymbol{x_j} - \boldsymbol{x})^2 + (\boldsymbol{y_j} - \boldsymbol{y})^2 + (\boldsymbol{z_j} - \boldsymbol{z})^2} \tag{3.9}$$

Likewise, using the same formula for range differences R_{ik} , R_{kj} , and R_{kl} produces the following equations:

$$\boldsymbol{c \times TDOA_{ik}} = \sqrt{(\boldsymbol{x_i} - \boldsymbol{x})^2 + (\boldsymbol{y_i} - \boldsymbol{y})^2 + (\boldsymbol{z_i} - \boldsymbol{z})^2} - \sqrt{(\boldsymbol{x_k} - \boldsymbol{x})^2 + (\boldsymbol{y_k} - \boldsymbol{y})^2 + (\boldsymbol{z_k} - \boldsymbol{z})^2} \tag{3.10}$$

$$\boldsymbol{c \times TDOA_{kj}} = \sqrt{(\boldsymbol{x_k} - \boldsymbol{x})^2 + (\boldsymbol{y_k} - \boldsymbol{y})^2 + (\boldsymbol{z_k} - \boldsymbol{z})^2} - \sqrt{(\boldsymbol{x_j} - \boldsymbol{x})^2 + (\boldsymbol{y_j} - \boldsymbol{y})^2 + (\boldsymbol{z_j} - \boldsymbol{z})^2} \tag{3.11}$$

$$\boldsymbol{c \times TDOA_{kl}} = \sqrt{(\boldsymbol{x_k} - \boldsymbol{x})^2 + (\boldsymbol{y_k} - \boldsymbol{y})^2 + (\boldsymbol{z_k} - \boldsymbol{z})^2} - \sqrt{(\boldsymbol{x_l} - \boldsymbol{x})^2 + (\boldsymbol{y_l} - \boldsymbol{y})^2 + (\boldsymbol{z_l} - \boldsymbol{z})^2} \tag{3.12}$$

Solving the four equations with three unknowns produces an exact solution for the location of the unknown emitter at (x, y, z). The solution is presented in a set of equations in which the measured values for the arrival time of the transponder signal at each of the four sensor locations delivers the necessary information to calculate the position of the aircraft transmitting the signal. For the purpose of simplicity, the equations will be solved in terms of R_{ij}, R_{ik}, R_{kj} and R_{kl}.

Assuming a network of four RF sensors at locations *i*, *j*, *k* and *l* placed in a geometrical configuration surrounding an airspace, the solution for the aircraft position is as follows:

$$\boldsymbol{x} = \boldsymbol{Gz} + \boldsymbol{H} \tag{3.13}$$

Where,

$$\boldsymbol{G} = \frac{\boldsymbol{E} - \boldsymbol{B}}{\boldsymbol{A} - \boldsymbol{D}} \tag{3.14}$$

$$\boldsymbol{H} = \frac{\boldsymbol{F} - \boldsymbol{C}}{\boldsymbol{A} - \boldsymbol{D}} \tag{3.15}$$

and,

$$\boldsymbol{A} = \frac{\boldsymbol{R_{ik} x_{ji} - R_{ij} x_{ki}}}{\boldsymbol{R_{ij} y_{ki} - R_{ik} y_{ji}}} \tag{3.16}$$

$$\boldsymbol{B} = \frac{\boldsymbol{R_{ik} z_{ji} - R_{ij} z_{ki}}}{\boldsymbol{R_{ij} y_{ki} - R_{ik} y_{ji}}} \tag{3.17}$$

$$\begin{aligned} \boldsymbol{C} = {} & \frac{\boldsymbol{R_{ik}\left({R_{ij}}^2 + {x_i}^2 - {x_j}^2 + {y_i}^2 - {y_j}^2 + {z_i}^2 - {z_j}^2\right)}}{\boldsymbol{2\left(R_{ij} y_{ki} - R_{ik} y_{ji}\right)}} \\ & - \frac{\boldsymbol{R_{ij}\left({R_{ik}}^2 + {x_i}^2 - {x_k}^2 + {y_i}^2 - {y_k}^2 + {z_i}^2 - {z_k}^2\right)}}{\boldsymbol{2\left(R_{ij} y_{ki} - R_{ik} y_{ji}\right)}} \end{aligned} \tag{3.18}$$

$$\boldsymbol{D} = \frac{\boldsymbol{R_{kl} x_{lk} - R_{kj} x_{lk}}}{\boldsymbol{R_{kj} y_{lk} - R_{kl} y_{jk}}} \tag{3.19}$$

$$E = \frac{R_{kl}x_{kj} - R_{kj}x_{lk}}{R_{kj}y_{lk} - R_{kl}y_{jk}} \tag{3.20}$$

$$F = \frac{R_{kl}({R_{kj}}^2 + {x_k}^2 - {x_j}^2 + {y_k}^2 - {y_j}^2 + {z_k}^2 - {z_j}^2)}{2(R_{kj}y_{lk} - R_{kl}y_{jk})} - \frac{R_{kj}({R_{kl}}^2 + {x_k}^2 - {x_l}^2 + {y_k}^2 - {y_l}^2 + {z_k}^2 - {z_l}^2)}{2(R_{kj}y_{lk} - R_{kl}y_{jk})} \tag{3.21}$$

Likewise,

$$y = Iz + J \tag{3.22}$$

Where,

$$I = AG + B \tag{3.23}$$

$$J = AH + C \tag{3.24}$$

z is solved for using the following equation which produces two possible solutions. Only one of these is above the surface of the earth, so the other is eliminated as a possible solution.

$$z = \frac{N}{2M} \pm \sqrt{\left(\frac{N}{2M}\right)^2 - \frac{O}{M}} \tag{3.25}$$

Where,

$$\boldsymbol{M = 4R_{ik}{}^2(G^2 + I^2 + 1) - L^2} \tag{3.26}$$

$$\boldsymbol{N = 8R_{ik}{}^2[G(x_i - H) + I(y_i - J) + z_i] + 2LK} \tag{3.27}$$

$$\boldsymbol{O = 4R_{ik}{}^2[(x_i - H)^2 + (y_i - J)^2 + z_i{}^2] - K^2} \tag{3.28}$$

$$\boldsymbol{K = R_{ik}{}^2 + x_i{}^2 - x_k{}^2 + y_i{}^2 - y_k{}^2 + z_i{}^2 - z_k{}^2 + 2x_{ki}H + 2y_{ki}J} \tag{3.29}$$

$$\boldsymbol{L = 2(x_{ki}G + y_{ki}I + z_{ki})} \tag{3.30}$$

Equation (3.25) produces a plus and minus *'z'* term. The minus term is eliminated as it resides below the surface of the earth. Taking the plus term as the solution for z and substituting this result into equations (3.13) and (3.22) produces the desired results for all three coordinates, and the hence, the location of the aircraft at position (*x, y, z*) [14].

The solutions above represent an ideal set of equations to solve for three-dimensional aircraft positions given the TDOA measurements from the multilateration network of sensors. These equations produce ideal solutions which give exact locations based on an *ideal measurement system* with *infinitely precise mathematical computations*, neither of which exist due to measurement error. Measurement error introduces a non-ideal component to the solutions that results in singularities, or divergences, at specific locations within the geometry of the multilateration system. This research project introduces a new methodology for identifying and resolving the singularities introduced by measurement error in a fixed geometry multilateration system. Introducing a '*software-based rotational geometry*' eliminates this uncertainty which, otherwise, compromises the reliability of multilateration systems. The solution presented in section 4.3.2.1 details the implementation of this methodology.

3.2.1 Sensor Geometry

Critical to the success of the multilateration system is the geometric configuration of the sensors. In order to maximize the system accuracy, attention to the layout of the sensors must turn to Geometric Dilution of Precision (GDOP). GDOP is a GPS term that characterizes the strength of satellite configuration on GPS accuracy. A direct correlation is made between GPS and multilateration geometry, and the same calculations for GDOP are used for both systems. For instance, when satellites are close together in the sky, the geometry is said to be weak and the GDOP value is high. When the satellites are far apart relative to the distance from the receiver, the geometry is strong and the GDOP value is low. The relationship is identical for the sensors in a multilateration system and their positions relative to the transmitter.

GDOP is defined by the geometry's relationship to the H matrix:

$$\boldsymbol{H} = \begin{bmatrix} \boldsymbol{a_{x1}} & \boldsymbol{a_{y1}} & \boldsymbol{a_{z1}} & \mathbf{1} \\ \boldsymbol{a_{x2}} & \boldsymbol{a_{y2}} & \boldsymbol{a_{z2}} & \mathbf{1} \\ \boldsymbol{a_{x3}} & \boldsymbol{a_{y3}} & \boldsymbol{a_{z3}} & \mathbf{1} \\ \boldsymbol{a_{x4}} & \boldsymbol{a_{y4}} & \boldsymbol{a_{z4}} & \mathbf{1} \end{bmatrix} \tag{3.31}$$

where, $a_i = (a_{xi}, a_{yi}, a_{zi})$ are the unit vectors pointing from the mobile to the location of the i^{th} sensor [15].

GDOP is then calculated from,

$$GDOP = \sqrt{D_{11} + D_{22} + D_{33} + D_{44}} \tag{3.32}$$

Where,

$$(H^T H)^{-1} = \begin{bmatrix} D_{11} & D_{12} & D_{13} & D_{14} \\ D_{21} & D_{22} & D_{23} & D_{24} \\ D_{31} & D_{32} & D_{33} & D_{34} \\ D_{41} & D_{42} & D_{43} & D_{44} \end{bmatrix} \tag{3.33}$$

Through GDOP analysis and experimental trials, the optimal geometry for this four sensor, three-dimensional multilateration system was determined to be a geometry that will be referenced as a ‘centered equilateral triangle’. This is a layout of four sensors in which three of the sensors are the vertices of an equilateral triangle with the fourth

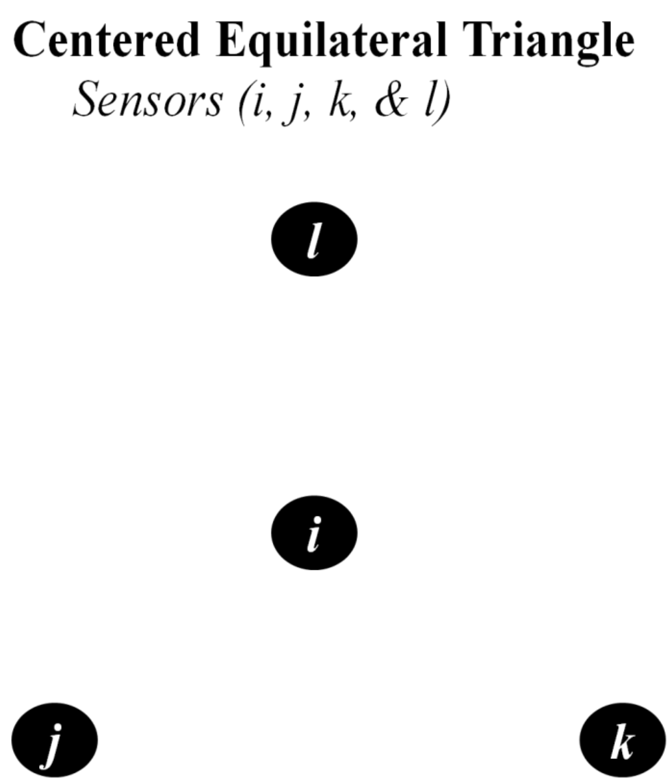

Figure 3. 3 - Graphical representation of ideal 'centered equilateral triangle' sensor layout.

placed at the center point of the triangle. Figure 3.3 is an illustration. For optimal multilateration performance, the network of RF sensors should follow this pattern as closely as possible. Actual deployment, however, is based on the availability of locations which are in the desired sensor positions, and will rarely fulfill the exact geometry that is sought.

Graphical representation of the GDOP analysis of a centered equilateral triangle is given in Figure 3.4. The graph illustrates the magnitude of GDOP throughout a constant altitude plane (1000 meters) inside and outside the geometrical configuration of sensors. Notice the center 'sweet spot' with rapid degradation just outside the network of sensors.

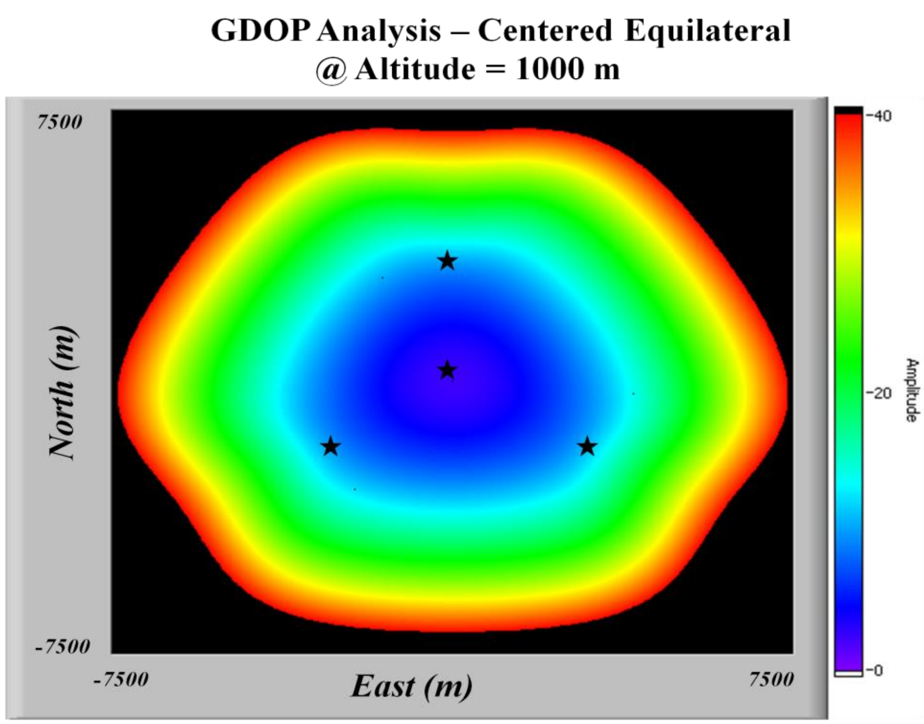

Figure 3. 4 - GDOP analysis of ideal geometry for four sensor multilateration system.

GDOP Analysis – Square Geometry
@ Altitude = 1000 m

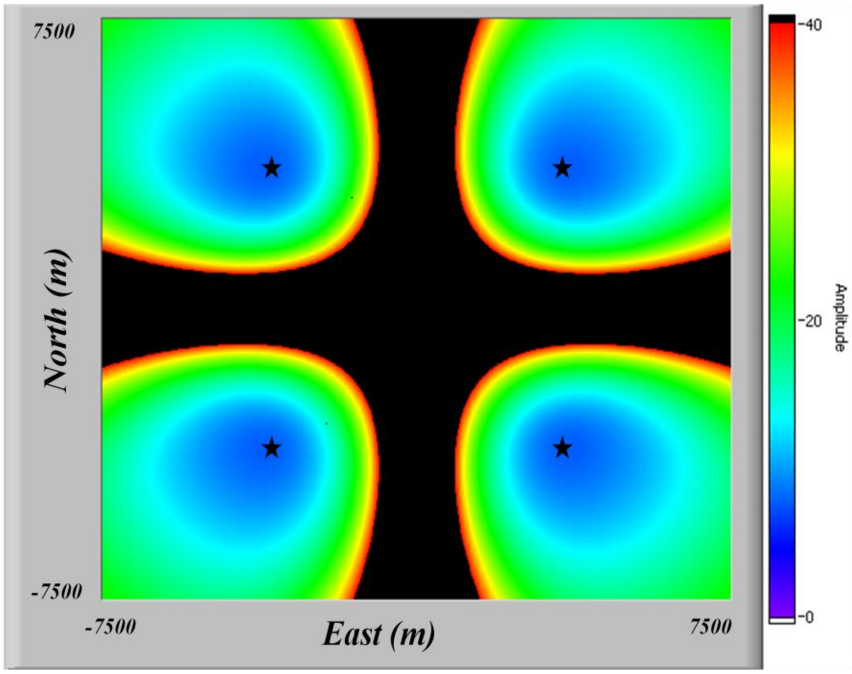

Figure 3. 5 - GDOP analysis of square geometry.

For comparison, a similar GDOP analysis is also illustrated in Figure 3.4 which represents the same calculations, this time for a square at an altitude of 1000 meters.

3.2.1 Multilateration Coordinate Systems

A few different coordinate systems are used when working with three-dimensional position measurements on or above the surface of the earth. Two Cartesian coordinate systems are used in this research project. They are Earth-Centered-Earth-Fixed (ECEF) and East, North, Up (ENU).

The main coordinate system used for all locations, measurements and calculations is Earth-Centered-Earth-Fixed (ECEF) [16]. This is a coordinate system (XYZ) in which the center of the earth is the origin, and the polar axis is the Z-axis. The X-axis is defined by the intersection of the plane defined by the Prime Meridian and equatorial plane. The Y-axis completes a right handed orthogonal system by a plane 90 degrees east of the X-axis and its intersection with the equator. This coordinate system, unlike the ECI (Earth-Centered-Inertial) system, is fixed relative to the surface of the earth. Unlike ECI, the

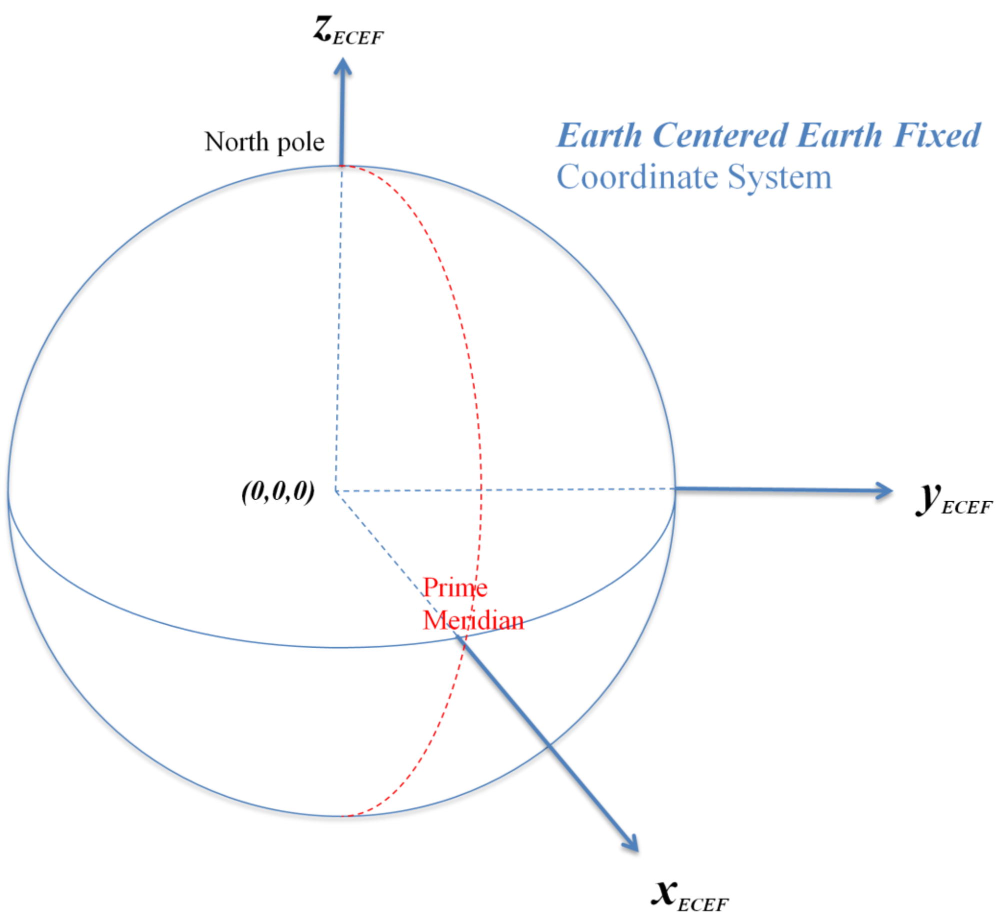

Figure 3. 6 - ECEF coordinate system.

ECEF coordinate system rotates with the earth. Therefore, a body at rest on the surface of the earth or in the air at a fixed point above the surface is at a fixed point (x, y, z) during the earth's rotation. Figure 3.5 is an illustration of the ECEF coordinate system.

Another more intuitive representation of the position data that is referenced in this document is the East, North, Up (ENU) coordinate system [17]. This is a Cartesian coordinate system that represents the data in terms of East, North and Up. The East-North plane is tangential to the surface of the earth with North in the direction of the polar axis, and the 'Up' coordinate is the distance in the direction normal to the surface of the earth (Figure 3.6).

The conversion from ECEF to ENU can be performed by the following calculation:

$$\begin{bmatrix} E \\ N \\ U \end{bmatrix} = \begin{bmatrix} -sin\lambda & cos\lambda & 0 \\ -sin\phi\ cos\lambda & -sin\phi\ sin\lambda & cos\phi \\ cos\phi\ cos\lambda & cos\phi\ sin\lambda & sin\phi \end{bmatrix} \begin{bmatrix} X_{ECEF} \\ Y_{ECEF} \\ Z_{ECEF} \end{bmatrix} \tag{3.31}$$

In the above equations:

$\lambda = Longitude$

and

$\phi = Latitude$

All calculations are made first with ECEF coordinates with the origin at the center of the earth. The data is then translated to the surface of the earth at the central point of the multilateration system network, thereby creating a coordinate system with the origin at the central point of the geometrical configuration. For the purpose of presentation, all position data is then translated to ENU retaining the central origin at the center of the configuration.

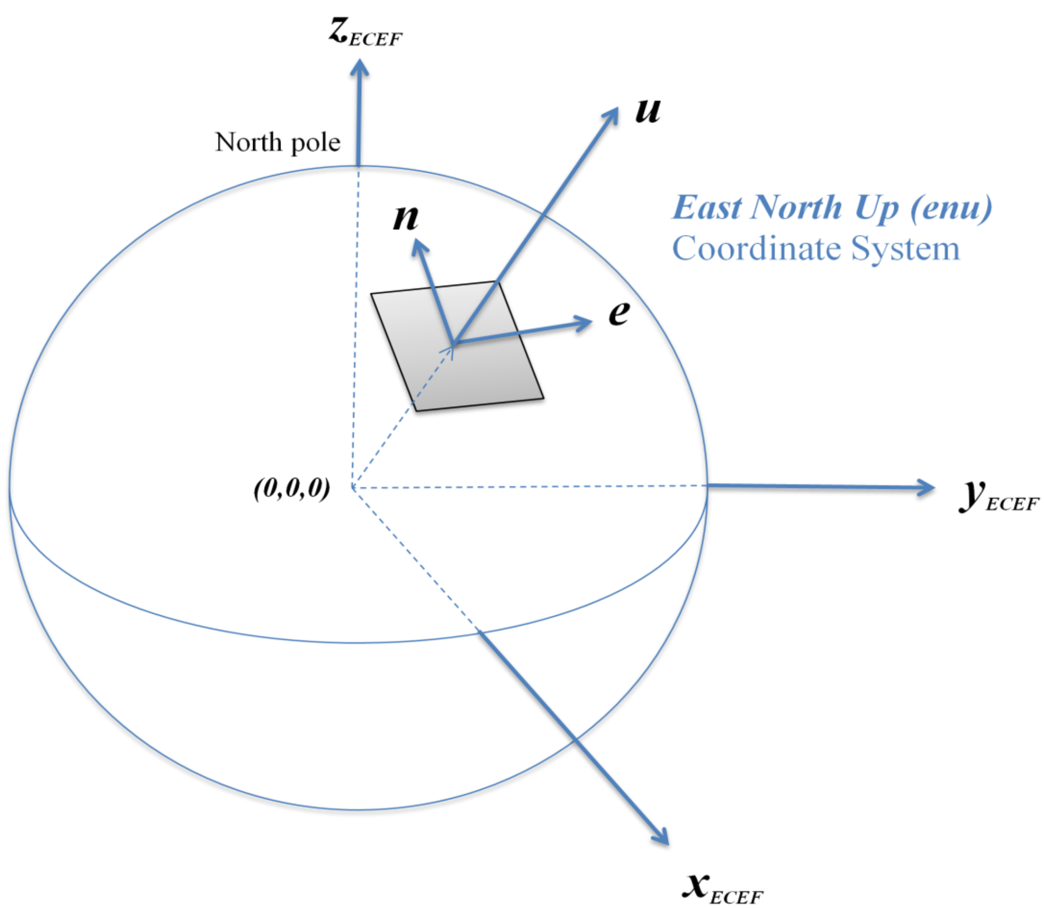

Figure 3. 7 - ENU coordinate system.

3.3 Architecture of System

New algorithms and methodologies have been developed to implement the above described multilateration system implementing a unique methodology for applying TDOA methods to locate aircraft in three dimensions. A passive network of four 'listen only' RF sensors were developed which have the bandwidth necessary to acquire, identify and timestamp the arrival of all Mode A/C broadcasts from aircraft within the geometry of the network of sensors.

Successful implementation of this new methodology requires a system design with three main components. These three key components of the system include:

1. Unique RF sensor design consisting of a custom software-defined spectrum analyzer/datalogger capable of identifying the message being transmitted by the aircraft's transponder and timestamping the arrival of the signal.
2. Central Processing Station for data reduction with unique algorithm for filtering and correlating data from each sensor and computing the location estimate of the unknown aircraft.
3. Communications infrastructure for networking the sensors and the Central Processing Station.

Both the RF sensor and the Central Processing Station have requirements that are not available in commercial products. This dictates that each sensor would have to be developed by creating new algorithms to accomplish the desired tasks. Each is based on a PC-based computing platform to deliver the processing power and the storage capability that will be necessary to fulfill the requirements.

3.3.1 RF Sensor

The development of a unique algorithm for precisely measuring the time of arrival of Mode A and Mode C transponder transmissions with the precision necessary to compute accurate position fixes requires the development of several new designs both in hardware and in software.

The Mode A/C message being transmitted by the aircraft's transponder is a low power RF transmission which dictates the need for adequate RF hardware for filtering and amplification. Likewise, the sophistication built into the spectrum analyzer which acquires the transponder signal has the requirement of acquiring the signal, demodulating it and processing the time domain binary pulse coded message (Figure 3.7). Additionally, it requires a timing device that accurately measures the time of arrival of the leading edge of the message, as this is the cornerstone for the TDOA methodology.

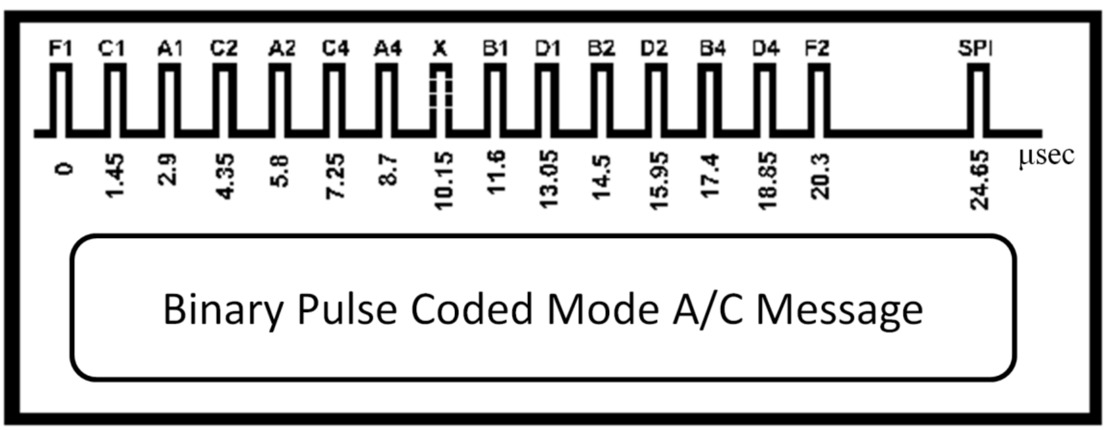

Figure 3. 8- Format of the Mode A/C message (described in detail in Chapter 4).

At the core of the time of arrival measurement device is a GPS-based timer capable of measuring 'time events' with an accuracy of ± 30 nanoseconds. Working in concert with the spectrum analyzer, this GPS-based event timer is capable of producing correlated pairs of Mode A/C transponder messages and their precise time of arrival timestamps. This data is the necessary information to accurately calculate the three dimensional position of nearby aircraft.

Several challenges are expected to be presented in realizing the RF sensor design being proposed. As in any engineering solution, the implementation of such a system requires dealing with and solving many non-ideal artifacts associated with RF instrumentation such as problems with Signal-to-Noise (S/N), bandwidth, saturation, signal collision, multipath, group delay, etc. A combination of hardware and software must be designed to reduce the effect these problems introduce in the form of measurement error. Below is a list of the challenges that were solved during the implementation of the multilateration RF sensor model:

- RF signal conditioning solution to provide optimal Signal/Noise in order to extract the necessary data from a low power transmitter
- Development of digital signal processing solutions associated with partial or overlapping Mode A/C messages
- Software development of unique algorithms to filter, decode and log Mode A/C data and timestamps
- Development of methodology for quantifying measurement error for each sensor associated with group delay in the filter/amplifier/downconverter
- Solution to 'sensor saturation' as a result of heavy air traffic outside the geometry that saturates only one or possible only two of the sensors and competing with legitimate targets for their bandwidth
- Loss of signal to individual sensors caused by airplane banking maneuvers
- Software driver development for instrumentation

3.3.2 Central Processing Station

The multilateration position solution calculations must be performed by a host computer which processes Mode A/C messages along with their times of arrival from each of four RF sensors. This process requires the development of new algorithms which are capable of filtering false data, correlating timestamps from the network of RF sensors, correcting for calibration offsets and computing the position solution from multiple aircraft in a given airspace.

A critical feature of the Central Processing Station is the ability to adaptively filter mathematical divergences which result from poor geometrical positioning and measurement error. The multilateration system is subject to gross inaccuracies that can result from a combination of non-ideal sensor location and time of arrival measurements that are in error. Below is a list of challenges that were solved during the implementation of the multilateration Central Processing Station model:

- Development of data reduction, cross correlation and filtering algorithm
- Development of adaptive solution to eliminate mathematical divergences (singularities) in solution equations caused my measurement error
- Development of adaptive solution to optimize sensor geometry as it applies to the TDOA solution equations

3.4 Procedure for Implementation of Concept

In order to analyze the effectiveness of this new approach to locating aircraft, a theoretical proof of concept for the multilateration system was designed so mathematical position solutions could be acquired from empirical data gathered from aircraft at known positions. Although the goal of the system is to provide real-time aircraft positions, for the purpose of this research, the conceptual design was implemented without the communications infrastructure. Although this proof of concept does not provide real-time position calculations, the system will validate the real-time approach and the actual solution accuracy will be identical to that of a real-time system deployment. Using this method of validating the system performance, truth flights can be flown and the multilateration system solutions can be post processed for comparison to actual positions taken from the GPS truth data recorders.

Using this experimental method, individual RF sensors operate autonomously as dataloggers which store transponder squawks and their arrival times. This data is then compiled over time and then retrieved from each unit for the purpose of testing the proposed algorithms in the Central Processing Station.

This experimental data, when compared to GPS-based truth data, is capable of characterizing the multilateration system by validating the accuracy of the system. From this data, error analysis can be performed by correlating multilateration position estimates with actual GPS-based truth data taken during flight tests. This comparison validates the system design and algorithm implementation. These results are presented in chapter 5.

CHAPTER 4

System Development Architecture

4.1 Overview

The implementation of the architecture described in the previous chapter will be discussed in detail in terms of hardware and software components that had to be developed in order to realize the conceptual design. The two main pieces of the system which include the RF sensor and the Central Processing Station will be discussed in detail, including detailed information regarding the Mode A/C message which must be received, decoded and timestamped.

4.2 RF Sensor Design

The multilateration system is dependent on a network of passive RF sensors capable of sensing, identifying and timestamping the arrival of the Mode A/C signal emitted from the transponders of nearby aircraft. The RF sensor is the key component of system and the one with the most complexity.

The sensor contains two main components. At the core of the system is a PC-based software-defined spectrum analyzer/datalogger with newly developed software algorithms which give it the capability of triggering on RF signals of which power in band criteria are met in the frequency range and bandwidth of interest. Utilizing a PC-based architecture gives it the additional functionality of providing the other features necessary for successful operation. The main features are software programmable analog signal threshold, adaptive software filtering, demodulation/decoding algorithms, serial communications with external instrumentation as well as datalogging and local storage capability.

Working in concert with the software-defined analyzer is a GPS-based event timer capable of autonomous operation (without the synchronization of a local reference transmitter and the dependence on line of sight operation). This autonomy is a feature that does not exist in multilateration technology today. Without the dependence on a local transmitter, the geographical positioning of the sensor network can be extended to areas which have limited or no line of sight access from the sensors to the central processing station.

This GPS-based event timer has the accuracy and bandwidth to service up to 100 events per second with ±30 nanosecond resolution. This provides the functionality necessary for each sensor to receive time of arrival information on up to 100 individual Mode A/C squawks per second. Figure 4.1 illustrates the main components of the RF sensor which will be discussed in greater detail in section 4.2.2.

During operation the digitizer in the analyzer has the capability of arming its analog trigger to detect RF transmissions from nearby aircraft transponders at a center frequency of 1090 MHz (Mode A/C transponder frequency). Upon receipt of an RF signal with sufficient energy to rise above the software defined threshold of the digitizer, the signal is digitized, demodulated and decoded. Simultaneously, an output trigger is sent to the GPS timer requesting the timestamp of the signal.

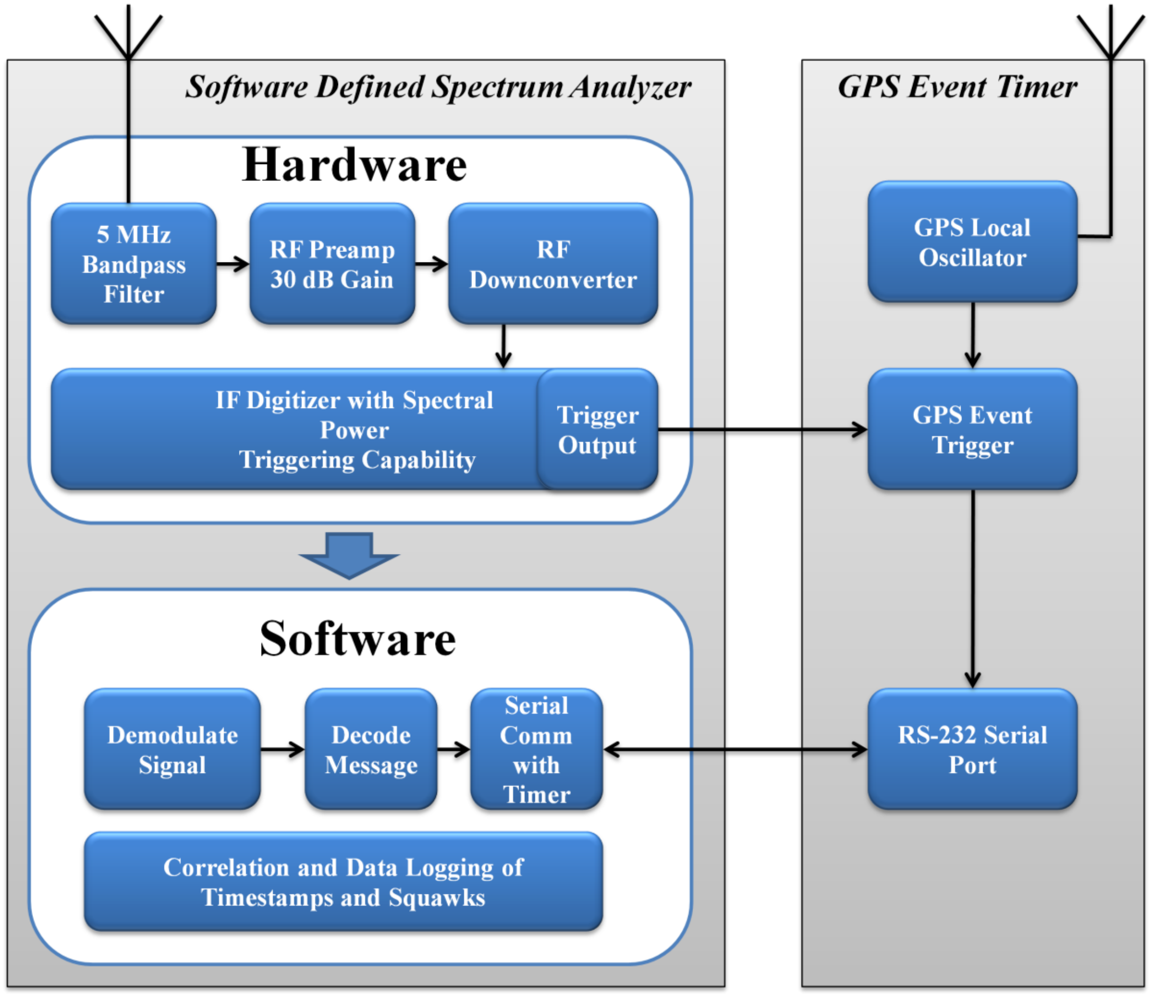

Figure 4. 1 - Block diagram of the RF sensor design.

After the software decodes the message and validates the authenticity of the Mode A/C message (message is in the proper format of a Mode A/C reply), the information is stored along with its corresponding time of arrival information. This data is cataloged for post processing so there is a one-to-one pairing of Mode A/C messages and their corresponding timestamps. A system level flowchart which characterizes the ideal path of the signal is illustrated in Figure 4.2.

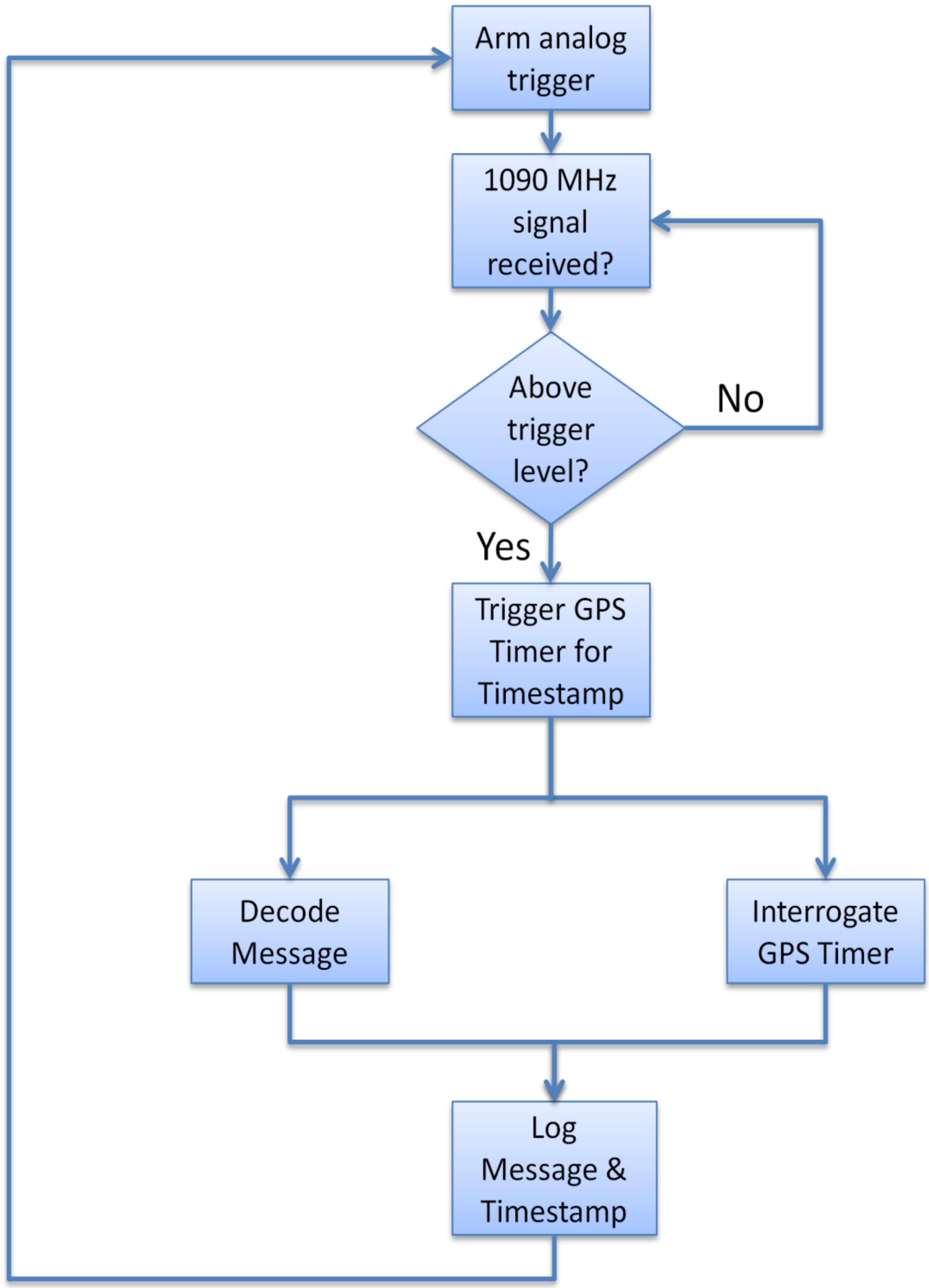

Figure 4. 2-Ideal path of signal flow through the RF sensor.

4.2.1 The Mode A/C Message Format

The Mode A/C transponder signal is a message in binary coded pulse trains containing IDENT (Mode A) or pressure-based altitude (Mode C) information. The message is a Pulse Position Modulated (PPM) bit stream Amplitude Modulated (AM) on a carrier of 1090 MHz. Upon interrogation by ATC, the transponder replies with a

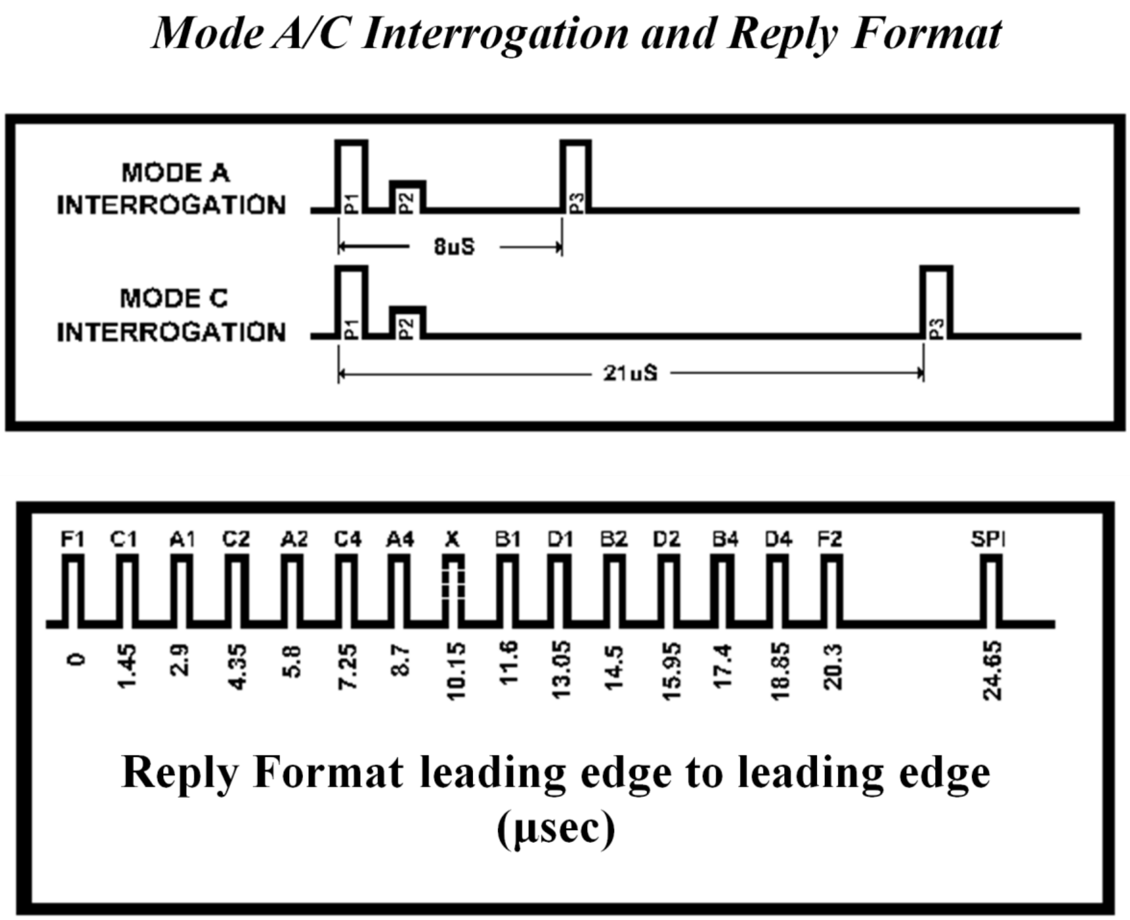

Figure 4. 3 - Mode A/C interrogation (top) and transponder reply format (bottom) [18].

message that has up to fifteen pulses (interrogation and reply format are shown in Figure 4.3). Three of these are framing pulses at the beginning, middle and end of the message.

The remaining twelve pulses represent four octal (three bit) digits which represent either the IDENT (Mode A) or the altitude (Mode C) of the aircraft. Figure 4.3 is an illustration of the transponder message which has 4096 unique messages that can be broadcast. The total spacing between the first and last framing pulse is 20.3 microseconds where each pulse is .45 microseconds with a spacing of 1.45 microseconds [19].

When decoded properly, a four digit message ABCD which ranges between 0000 and 7777 will be observed. In the case of a Mode A interrogation by ATC, the message represents a unique IDENT that was assigned to the aircraft upon entering a controlled airspace. In the case of a Mode C interrogation by ATC, the reply message represents pressure-based altitude which is can be obtained by correlating the message with the altitude code lookup table located in Appendix A. The Mode C altitude codes correspond to one of 1280 altitude codes, one for each 100 foot increment from -1200 ft to 126,700 ft. This measurement is performed by the onboard pressure based altitude sensor.

In order to determine the values of the four octal digits, each pulse has to be examined for its position in the pulse train and correlated with the appropriate bit in each of four separate three bit numbers. For instance, the *A* digit is represented as a 3-bit binary number whose least significant bit is *A1* and most significant bit is *A4*. The binary representation of *A* is (*A1 A2 A4*) which can be 000 thru 111 (0 through 7). Therefore the weighting factor of each is as follows:

$$A = A1 \times 1 + A2 \times 2 + A4 \times 4$$

The same holds true for the other three digits *B*, *C* and *D*.

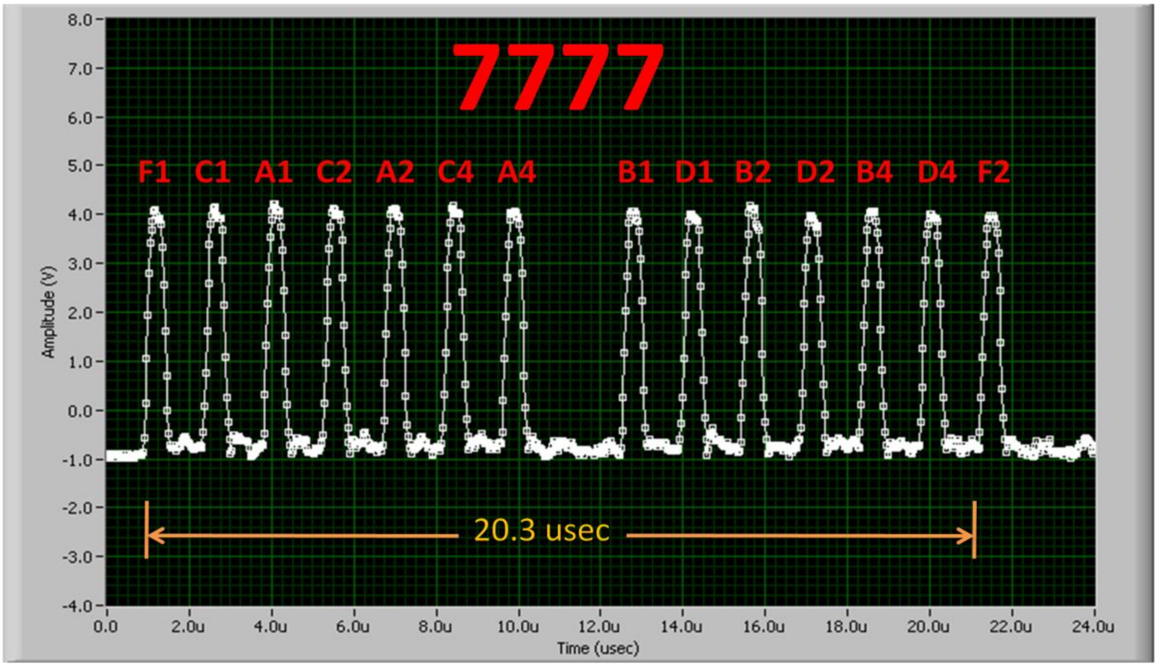

Figure 4. 4 - Actual digitized waveform of a transponder reply representing a '7777'.

In either case (Mode A or Mode C) the key to the success of the multilateration system is for the sensor to be capable of extracting two pieces of information from the signal – the precise time of arrival of the leading edge of the first framing pulse (F1) which represents the precise time of arrival of the signal at a given sensor and the four digit message that is being sent (ABCD). These two parameters when correlated with other sensors in the multilateration network give us the data that we need to perform position estimations using the TDOA algorithm described in chapter 3.

4.2.2 Software-Defined Spectrum Analyzer/Datalogger

The capturing, decoding, and timestamping of the Mode A/C transponder signal is made possible by the development of new software algorithms and hardware with the appropriate gain and bandwidth to capture all squawks within the geometry of the multilateration network. The analyzer must be sensitive enough to detect the signal of interest, but also filter out the signals which are not of interest but well above the noise floor of the system at nearby center frequencies.

The message broadcast from the transponder is done so at very low power levels which dictates a need for a high gain RF front end and antenna to provide adequate Signal-to-Noise ratio (S/N) to discern the signal of interest from other forms of RF energy nearby. The design of the spectrum analyzer therefore includes the need for the appropriate antenna, bandpass filter, and amplification to get the signal of interest to a level that diminishes the possibility of noise being falsely interpreted as actual Mode A/C signals from nearby aircraft.

Getting Signal-to-Noise to an adequate level is critical for the RF sensor, as it is bandwidth limited on the number of actual interrogations that can be adequately serviced by the GPS based event timer. If too many false signals are received (and hence timestamps requested), there will not be adequate bandwidth to handle the required amount of air traffic in a given geographical configuration. Figure 4.5 shows the block diagram of the RF front end of the signal analyzer.

The antenna that was chosen is a DME (Distance Measuring Equipment) omni-directional (360 degree operational pattern) antenna. It is a broadband omni-directional antenna designed for operation from 960 to 1215 MHz consisting of a 10-element, collinear dipole phased array. RG8 low loss cable was used for connectivity between the antenna and the analyzer.

In order to meet the gain/bandwidth requirements for the sensor, a bandpass cavity filter stage was added to pre-filter out all unwanted noise in the frequency band just outside of the 1090 MHz center frequency. The cavity filter is a 5 MHz bandpass filter with 60 dB attenuation at the cutoff frequencies (1087.5 MHz and 1092.5 MHz) centered at 1090 MHz. This filtering solution is necessary before the signal reaches the broadband preamp. It helps eliminate false triggers that would otherwise occur as a result of the many different dedicated communications transmissions standards near the 1 GHz range. It also eliminates false triggering that could occur as a result of the interrogation signal that is sent from ATC which is centered at 1030 MHz.

Given the geographical range of operation for the proof of concept design of approximately 8 to 10 miles, additional amplification was needed to boost the signal. An additional gain stage was added in the form of a 30 dB fixed gain broadband RF preamplifier. This RF front end is shown if Figure 4.5.

The output of the preamp is then fed into a 2.7 GHz RF downconverter with 20 MHz real-time Bandwidth which downconverts the signal to an Intermediate Frequency

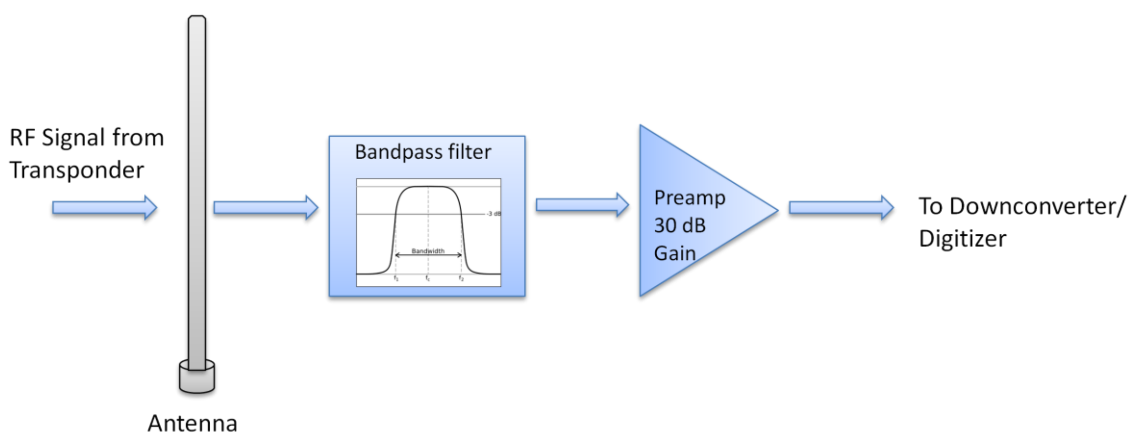

Figure 4. 5 - RF front end for the spectrum analyzer.

(IF) for digitization by an IF digitizer. The IF digitizer is a 100 MHz 14-bit, 100 MSample/sec digitizer with software configurable analog triggering capability.

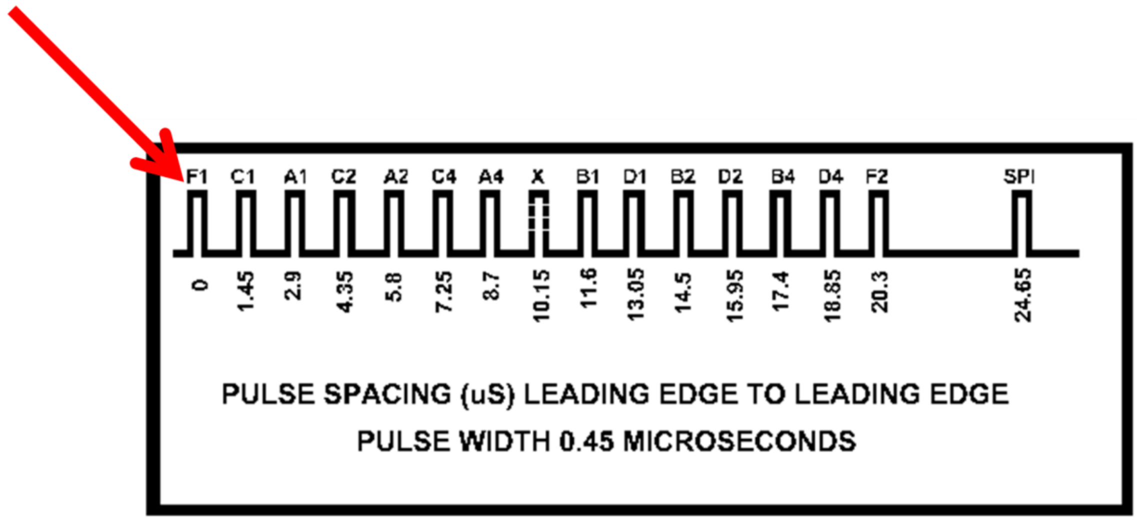

Figure 4. 6 - Mode A/C reply framing pulse (triggering edge for event timer).

The analog triggering functionality of the digitizer provides the necessary triggering mechanism for interrogating the GPS event timer for a timestamp corresponding to the arrival of the Mode A/C signal. When the leading edge of the Mode A/C message framing pulse (Figure 4.6) rises out of the noise floor threshold specified by the software, the analog trigger generates a pulsed output for export in the form of a TTL 5 Volt pulse with a width of 100 nanoseconds. This output signal from the digitizer is routed to the GPS event timer where the leading edge triggers the timer to produce the precise timestamp of the event with ±30 nanosecond resolution. The analog trigger is then immediately rearmed to begin waiting for the next signal to arrive. The GPS event timer system specifications allow for a maximum of 100 individual triggers/second to be timestamped (hence the need for limiting the number of false triggers allowing for maximum use of event timer's bandwidth).

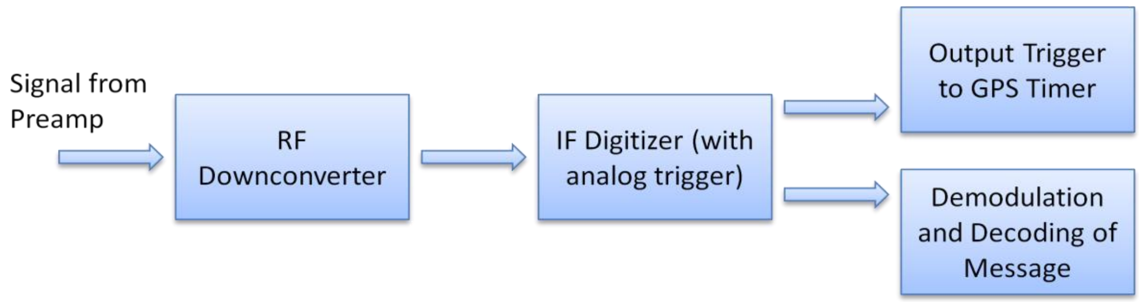

Figure 4. 7 - Signal flow through the spectrum analyzer.

While the bandpass filter and the preamp extend the range of the analyzer to reach the necessary distance for the multilateration system requirements, the filter has a negative effect on the system as well. As expected, one of the negative effects of the bandpass filter is that it alters the shape of the pulses. This rounding effect alters the rise time of each pulse, hence adding error to the time of arrival measurement. In Figure 4.8 the reader can see that even though these two examples are both from the same Mode A

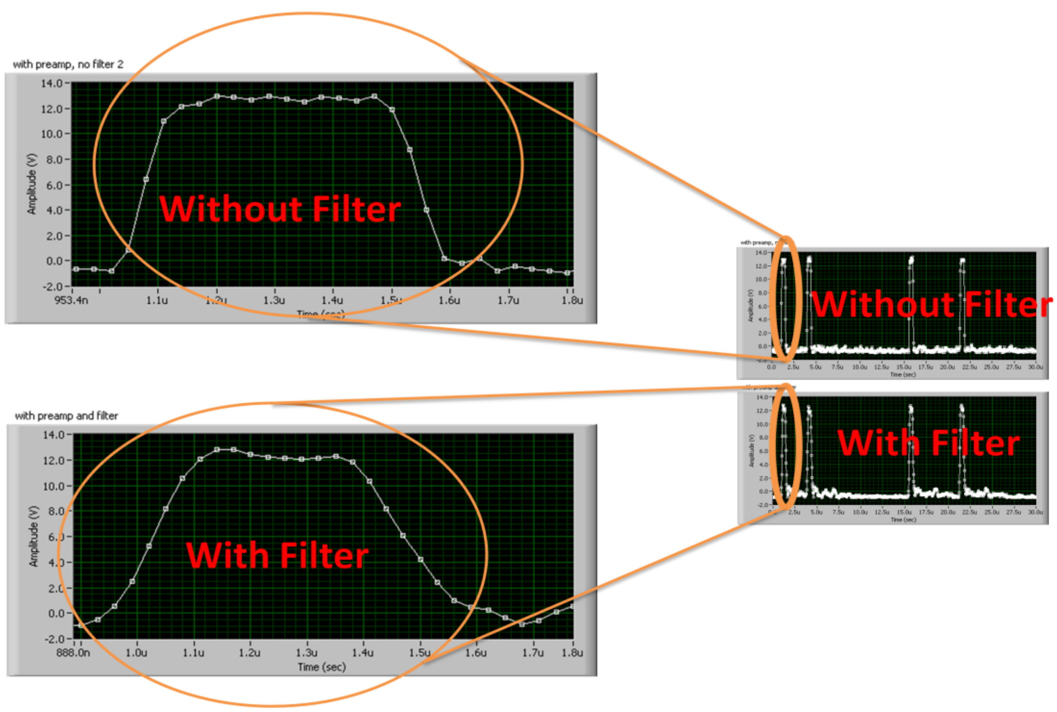

Figure 4. 8 - Rounding effects of the bandpass filter.

message (1200), with the same sampling rate from the digitizer, the Δt for the signal to reach its amplitude is larger for the sample that was taken from the system using the filter. The reason this is a source of error is due the fact that the analog trigger is set to act on the first crossing of the trigger level. This 'lag' caused by the presence of the filter leads to a delay in the trigger sent to the timer, hence causing a slight distortion in the time of arrival measurement. Although the difference is extremely small (nanoseconds), it does introduce a small amount of error in the time of arrival measurement. This error is a necessary tradeoff to get the extended range that the filter and the amplifier provide. This error has been included in the system's overall error budget.

4.2.2.1 Software and Digital Signal Processing

The software development of each sensor consisted of new algorithms which provide functionality of a spectrum analyzer, filter, decoder, timer and datalogger wrapped up in a single PC-based platform. This was accomplished using a PXI instrumentation platform with custom developed LabVIEW source code to perform the required instrumentation tasks as well as the real-time demodulation and digital signal processing to extract the Mode A/C message.

Figure 4.9 is a system level flowchart of the software routine that illustrates the sequential operation of the algorithm for capturing, identifying and timestamping the Mode A/C transponder signals.

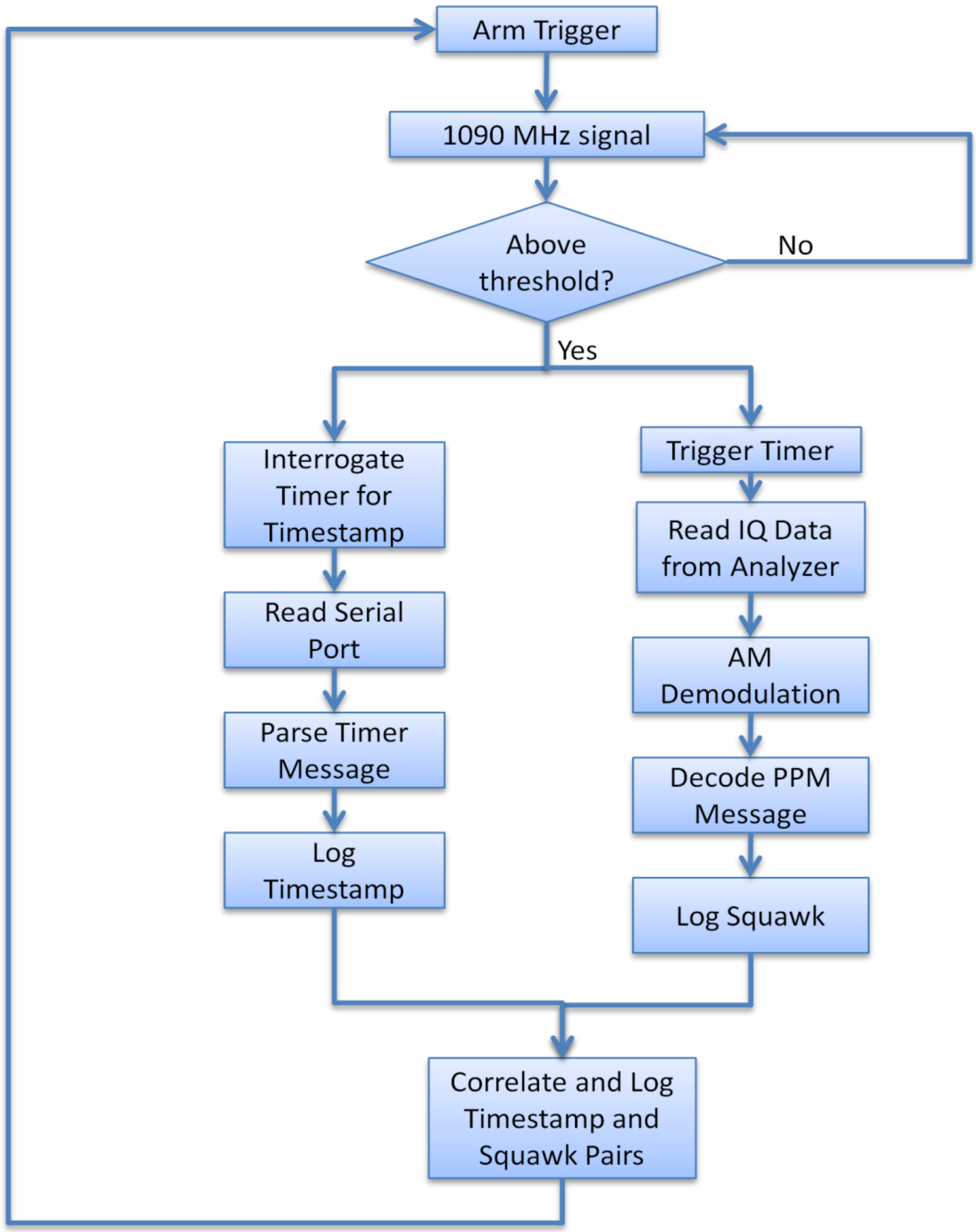

Figure 4. 9 - System level flowchart for the spectrum analyzer.

Figure 4.10 is a screen shot from the system that illustrates the actual waveform that is produced as a result of the AM demodulation step. This analog waveform represents the four digit octal code for a transponder emitting the code '7777'. Notice the absence of the middle framing pulse which may or may not be present, but it is considered a ‘don’t care’ bit.

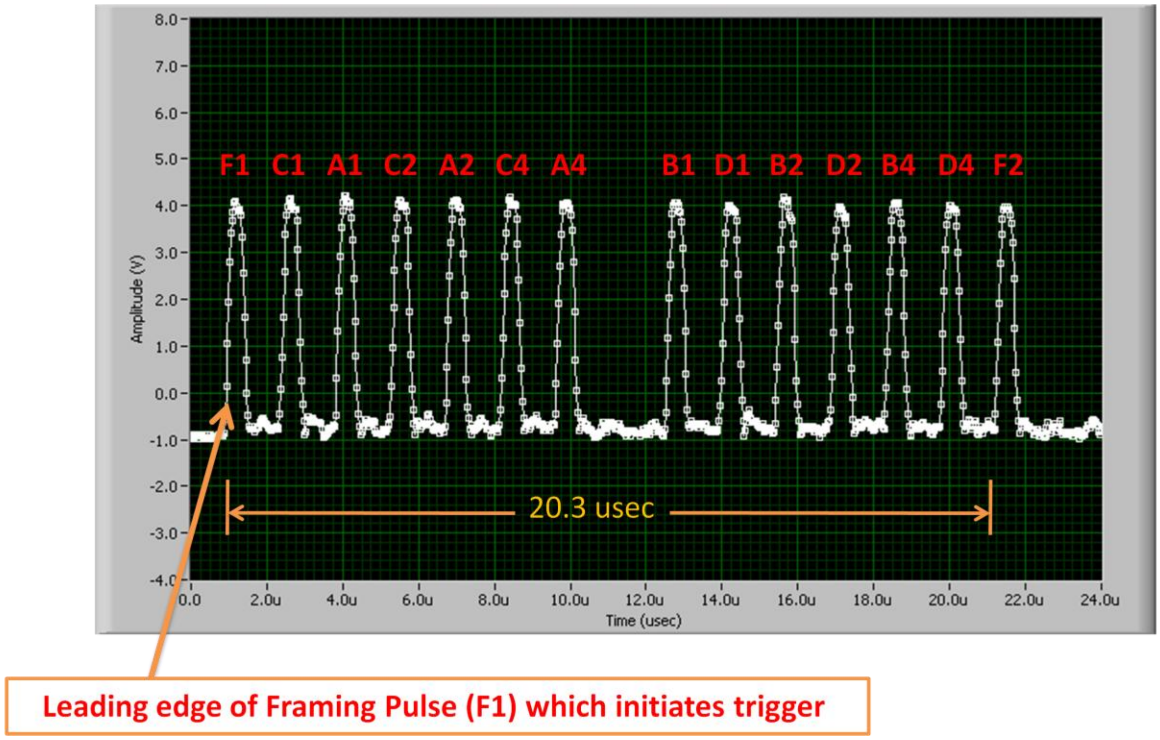

Figure 4. 10 - Actual screen shot of digitized '7777' illustrating leading edge of framing pulse.

There are two main threads that are running simultaneously in order for the sensor to implement the model. One is relatively simple, and the other is quite complex. Those two threads are as follows:

1. Interrogation of the GPS-based event timer and the acquisition of timestamp information which includes the parsing of the timestamp and datalogging the results in a manner that maintains the correlation with the RF message that was received by the digitizer in a separate thread.
2. The acquisition of the I/Q measurement, AM demodulation of the signal and decoding of the Pulse Position Modulation (PPM) coding scheme

The first of these tasks is essentially a routine for serial communications with the event timer. Constant communications are necessary to gather and parse timestamps and correlate with them with the appropriate squawk. The timestamp format from the event timer is as follows:

Day : Hour : Minute : Second : Nanosecond

This data is parsed and paired with its associated squawk (taken from the routine described below) and stored in data packets of the following format in each of the four sensors:

Squawk : Day : Hour : Minute : Second : Nanosecond

The second of the two tasks is considered to be the more complex of the two primarily due to the decoding of the binary coded PPM pulse train which contains the Mode A/C message (squawk). This requires the development of a new algorithm for decoding the pulse positions to produce the four digit octal code representing the squawk. It also dictates the need for developing the necessary digital signal processing to identify and filter non-ideal measurements. Otherwise, these non-ideal factors may cause the mis-identification of the squawk due to false triggers, interlaced messages from multiple aircraft, overlapping messages from multiple aircraft or unwanted pulses interlaced into signal as a result of multipath.

The algorithm developed for decoding the binary coded PPM pulse train which represents the Mode A/C message is represented in a flow chart in Figure 4.11.

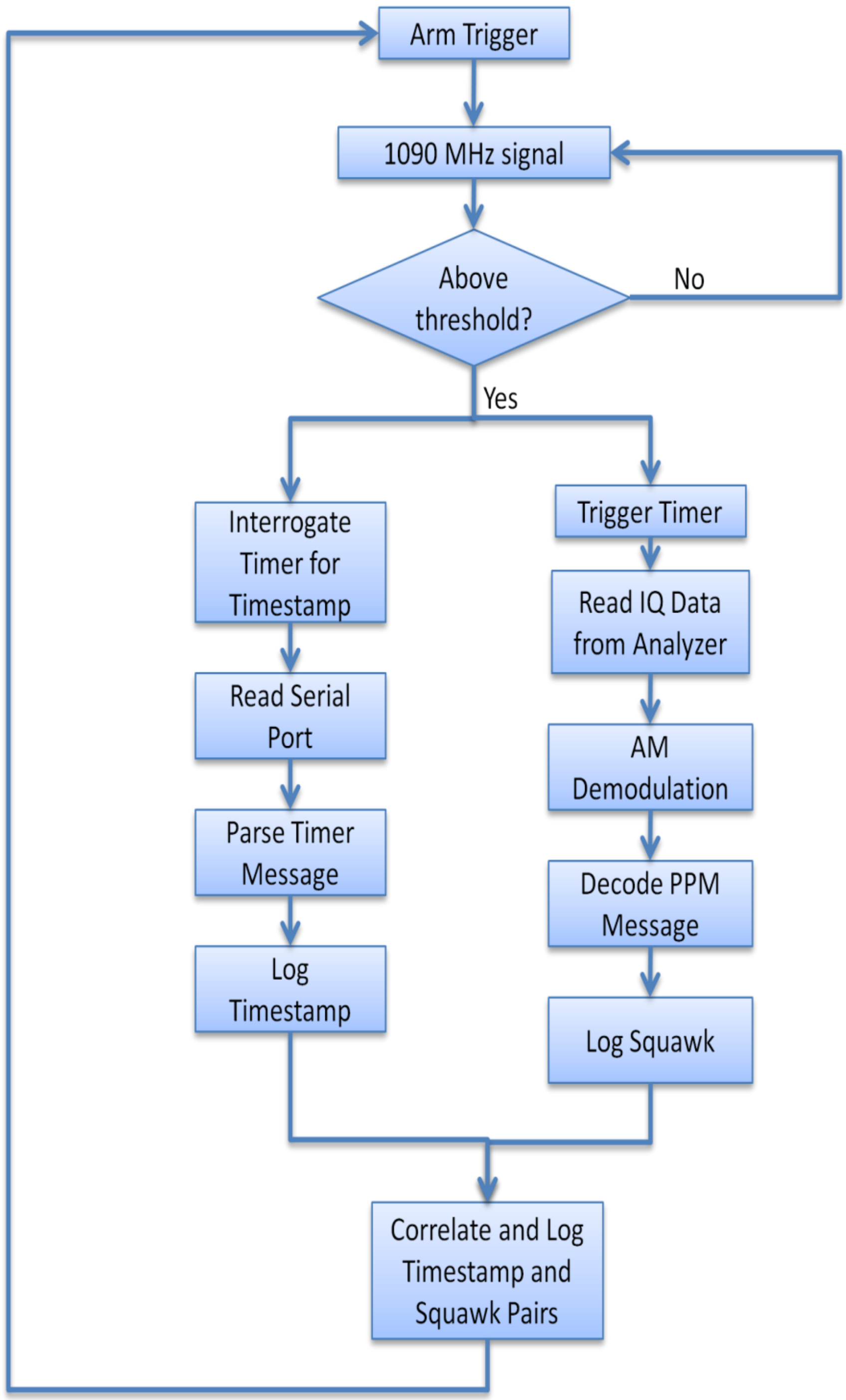

Figure 4. 11 - Algorithm for decoding PPM message.

Below are illustrations of two different squawks, one Mode A (IDENT) and one Mode C (altitude) along with the computation of their 4-digit, 3-bit octal codes.

The Mode A IDENT squawk show in Figure 4.12 was decoded properly as a '1200' by the algorithm that was developed for the analyzer. Below is the computation of each digit:

$$\mathbf{A = A1 \times 1 + A2 \times 2 + A4 \times 4}$$

$$\mathbf{= 1 \times 1 + 0 \times 2 + 0 \times 4}$$

$$\mathbf{= 1}$$

Likewise, *B* = 2, *C* = 0, *D* = 0 to make up the Mode A IDENT of '1200'.

Using the same algorithm and calculations, Figure 4.13 illustrates a squawk of '0760'. This is marked as a Mode C broadcast since it is one of the 1280 altitude codes. '0760' corresponds to a pressure-based altitude of 1600 ft MSL.

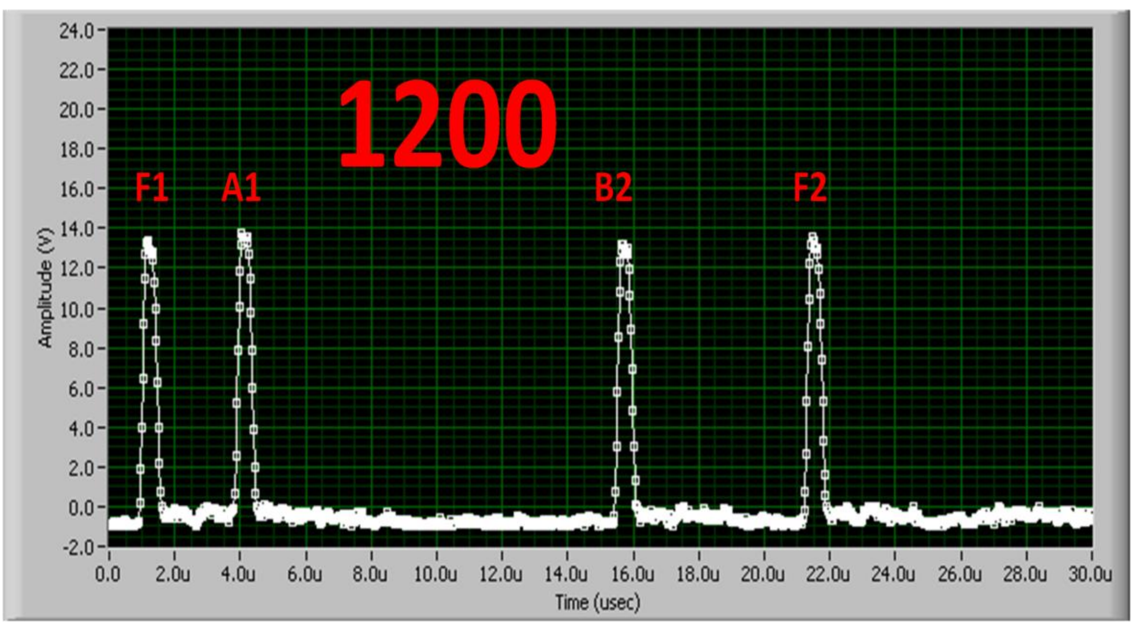

Figure 4. 12 - IDENT sqawk '1200' screen shot from the spectrum analyzer.

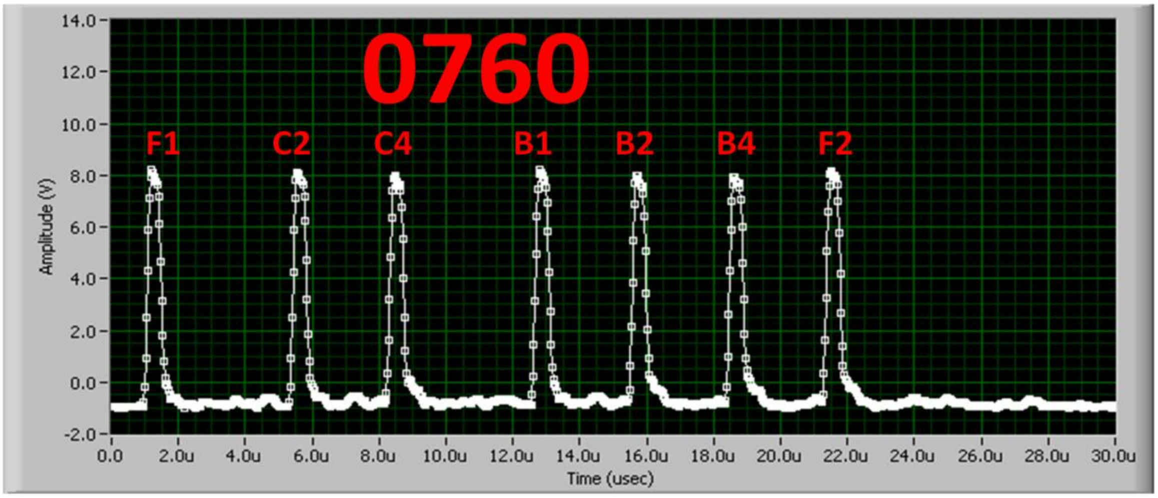

Figure 4. 13 - Altitude squawk '0760' screen shot from the spectrum analyzer.

The bulk of the software effort was in developing a new algorithm to filter false triggers as well as interlaced and overlapped messages that are caused by any of the following:

1. *Interlaced* pulses due to multiple aircraft being interrogated within 20.3 microseconds of each other.
2. *Overlapping* pulses due to multiple aircraft being interrogated within 20.3 microseconds of each other.
3. Interlaced pulses due to multipath reflections of the same transmission.
4. Message fragments due to message being transmitted simultaneously to the rearming of the trigger.
5. False triggers due to RF noise that was not attenuated by the bandpass filter.

Examples of each of these types of non-ideal waveforms are illustrated in the following figures which are actual digitized waveforms sampled by the RF sensor. The first is an example of interlaced or overlapped pulses due to multiple aircraft being interrogated within 20.3 microseconds of each other. This type of signal collision results in two or more messages from different aircraft merged into the same waveform. The algorithms developed are capable of adaptive filtering data collisions such as that shown in Figure 4.14. The software was developed to provide the necessary digital signal processing to detect the presence of interlaced messages by filtering on pulse amplitude differences. Although the filtering methodology is capable of recognizing the fact that there are two interlaced messages and identifying both, it is only capable of exporting a trigger to the timer for one of them. Therefore, the signal that initiated the trigger with the leading edge of its framing pulse (as indicated on in the figure by message '0140') is considered the 'message of interest' and hence the one in which the timer will be providing a timestamp. In this case, the second message is simply filtered.

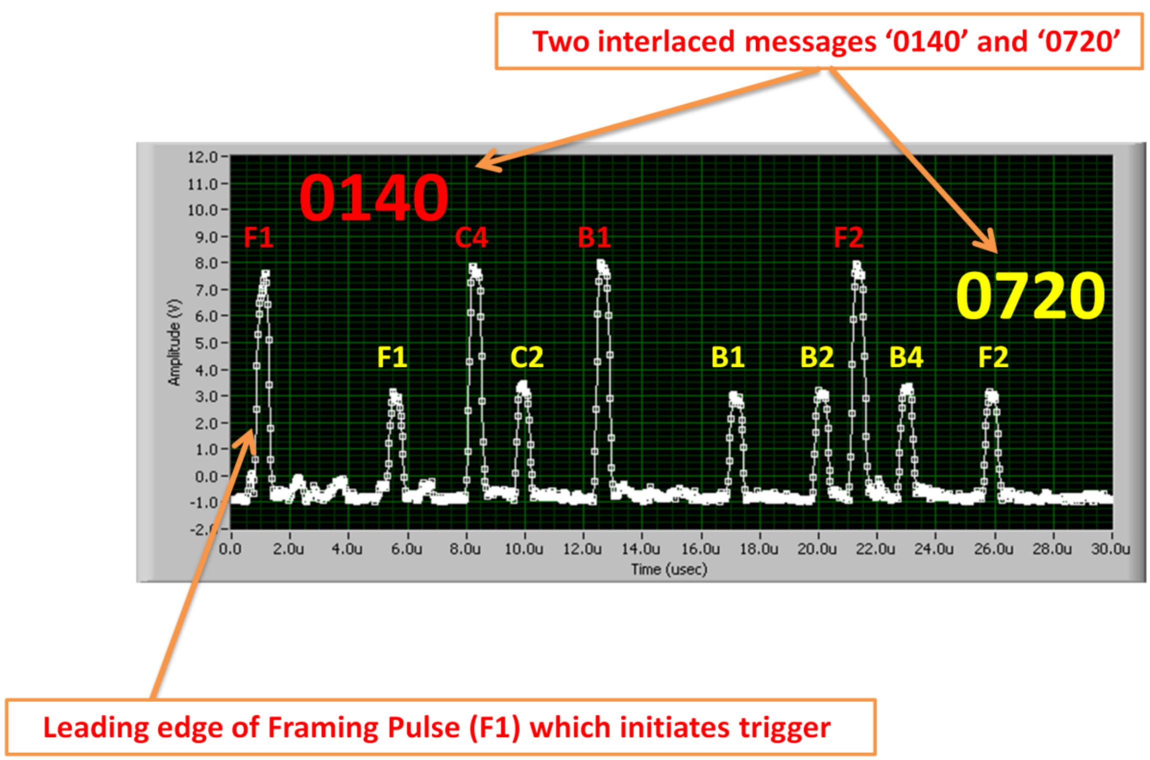

Figure 4. 14 - Interlaced messages '0140' and '0720'.

Simply throwing out the interlaced message solves this problem and does not have a negative effect on the overall perform of the system. The overabundance of Mode A/C squawks provides more than enough data for successful implementation of the multilateration system without these filtered messages being timestamped. Figure 4.15 illustrates a similar data collision, except in this interlaced message there is also an 'overlap' of two pulses. This too is filtered out by the signal processing software.

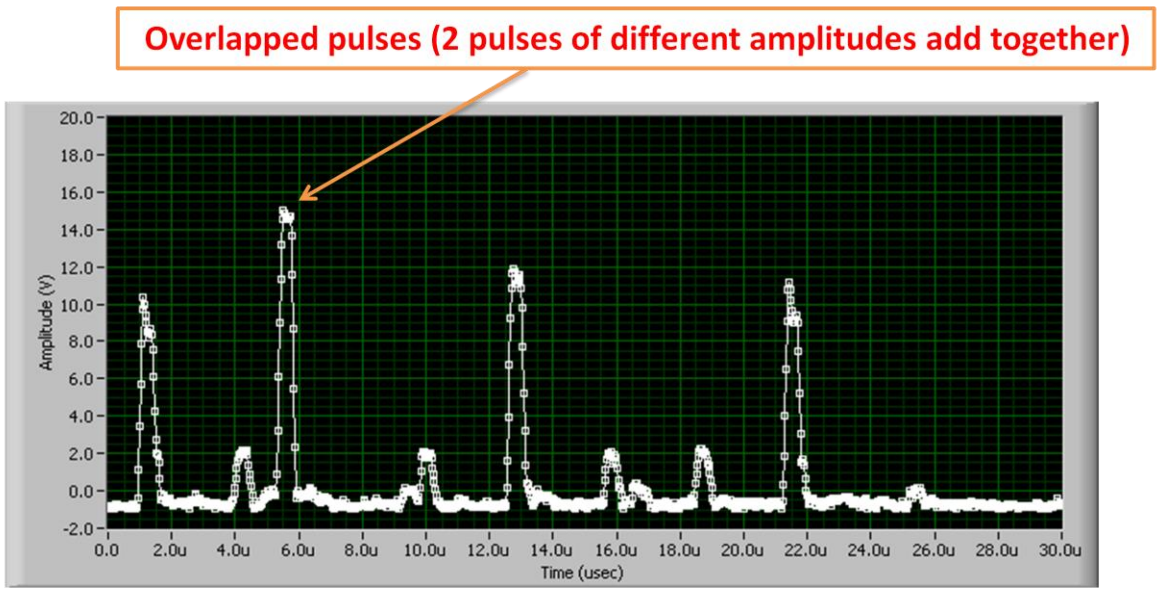

Figure 4. 15 - Interlaced and overlapping pulses in collision.

Like interlaced messages that a result from two or more aircraft being interrogated nearly simultaneously, another need for filtering exists as a result of signal multipath. The digital signal processing algorithm uses a method similar to the previously described filter to detect the presence of multipath. Using the same method of noise recognition, the algorithm is capable of filtering the signal due to multipath as they are always lagging the 'actual' signal in time and signal strength. FIGURE 4.16 illustrates an actual message exhibiting erroneous data due to multipath.

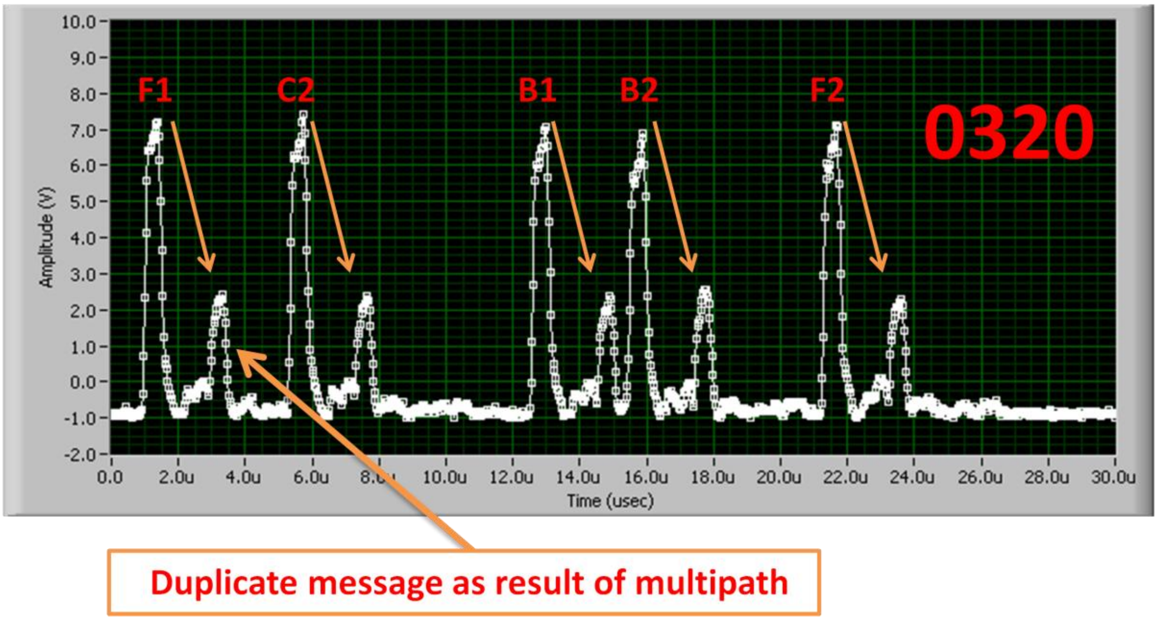

Figure 4. 16 - Interlaced messages due to 'echo' of multipath.

Fragmented messages are another source of erroneous data that the software must be capable of recognizing to protect the integrity of the multilateration data. The most common form of fragmenting occurs as a result of the rearming of the digitizer trigger occurring simultaneously with the presence of a transponder message being received by

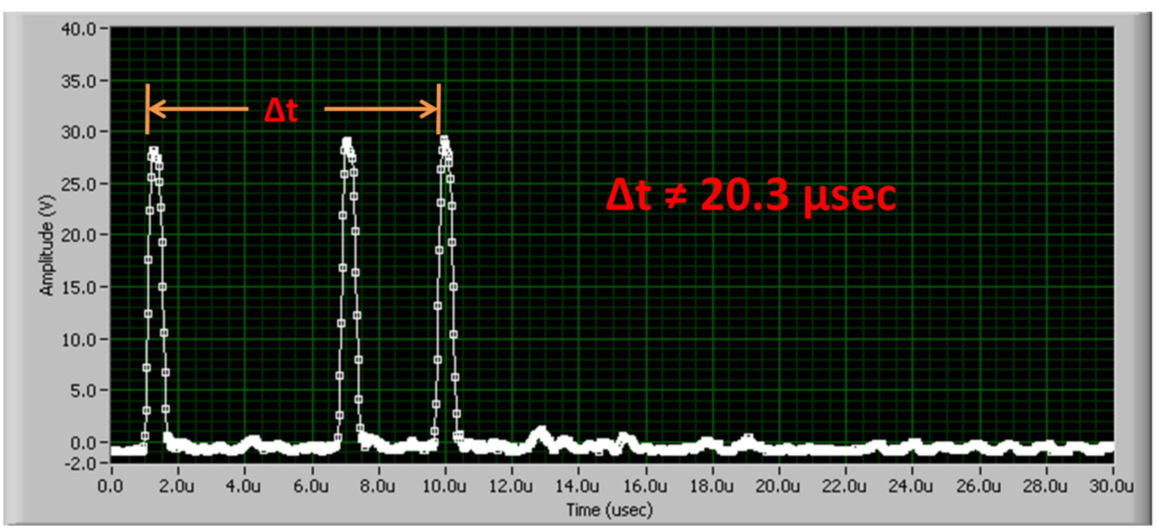

Figure 4. 17 - Fragmented message due to the trigger re-arming in the middle of a message broadcast.

the system. If a message partially finished at the moment that the trigger is rearmed, then the digitizer will immediately trigger on the first pulse it sees (in this case a pulse that is not the framing pulse). The software filter can discern this type of fragmented message by filtering on messages which are not of the proper length from the framing pulses F1 to F2 (Figure 4.17).

4.2.2.2 Group Delay System Calibration

Group delay is the measure of how long it takes a signal to traverse a network, also known as the transit time [20]. In the case of the RF sensor design, group delay would be the time, Δt, from the instance when the antenna is excited with electromagnetic energy to the time that the TTL output trigger from the digitizer appears at the input of the GPS event timer. In other words, the group delay is the time of transit for the signal to pass through the antenna, the cavity filter, the preamp, the downconverter and the digitizer. Since precise times of arrival measurements are key to the multilateration system accuracy, group delay must be a consideration for potential measurement error.

Any significant differences in group delay from one RF sensor to the next in the multilateration system network must be known so adjustments can be made to correct for the error caused by the inconsistencies from one sensor to the next. These differences, if known and consistent, can be canceled as part of a system level calibration. The actual group delay of each sensor is not the critical factor, instead the important calibration information resides in the *relative* difference in group delay among the individual sensors of the network.

The cause for inconsistencies in group delay from one sensor to the next is due to the non-ideal components that make up the system. Some of these non-ideal components include:

- Differences in cable lengths
- Variations in electronic components
- Cable impedance and insertion loss
- Digitizer triggering latency

In order to characterize the group delay associated with each individual sensor relative to the others, before deployment each sensor antenna was placed in a grid with the minimum possible spacing (4 feet square) for the purpose of performing a test which determines the relative differences in group delay among the sensors. A test was developed to measure the calibration offsets for each system relative to a baseline. Data was acquired for approximately one hour on each system in which Mode A/C signals were captured and timestamped in each sensor with the assumption that each antenna should receive the same RF signal. Since the systems were in the same location (insignificant separation for the purpose of the measurement being made) a network without group delay discrepancies would effectively have zero offsets with respect to a baseline system. This 'ideal' network of sensors would also have measurement precision bound by the event timer's specification for accuracy (in this case ± 30 nanoseconds). In reality each system did exhibit relative offsets with respect to the other systems.

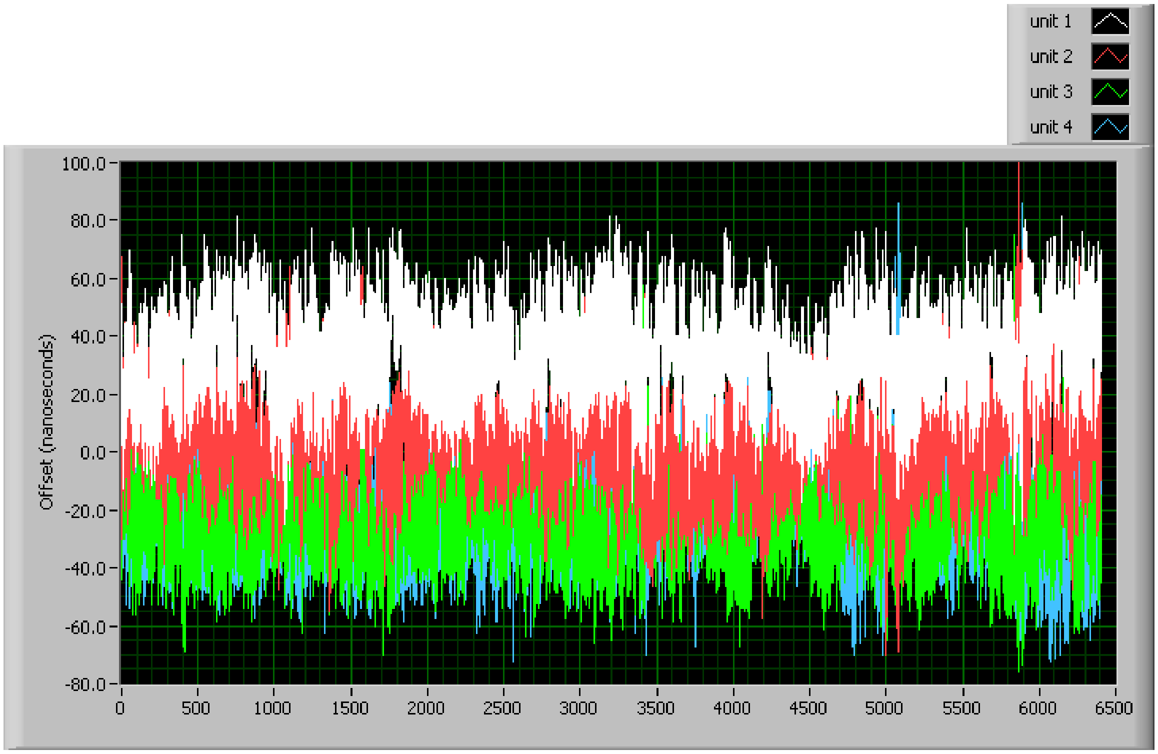

Figure 4. 18 - Relative offsets in group delay for all four units.

A graph illustrating the results is shown in Figure 4.18. The graph illustrates over 6000 measurements in which ‘simultaneous’ signals were received and timestamped. Each of the four sensors is represented by a unique color on the graph and compared to the baseline offset (in nanoseconds) relative to the other units. As these traces demonstrate, each sensor (unit 1, unit 2, unit 3 and unit 4) has a group delay that is biased over a large sample at consistent offsets relative to the other units. Also observed is the fact that the spread of measurement error is approximately 140 nanoseconds (+80 to -60). Ideally this measurement error without group delay effects would be 60 nanoseconds (the ± 30 nanoseconds measurement accuracy of the event timer).

These offsets were stored and built into the Central Processing software as calibration constants to be used as the final measurement adjustment before position

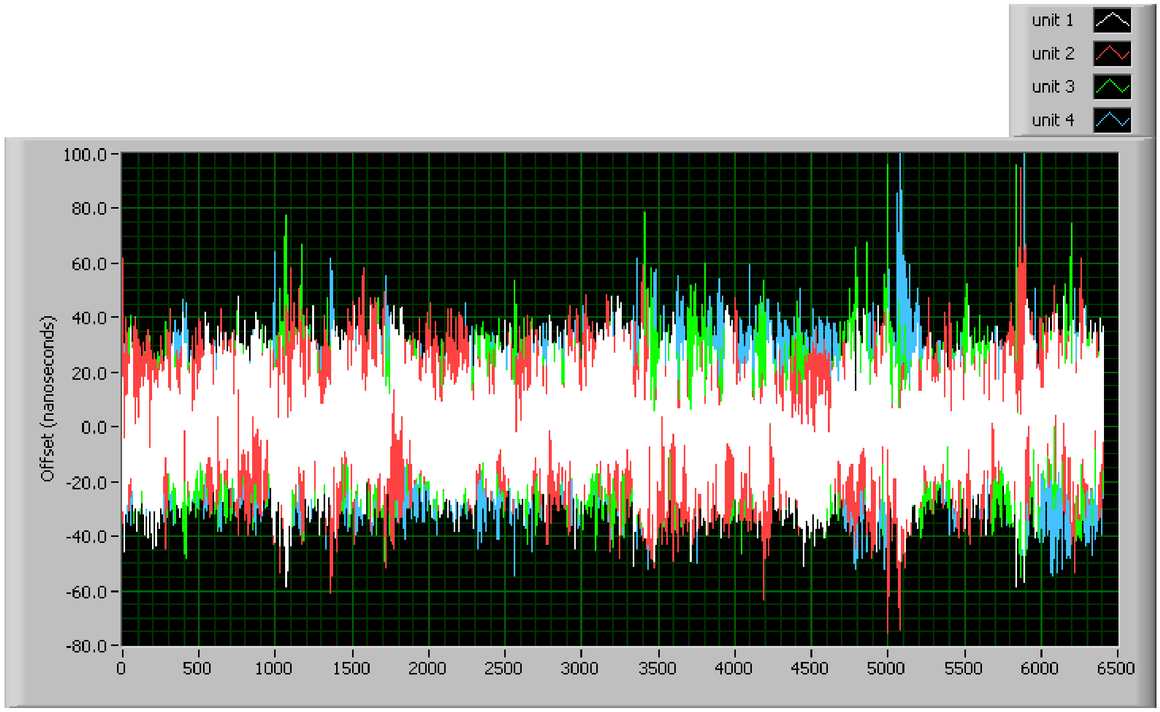

Figure 4. 19 - Calibrated group delay results (bias removed from each unit).

solution calculations were made. Figure 4.19 illustrates the effectiveness of the group delay calibration as the measurement resolution is reduced to ± 40 nanoseconds (improvement of nearly 2X).

4.3 Central Processing Station

The Central Processing Station is responsible for compiling data from each sensor and computing position solution estimates based on the time of arrival measurements and Mode A/C messages received at each sensor in the multilateration network. As discussed earlier, for the purpose of this proof of concept research, all position solution calculations are post-processed rather than being processed real-time. This does not alter the results in any way, but it does slightly alter the data reduction and correlation algorithms.

Critical to success for this research proof of concept is the development of algorithms capable of combating the weakness that exist in current implementations of multilateration systems.

One of the most significant weaknesses, and hence one of the biggest reasons for continued research in the area of multilateration system technology, is due to the singularities that exist within the geographical boundaries of the network of sensors. These singularities are the result of mathematical divergences that exist due to the sensitivity of the exact solution equations' sensitivity to measurement error. A unique solution to this problem will be presented in section 4.3.2 as a new approach to position calculation limits the effects of measurement error.

4.3.1 Data Reduction and Cross Correlation

Data packets from the RF sensors are formatted with squawk and timestamp for each trigger that was issued to the GPS-based event timer during the hours of operation. Cross correlation of this data across each of the four units produces the actual data that is used for position calculations. Each data packet has the following format:

Squawk : Day : Hour : Minute : Second : Nanosecond

The primary task for data reduction and correlation is to correlate data from each unit for the purpose of finding a squawk/timestamp match in *all units* that fits the criteria for being a valid time of arrival that can be used to compute a position solution. The criteria used for this correlation is that all four units have a squawk/timestamp match in which the time difference of arrival (TDOA) maximum among all four units is less than the maximum travel time for an RF signal to travel the maximum separation distance of any two sensors. This ensures that the same signal was received at each station from the same transponder, hence qualifying for a position solution to be calculated. This maximum RF signal travel time between any two sensors can be computed using the relationship between speed and distance. In this case it would be:

$$\boldsymbol{max\ TDOA < (max\ distance\ between\ any\ 2\ sensors) \div speed\ of\ light}$$

This reduction is performed only after the 'group delay calibration constants' have been subtracted from the timestamps from each sensor. This calibration step improves the overall quality of the measurement as described in section 3.2.2.2.

A set of valid TDOA's that meets the criteria for maximum allowable TDOA can be seen in the highlighted rows from each sensor in Figure 4.20. Once data from each

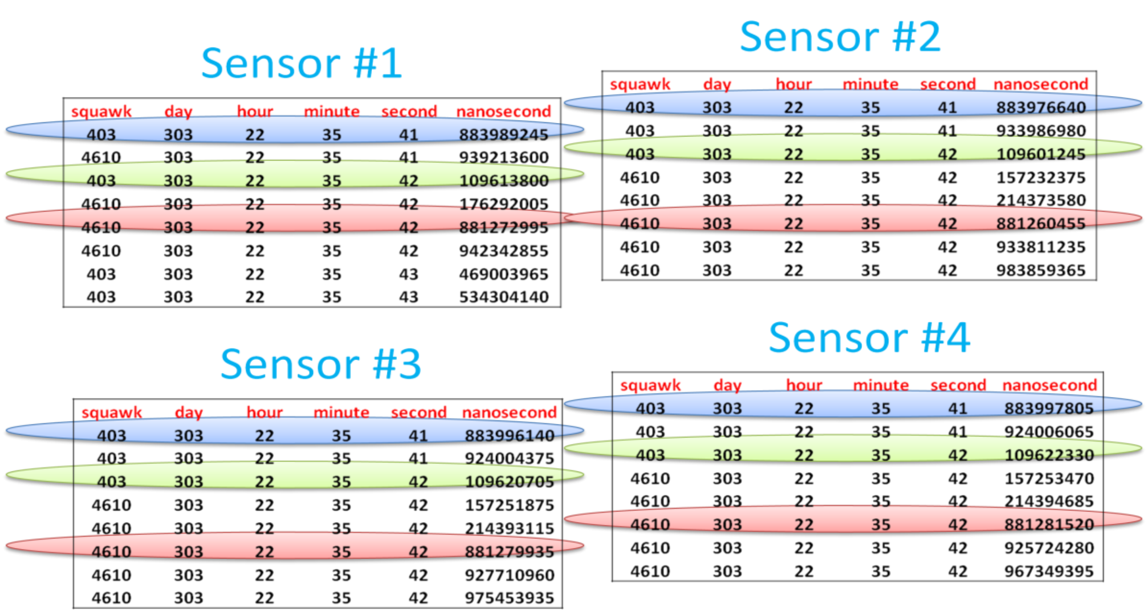

Sensor #1

squawk	day	hour	minute	second	nanosecond
403	303	22	35	41	883989245
4610	303	22	35	41	939213600
403	303	22	35	42	109613800
4610	303	22	35	42	176292005
4610	303	22	35	42	881272995
4610	303	22	35	42	942342855
403	303	22	35	43	469003965
403	303	22	35	43	534304140

Sensor #2

squawk	day	hour	minute	second	nanosecond
403	303	22	35	41	883976640
403	303	22	35	41	933986980
403	303	22	35	42	109601245
4610	303	22	35	42	157232375
4610	303	22	35	42	214373580
4610	303	22	35	42	881260455
4610	303	22	35	42	933811235
4610	303	22	35	42	983859365

Sensor #3

squawk	day	hour	minute	second	nanosecond
403	303	22	35	41	883996140
403	303	22	35	41	924004375
403	303	22	35	42	109620705
4610	303	22	35	42	157251875
4610	303	22	35	42	214393115
4610	303	22	35	42	881279935
4610	303	22	35	42	927710960
4610	303	22	35	42	975453935

Sensor #4

squawk	day	hour	minute	second	nanosecond
403	303	22	35	41	883997805
403	303	22	35	41	924006065
403	303	22	35	42	109622330
4610	303	22	35	42	157253470
4610	303	22	35	42	214394685
4610	303	22	35	42	881281520
4610	303	22	35	42	925724280
4610	303	22	35	42	967349395

Figure 4. 20 - Cross Correlation of each unit for common squawks and TDOA's.

sensor has been correlated with every other sensor and all data has been filtered except for those squawk/timestamp pairs which meet the above specified criteria, the data is ready for export to the solution equations for position calculation.

4.3.2 Position Calculation

The solution equations for calculating the aircraft position estimate were given in section 3.2. The inputs to these equations are in terms of R_{ij}, R_{ik}, R_{kj}, and R_{kl} which can be computed with the measured values for $TDOA_{ij}$, $TDOA_{ik}$, $TDOA_{kj}$ & $TDOA_{kl}$ as described in chapter 3. After the data reduction/correlation step is completed as explained in the previous section, these variables are known for each instance in which a transponder signal was received at each sensor. Since the units of time in the equation are in nanoseconds, the following substitutions will plug directly into the solution equations:

$$\boldsymbol{TDOA_{ij} = t_i - t_j} \tag{4.1}$$

where t_i is the calibration adjusted nanosecond value from the time of arrival measurement at the sensor located at position *i*. Likewise,

$$\boldsymbol{TDOA_{ik} = t_i - t_k} \tag{4.2}$$

$$\boldsymbol{TDOA_{kj} = t_k - t_j} \tag{4.3}$$

$$\boldsymbol{TDOA_{kl} = t_k - t_l} \tag{4.4}$$

The solution equations assume a geometrical configuration of sensors in which locations *i, j, k & l* are assigned to the four positions of the sensors in the multilateration network. This fixed geometry causes limitations on the system's overall accuracy at certain locations within the network in which singularities exist due mathematical divergences.

The exact solution equations being used to determine the aircraft positions are sensitive to the geographical assignments of the sensor positions *i, j, k & l* and their positions relative to the location of a given aircraft. Depending on the location of the aircraft, the assignments of sensor location may or may not be optimal for the solution equations to compute a solution that is not mathematically divergent. The most common contributor to divergence is when one of the terms of the equation experiences a denominator that approaches zero. As this mathematical divergence is being approached, the solution equation's sensitivity to measurement error is exaggerated, hence rendering its solution to be proned to unacceptable error. A new algorithm which combats these singularities will be presented in the following section. This new methodology implements a software-based variable geometry which acts as an adaptive filter to rid the multilateration system of these singularities.

4.3.2.1 Rotational Geometry

The concept of a *rotational geometry* of sensor locations is applied in order to overcome erroneous position calculations caused by mathematical divergences in the solution equations. These mathematical divergences will be filtered out by rotating the geometry of the *i, j, k & l* sensor locations in the software solution algorithm through twelve separate iterations for each position solution that is sought. This includes four major shifts as shown in Figure 4.21 and three secondary shifts at each major shift as

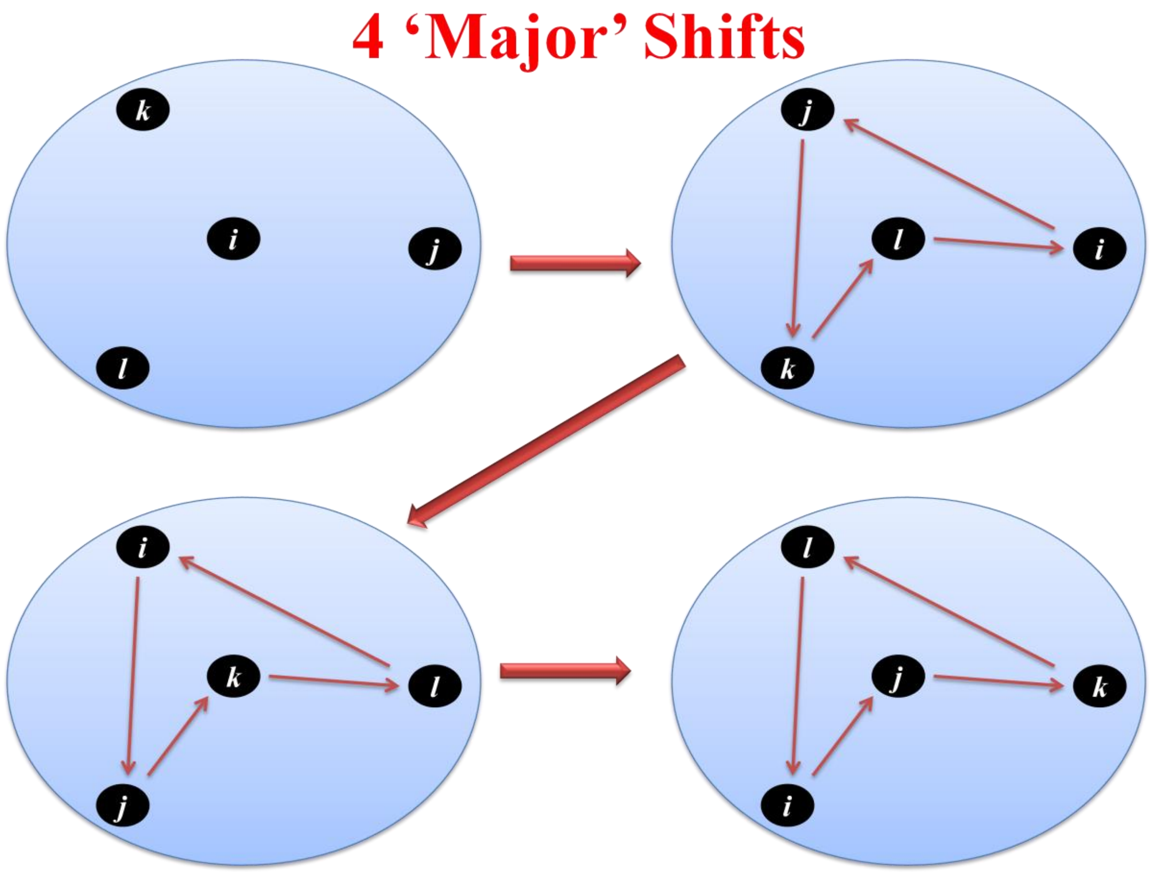

Figure 4. 21 - Four major shifts in the rotational gemoetry.

illustrated in Figure 4.22. The secondary shifts in Figure 4.22 illustrates the secondary shifts that are associated with the center sensor designation as the *'i'* location.

Although the position of each sensor relative to the location of the aircraft is actually fixed, its position relative to the solution equations is variable. In other words, each sensor's position relative to the solution equation can be one of four possible positions (i, *j, k or l*). The rotational geometry algorithm shifts the assignments of the sensor locations *i, j, k and l* through the twelve iterations and looks for common solutions among the results. Only when a minimum number of matches are found, will a solution be considered a valid aircraft position.

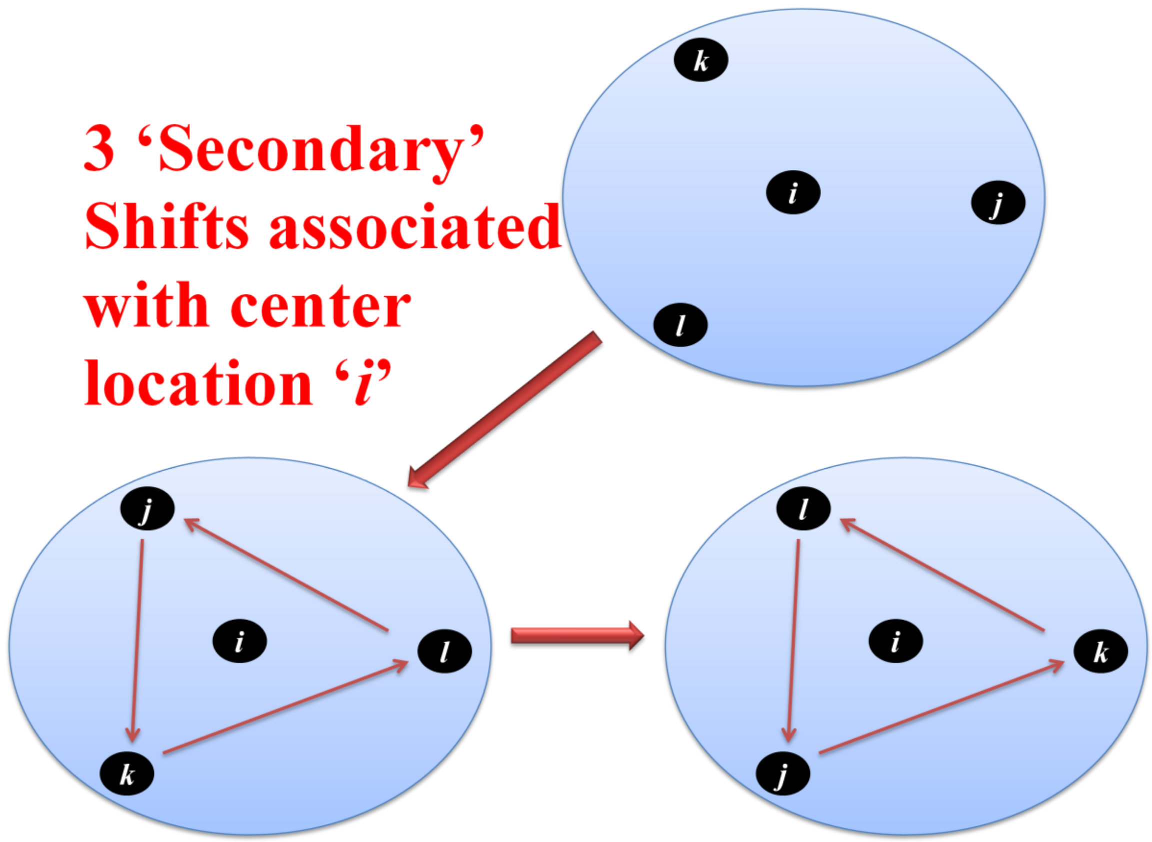

Figure 4. 22 - Three secondary shifts (rotations around center sensor).

This new rotational geometry algorithm will not allow a divergent solution to be produced as it requires four matching solutions out of the twelve rotational shifts. Only when at least four solutions are calculated whose results are separated by less than one meter each, will a solution be considered a valid one. This adaptive filter algorithm is capable of identifying and filtering non-optimal geometry for the locations of the sensors relative to the aircraft position even though the aircraft position is unknown. This does not affect the integrity of the mathematical computation as the solution is an exact solution which is valid for all sensor location assignments (given ideal conditions for measuring the absolute time of arrival). Instead, it isolates the geometries that have the poorest performance due to measurement error at certain aircraft locations and rejects their solution calculations. It rejects the solutions based on sensor assignments to locations which cannot tolerate the system measurement error of ±40 nanoseconds.

4.4 Sensor Network Geometry

In order to realize the benefits of the optimal geometry, an effort was made to implement a sensor geometry with as much correlation as possible to the centered equilateral triangle discussed in Chapter 3.

Four locations were identified as locations which fit the following criteria:

1. Positioned at a location whose coordinates relative to the other sensors is consistent with the optimal geometry previously discussed
2. Located at a place of business or residence with adequate space inside and outside to house the antenna, the antenna mounting fixture and the instrumentation (flat rooftop with inside access and available power for the instrumentation including access point for cables)
3. Location which provides reasonable line of sight to the Max Westheimer Airport airspace.
4. Located at a place of business or residence in which ownership/management are willing to cooperate and allow the installation of the equipment.

Four establishments were identified as the locations for the sensor network which provides geometry very similar to the centered equilateral triangle mentioned earlier. In realization, the network of sensors that were installed represents a centered triangle in which the range from the center to the vertices average approximately 2.5 miles. Adequate line of site was realized with roof-mounted installations in which each antenna was over 30 feet above ground level.

The University of Oklahoma North Base Campus Research Park at Max Westheimer airport in Norman, Oklahoma was the location chosen as the site for initial phase of research and development. This location (referred to as 'North Base'), which serves as the center point of the triangular geometry is located adjacent the main runway of the airport at the research park. This location will be referred to as the North Base sensor.

Sensor Location	ECEF Coordinates	ENU Coordinates (origin at North Base sensor)
North Base	X = -677730.7 m Y= -5171019.5 m X= 3660053.5 m	East = 0 m North = 0 m Up = 0 m
Rec Center	X = -673796.0 m Y = -5171741.4 m Z = 3659779.5 m	East = 3995.1 m North = -341.8 m Up = 8.8 m
Press	X = -679171.4 m Y = -5169174.4 m Z = 3662397.1 m	East = -1569.2 m North = 2869.2 m Up = .49 m
Borders	X = -680075.8 m Y = -5172436.7 m Z = 3657620 m	East = -2141.1 m North = -2974.2 m Up = -7.7 m

Table 4. 1 - Table of sensor locations with ECEF origin at the center of the earth. ENU coordinates origin is at North Base sensor.

The sensor located to the east of the North Base sensor was installed on top of the 12th Avenue Recreational Center at 1701 12th Avenue, NE. Its range to the North Base sensor is 2.5 miles and will be referenced as the 'Rec Center' sensor.

To the north and slightly west of the North Base sensor a sensor was installed on top of the University of Oklahoma Press Distribution Center at 2800 Ventura Dr. Its range to the North Base sensor is 2.0 miles and will be referenced as the 'Press' sensor.

To the south and west of the North Base location a sensor was installed on top of the Borders Bookstore at 300 Norman Center Ct. Its range to the North Base sensor is 2.3

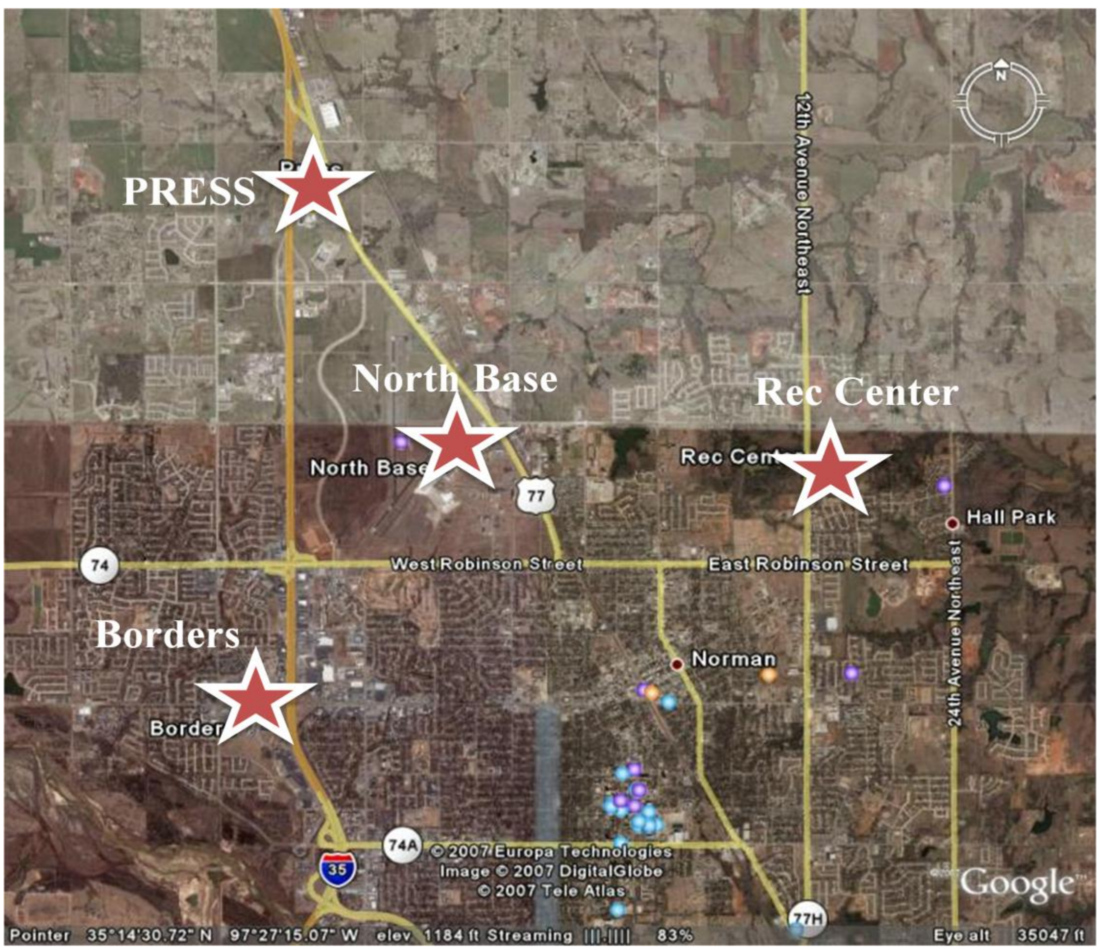

Figure 4. 23 - Aerial view of sensor network in relation to Norman, Ok.

miles and will be referenced as the ‘Borders’ sensor.

A table displaying each of the sensor locations along with their ECEF coordinates is located in Table 4.1. Also shown in this figure are the coordinates of each sensor expressed in terms of the ENU coordinate system.

A graphical representation of the layout is illustrated in Figure 4.24. This is an aerial map of the north side of Norman, Oklahoma with ‘North Base’ sensor located in the center of the equilateral triangle geometry.

4.4.1 GDOP Analysis of Sensor Network

The ideal geometry is obviously not achievable due to limitations of having access to the proper locations. Table 4.1 represents the locations for sensor installation

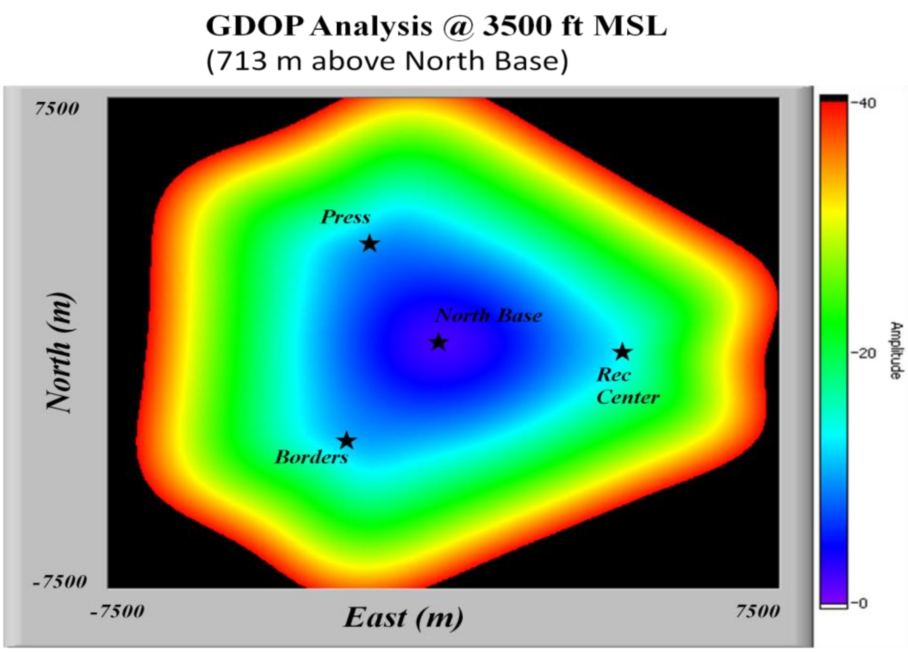

Figure 4. 24 - GDOP analysis of sensor network at 3500 ft MSL.

that best fit our needs based on availability. In order to visualize the expected effectiveness of the actual sensor locations that were chosen, the method of GDOP calculations presented in Chapter 3 were implemented. The GDOP analysis of the selected locations for the sensor network was performed at the two altitudes associated with the truth flight patterns that were going to be flown. Making altitude constant and calculating GDOP magnitude at each point on a grid around the geometry at constant altitude produces an array of data that can be visualized in the form of an intensity chart. These two constant altitudes included 3500 ft MSL (Mean Sea Level) and 5500 ft MSL. Figures 4.24 and 4.25 show the results of the test. These figures represent a GDOP profile based on a 1000 x 1000 element array implementation of Equation 3.32 at constant altitude. The GDOP map is a grid that consists of fifteen meter spacing between each element in the North and East direction.

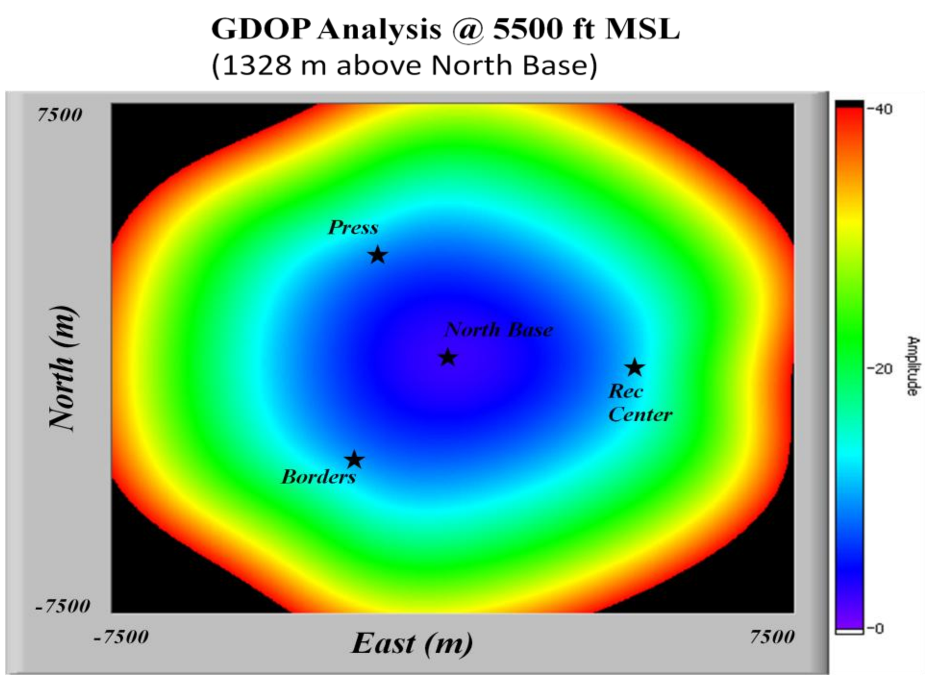

Figure 4. 25 - GDOP analysis for sensor network at 5500 ft MSL.

This visualization proves that the geometric configuration provides good GDOP results within the geometry with degradation beginning at the boundaries and getting progressively worse as you move away from the network of sensors. The multilateration system based on the geometry analyzed in Figure 4.24 and 4.25 should produce the desired results within the triangular geometry.

CHAPTER 5

Experimental Results

5.1 Experimental Objective

For the purposes of model validation of the proof of concept, truth flights were flown in areas inside and outside of the triangular geometry to log GPS-based truth data. This flight recorded data was used to compare the actual position of the aircraft to the multilateration system's estimation. The system used for acquisition of truth data was an Ashtec Z-Xtreme which has time/position accuracy of 0.20 meters and 0.001 seconds. The truth missions were flown while each of the four sensors logged Mode A/C squawks along with precise time of arrival data for the purpose of post-processing position solutions. The goal for the analysis of the data was to provide two-dimensional and three-dimensional ranging error calculations which compare the actual aircraft position to the multilateration system's solution estimation of position. This analysis provides the necessary data to determine the effectiveness of the multilateration system by quantifying error at locations both inside and outside of the multilateration sensor geometry.

5.2 Experimental Configuration

Each sensor was set for operation with a 300.0 mV trigger. This setting was chosen because it is the least sensitive setting possible which will ensure that each sensor has the range to capture the Mode A/C transmissions at a range of 6 to 7 miles (the maximum range needed for each sensor to be capable of capturing all transmissions from the planned truth flight route). The least sensitive trigger level that is still capable of capturing all transmissions is the optimal setting to eliminate false triggers due to RF noise, and it also helps eliminate the triggering of the sensor due to aircraft beyond the region of interest for the test.

After calibration of each sensor was performed using the group delay calibration methodology described in Chapter 4, each sensor was deployed to their locations in the centered triangle configuration around the Max Westheimer Airport. Each sensor was surveyed in for their exact ECEF and ENU coordinates (Figure 4.23).

For the purpose of logging data from the truth flights each sensor was configured to collect and store all squawk and timestamp data during the given window of operation for the truth flight. The data was stored locally on the hard drives of the sensors in correlated pairs (squawk/timestamp) in file sizes of 5000 data points (pairs) each. The units were configured to immediately begin new data files upon the completion of each file to guarantee continuous data collection throughout the duration of the test across the entire multilateration network.

Each truth mission was flown in the late evening for the purpose of maximizing the collection of valid squawks due to decreased traffic in the airspace being monitored. An optimal test for the system would be one in which the aircraft flying truth flights was the only one in the air within range of each sensor in the network. This is obviously not achievable due to the proximity of the Max Westheimer airport and the presence of several major traffic patterns nearby including Will Rogers International Airport and Tinker Air Force Base.

In order to have an absolute reference to a known target, the pilot flying the truth missions would climb to altitude and get assigned an IDENT distinguishing his airplane from any other planes in the controlled airspace surrounding the Max Westheimer airport. This allows for 100% confidence on correlation with IDENT squawks which is the necessary data to calculate multilateration error. Mode C altitude squawks can be used as well, but there is no way to guarantee that an altitude squawk is being transmitted by the plane flying the truth data as other planes at the same altitude could conceivably be transmitting the same message without any way to discern the difference between the truth plane and others.

The flight plan consisted of flight patterns which traversed the multilateration network geometry multiple times from multiple directions. Regular ‘left pattern’ and ‘right pattern’ traffic for touch-n-go’s on the main runway (taking off to the northeast) fit the desired tracks of interest because these patterns had multiple passes into and out of the triangular geometry. In order to provide continuous signal to all sensors, the pilot did not conduct touch-n-go’s, instead choosing to stay at altitude in the touch-n-go pattern (line of sight is lost on the corner sensors below 200 ft). Multiple passes were also flown in patterns well outside of the geometry to explore the degradation of accuracy experienced outside of the network.

Specifically, the flight data that was recorded include the following sequence of patterns:

1. Climb to altitude of approximately 3500 MSL
2. 1 left inside traffic pattern (counter-clockwise)
3. 1 left outside traffic pattern (counter-clockwise)
4. 1 right inside traffic pattern (clockwise)
5. 1 right outside traffic pattern (clockwise)
6. Traverse the triangle, climb to 2nd altitude 5500 MSL
7. Complete counterclockwise square pattern significantly outside of the triangular geometry.

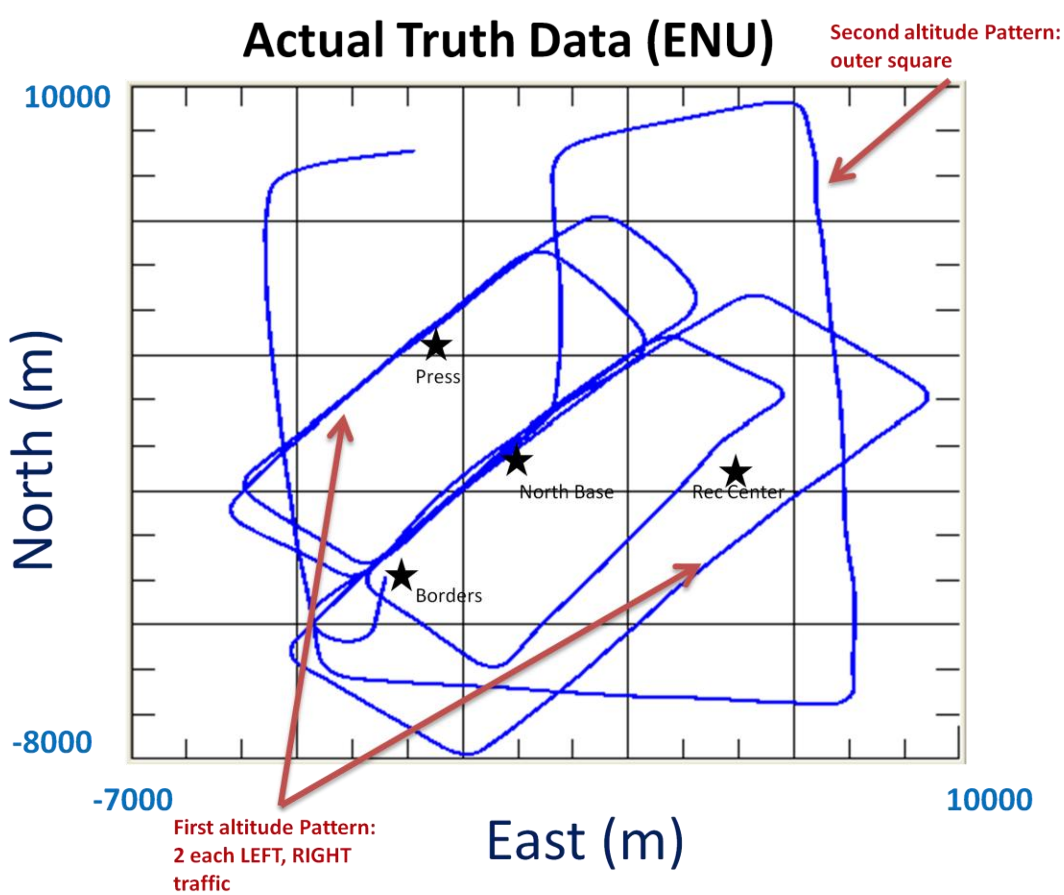

Figure 5. 1 - Complete truth flight path. Data taken from the Ashtec datalogger at .2 Hz sampling rate.

Figure 5.1 is the two-dimensional view (East-North plane) of the truth mission flight path. Left traffic patterns were flown in counter-clockwise direction, while right traffic patterns were flown clockwise. The outer square was flown in the counter-clockwise direction also.

Figure 5.2 is an illustration of the truth data with altitude perspective. This is a view looking from south to north, and the two distinct patterns at different altitudes are easily discernible. The first altitude is approximately 3500 ft MSL and the second in which the outer square loop is flown is at 5500 ft MSL.

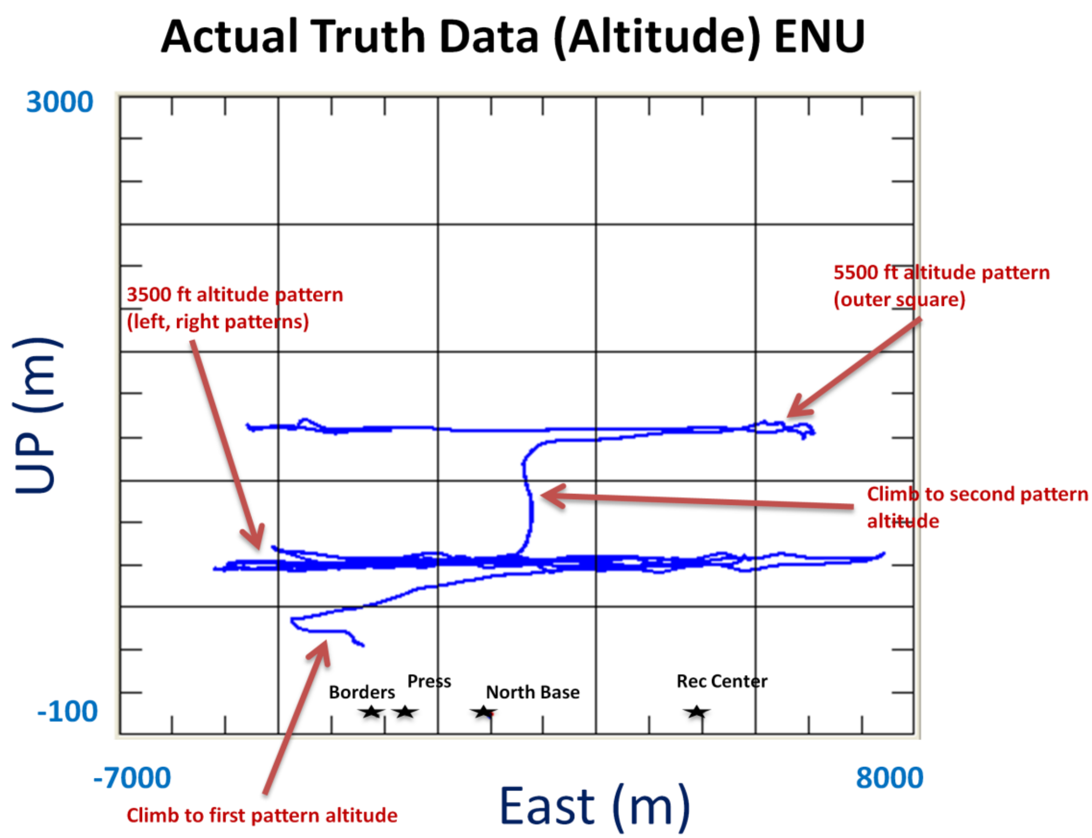

Figure 5. 2 - Truth flight path elevation view looking from south to north.

5.3 Experimental Results

The analysis of the test results produced data that validated the model of the multilateration system. Error profiles were correlated very closely with the theoretical expectations obtained from the GDOP analysis that was performed in Chapter 4.

The software-based rotational geometry and adaptive filter implemented the model successfully. It eliminated singularities that existed prior to the geometrical shifts that were executed in the new algorithms. The reader will see by looking at only the four major shifts that many mathematical divergences exist inside the geometric configuration. They are not only extreme, but also very repeatable.

The next eight figures represent the error analysis of the four major software shifts (without the three secondary shifts at each major shift). Both the elevation figures (3-dimensional) and the East-North figures (2-dimensional) are comparisons between the multilateration position estimates and the truth data. Elevation figures are accompanied by their three-dimensional error analysis. The East-North figures are accompanied by their appropriate two-dimensional error analysis.

The presence of the singularities without the rotational filter applied is obvious both in two and three dimensions. In each of the four major shifts, the reader can see that although there are segments of the flight where the multilateration system has a valid track, the divergences (both in 2-dimensions and 3-dimensions) are severe with error values changing from less than 20 meters to well over 30,000 meters in a matter of seconds.

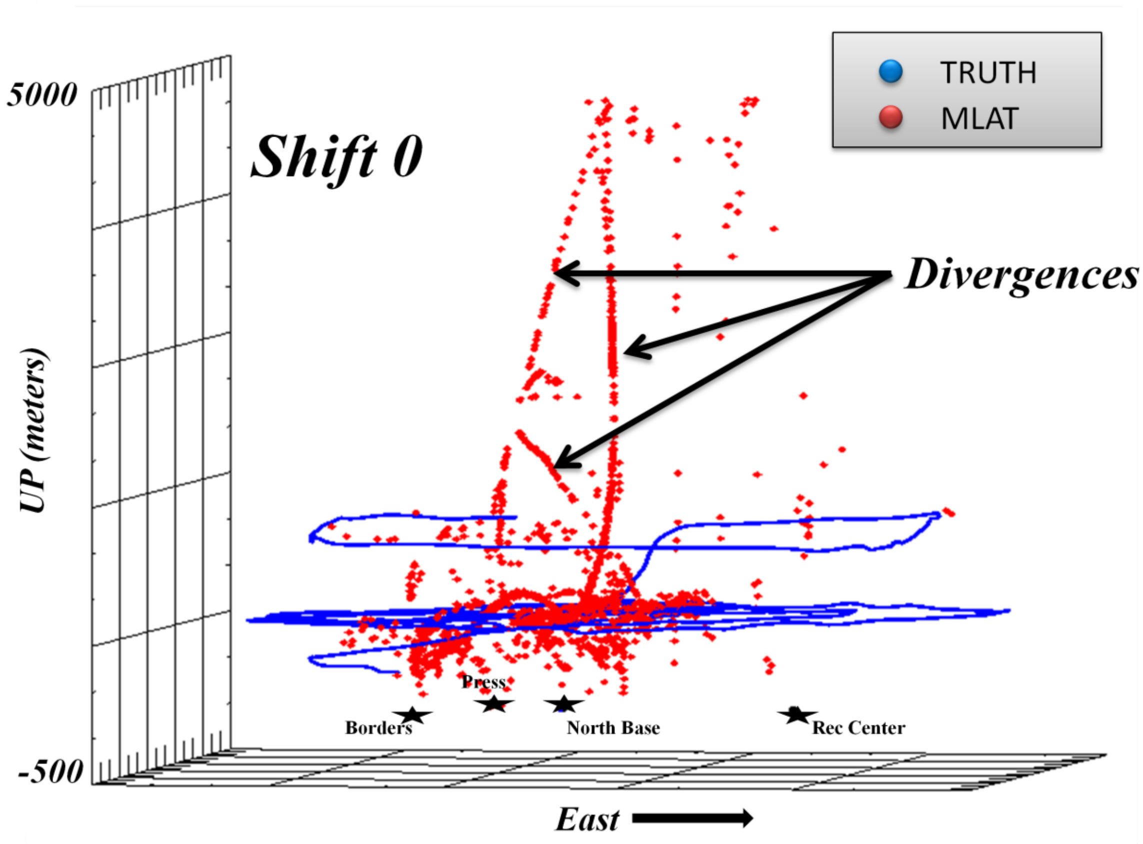

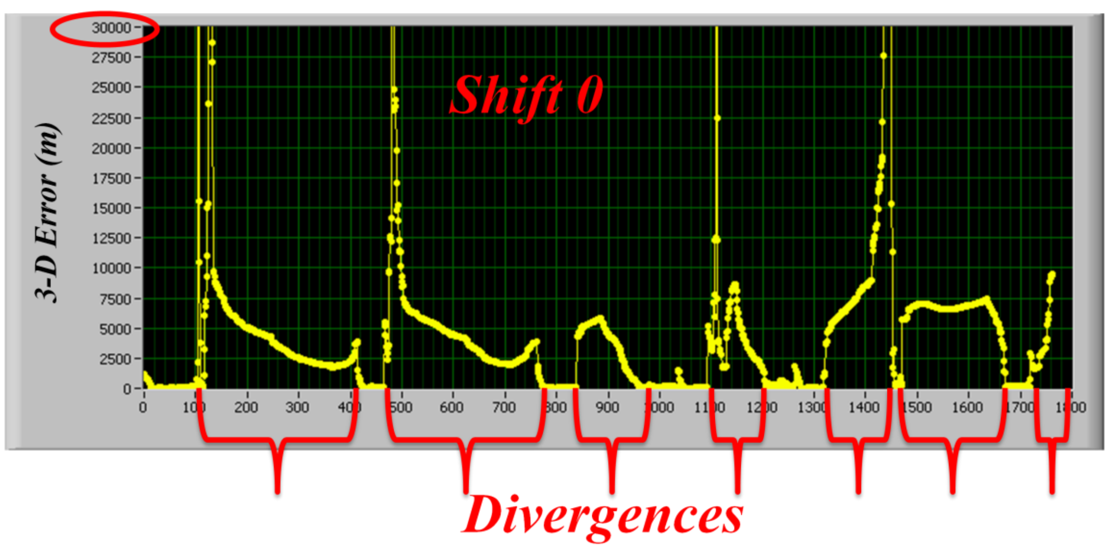

Figure 5. 3 - Shift 0 elevation view of MLAT vs. truth data (top). 3-D error analysis showing divergences (bottom).

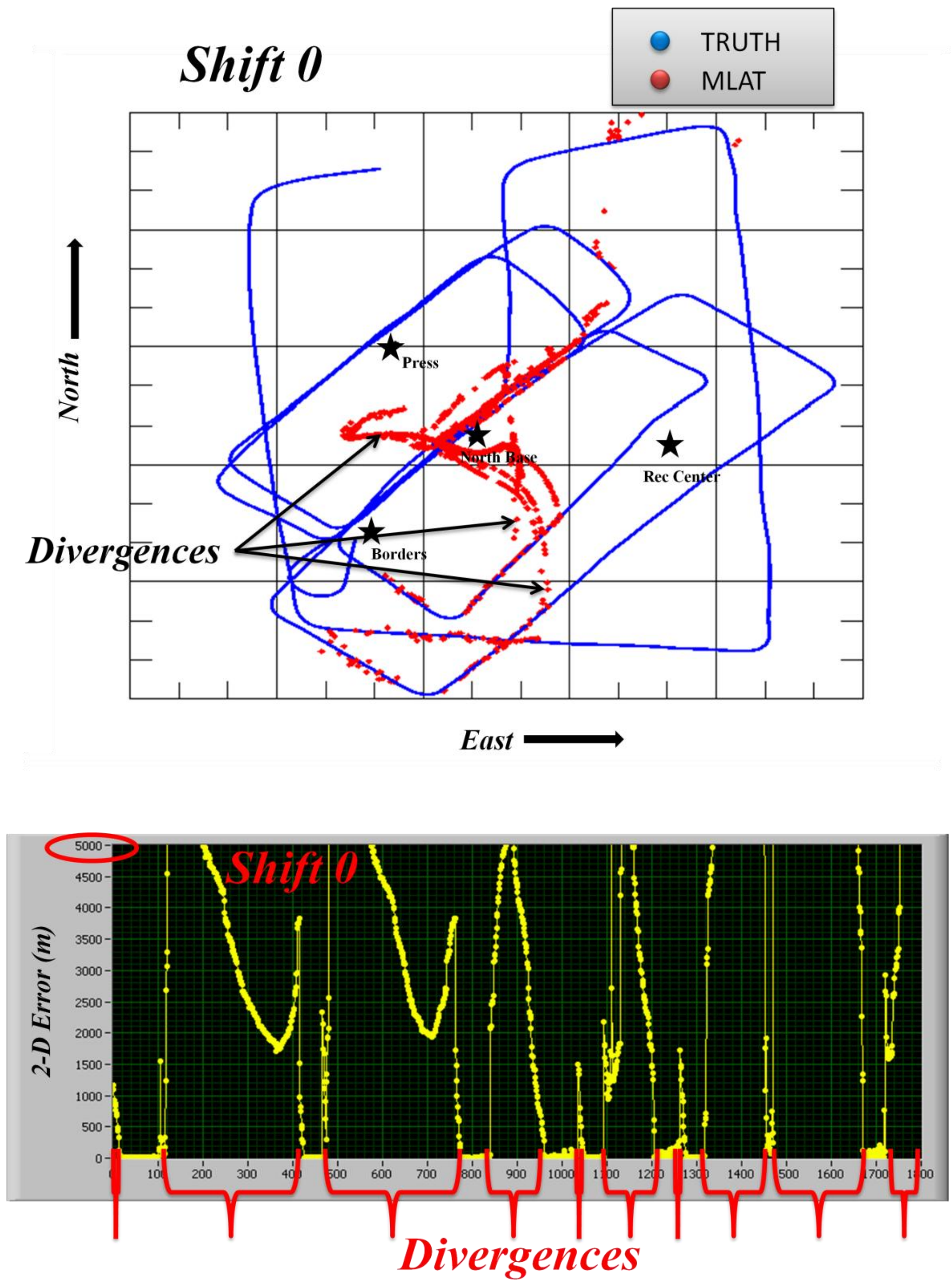

Figure 5. 4 - Shift 0 East-North view of MLAT vs. truth data (top). 2-D error analysis showing divergences (bottom).

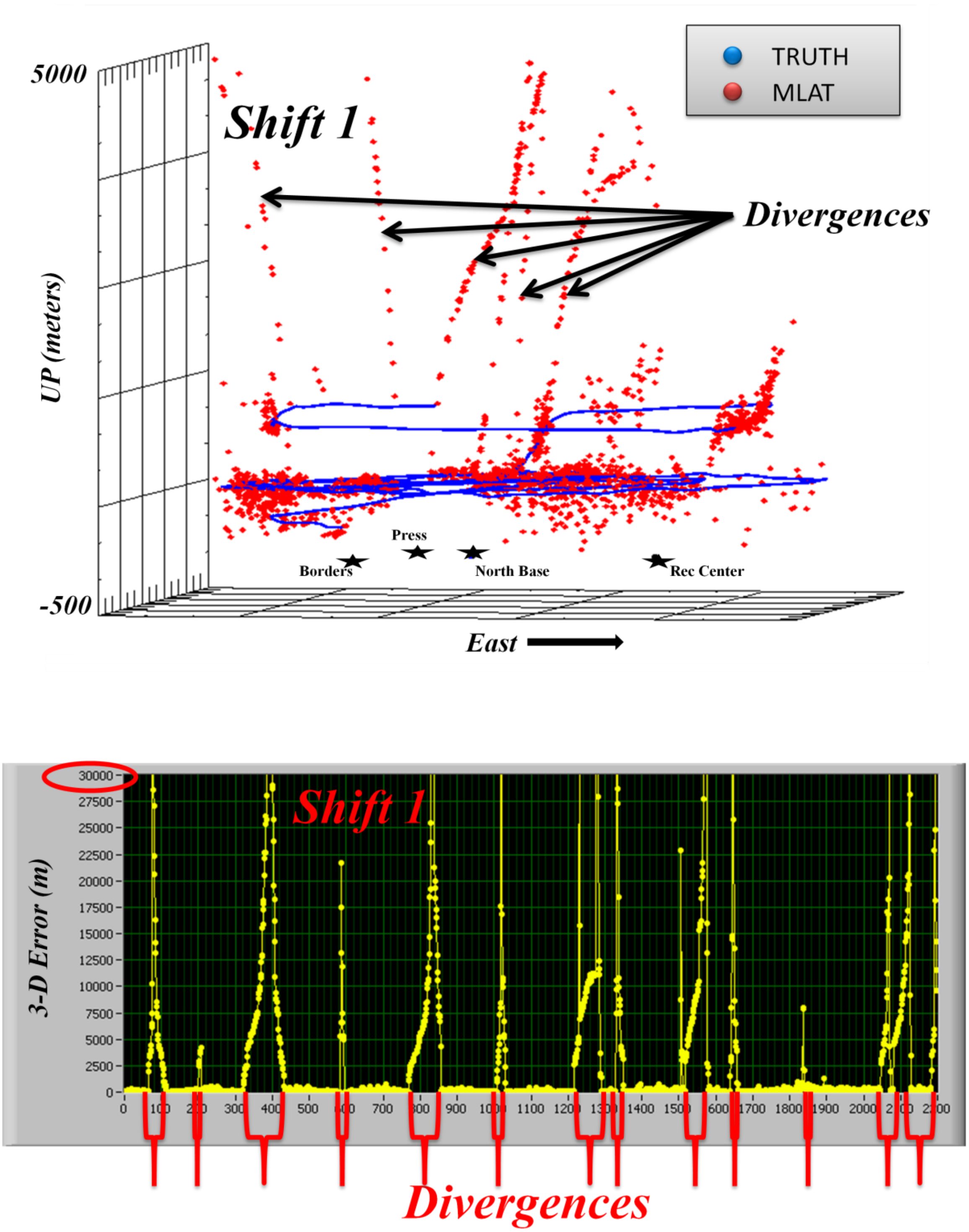

Figure 5. 5 - Shift 1 elevation view of MLAT vs. truth data (top). 3-D error analysis (bottom).

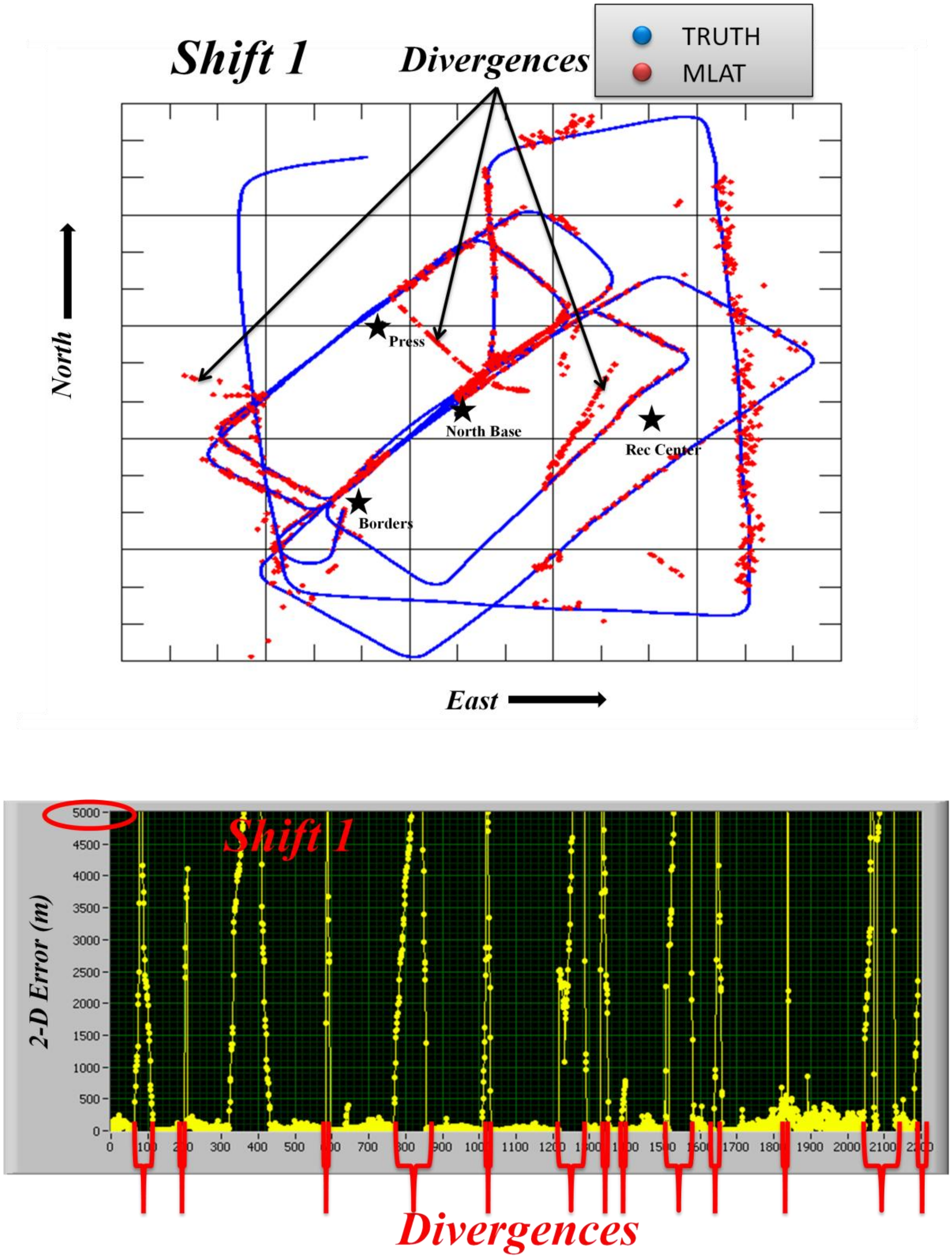

Figure 5. 6 - Shift 1 East-North view of MLAT vs. truth data (top). 2-D error analysis (bottom).

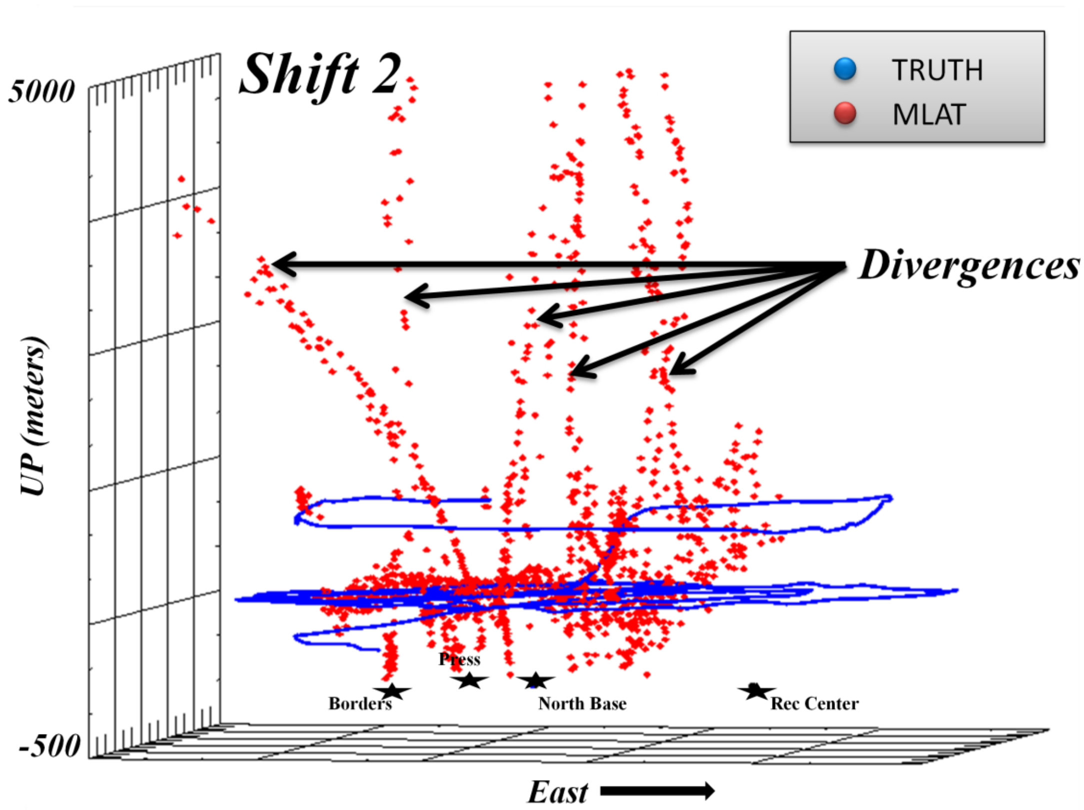

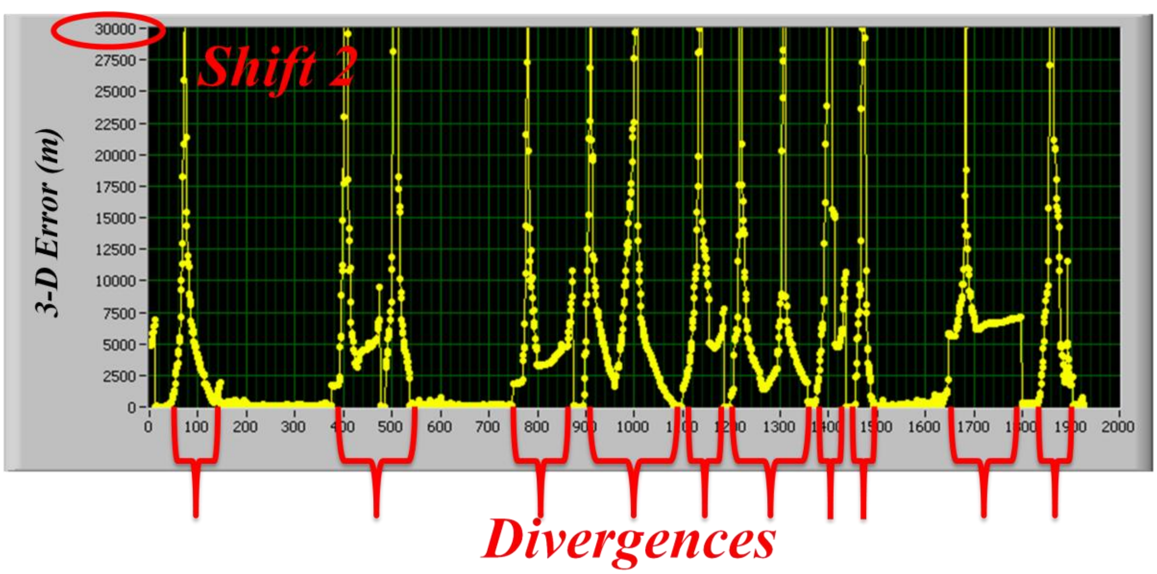

Figure 5. 7 - Shift 2 elevation view of MLAT vs. truth data (top). 3-D error analysis (bottom).

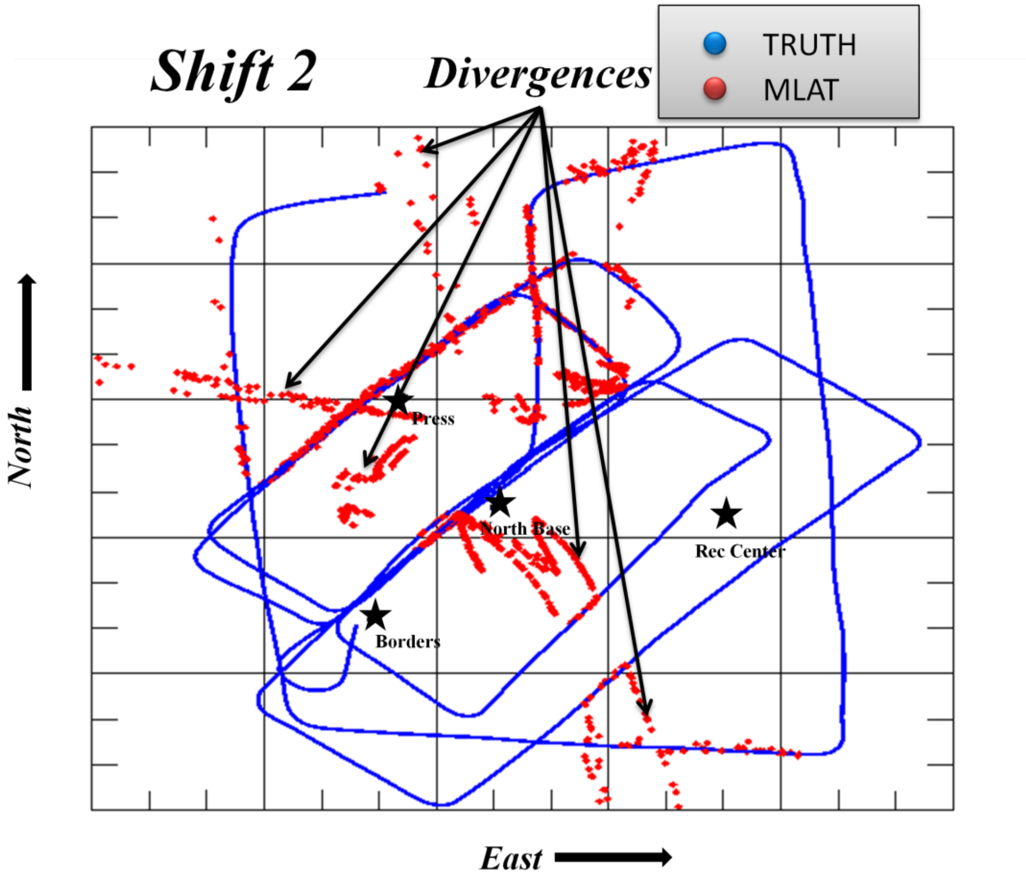

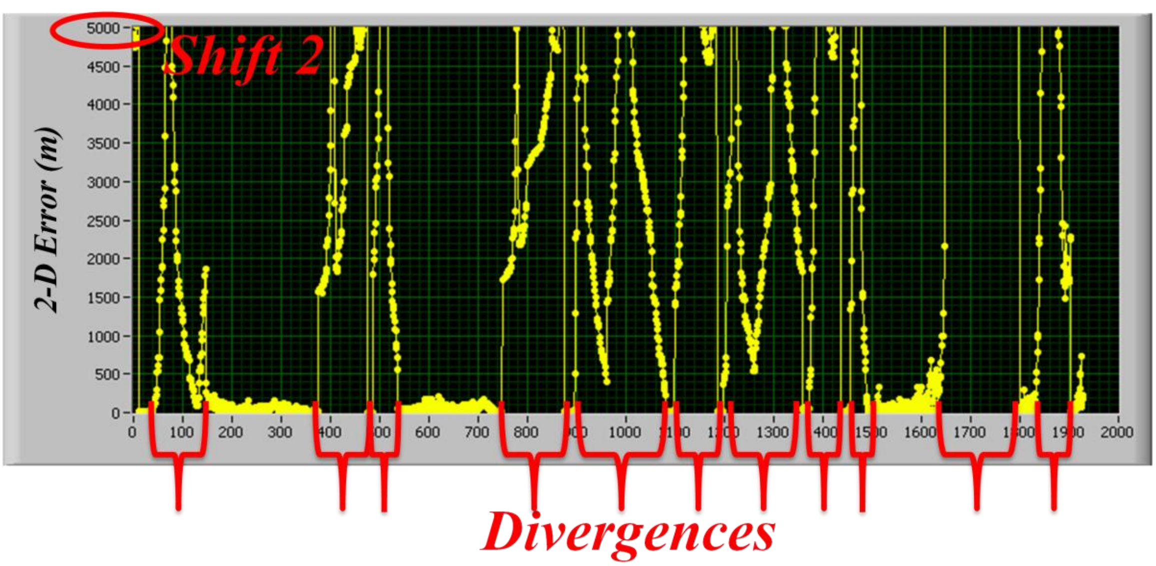

Figure 5. 8 - Shift 2 East-North view of MLAT vs. truth data (top). 2-D error analysis (bottom).

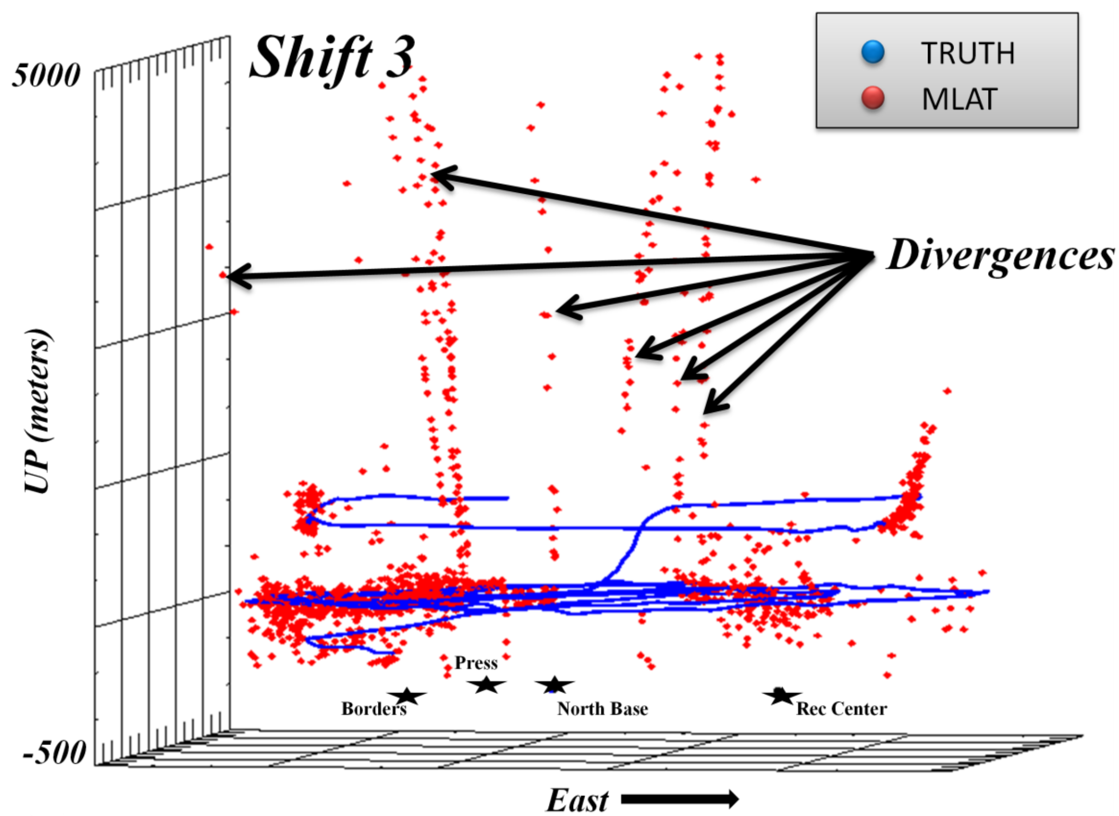

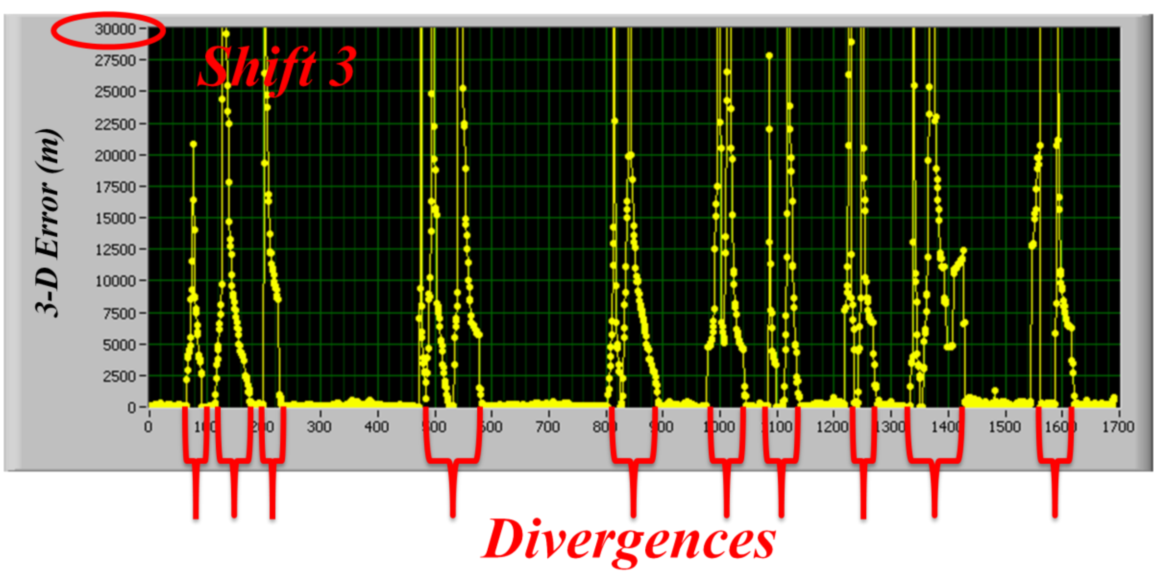

Figure 5. 9 - Shift 3 elevation view of MLAT vs. truth data (top). 3-D error analysis (bottom).

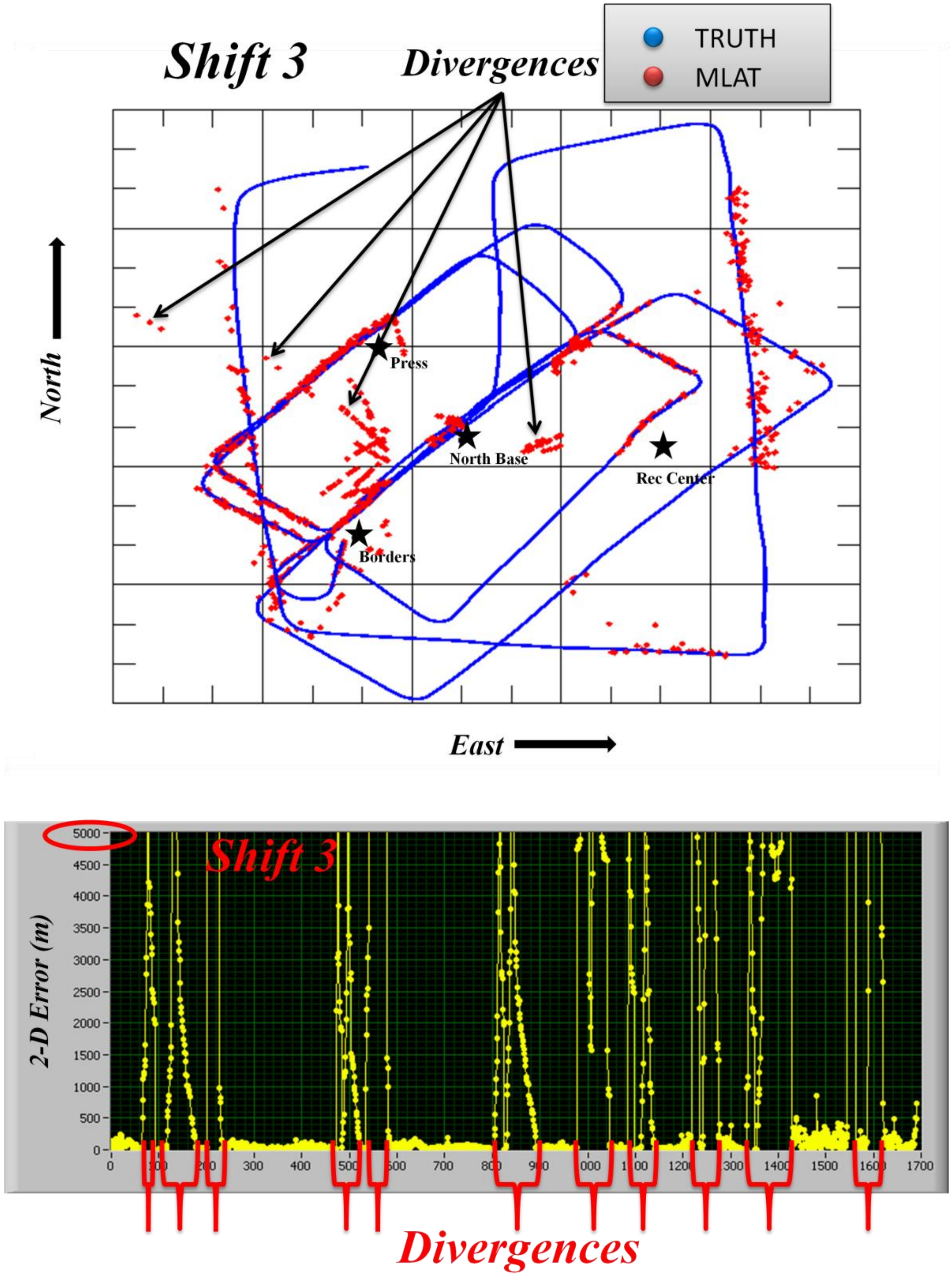

Figure 5. 10 - Shift 3 East-North view of MLAT vs. truth data (top). 2-D error analysis (bottom).

Figure 5.3 thru Figure 5.10 illustrate that the solution calculations are in fact susceptible to the singularities that exist within the geographical coverage area of the multilateration system. Each shift produces a different geometry with which the computations are made to find the position of the aircraft. Notice in equation 3.9 through equation 3.12 the formulas used in the solution equations only use time difference relationships between i-j, i-k, k-j and k-l. The process of using software to rotate the geometry varies the relationships of the sensors to their significance in the solution equations. This circulation of geometry accompanied with a demand for a minimum correlation confidence filters out divergences. This optimization routine guarantees that an erroneous position estimation caused by a singularity from an unknown aircraft will never be accepted as a valid solution.

The effectiveness of the rotational geometry can clearly be seen in Figure 5.11 and Figure 5.12 as 100% of the singularities are filtered out of the computed solutions. Error, both two-dimensional and three dimensional, are bound and very closely correlated with the GDOP analysis. The accuracy of the system clearly degrades outside the geometry as expected, but at all locations inside the triangle the system is extremely accurate. Like SSR, the system is susceptible to signal loss at severe bank angles as the transponder is usually located on the bottom surface of the aircraft (corners exhibit loss of track). Therefore, if one sensor in a four sensor network does not obtain a signal, the system is not capable of producing a solution. Another point worthy of consideration is that the data presented in Figure 5.11 and Figure 5.12, only IDENT squawks are being used. If altitude squawks were being used, the data rate would have increased by a factor of 2 or 3.

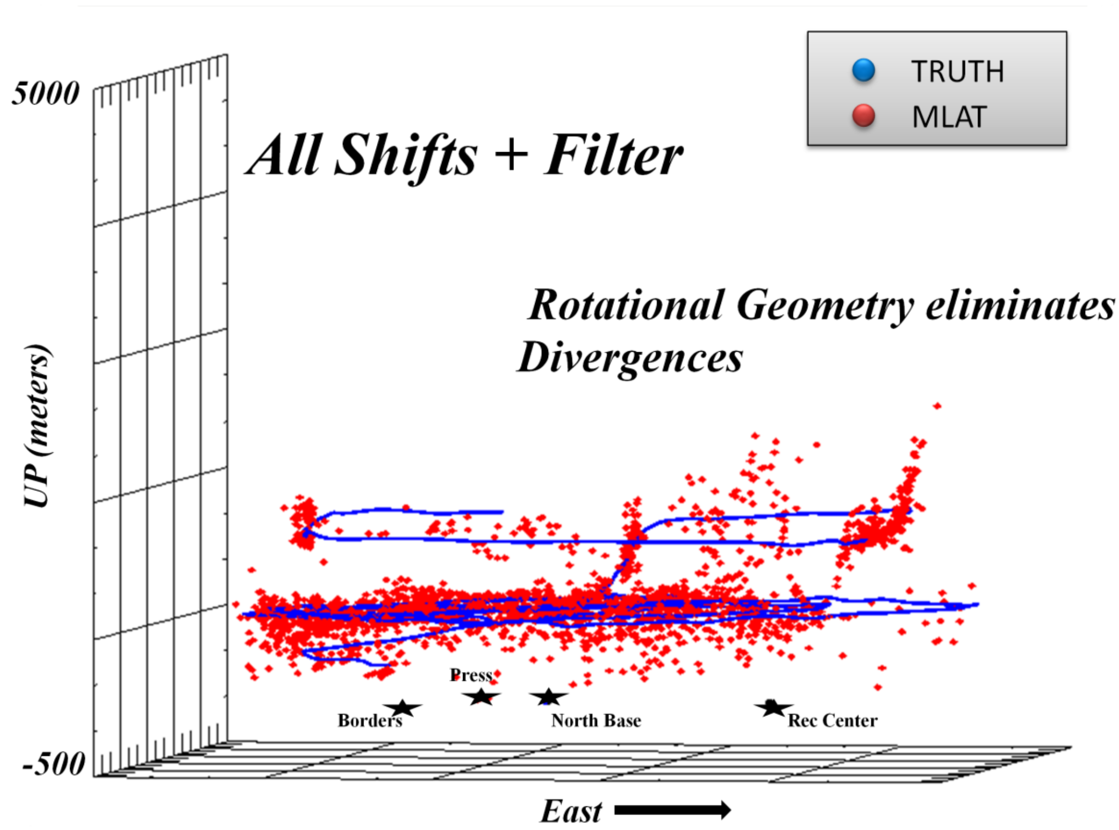

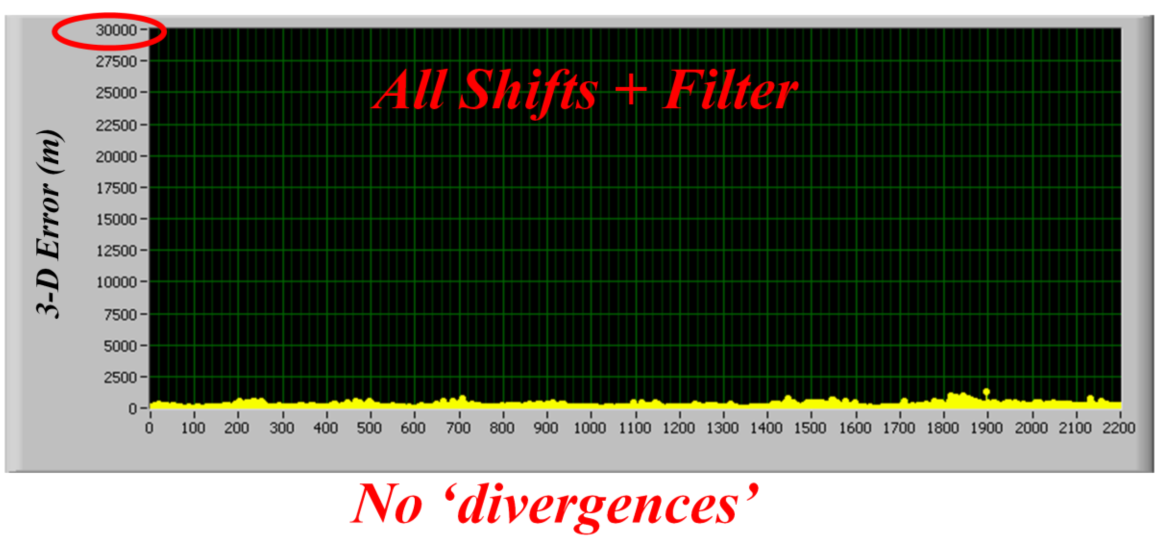

Figure 5. 11 - Elevation view of MLAT vs. truth data with all rotational shifts plus filter (top). 3-D error analysis (bottom).

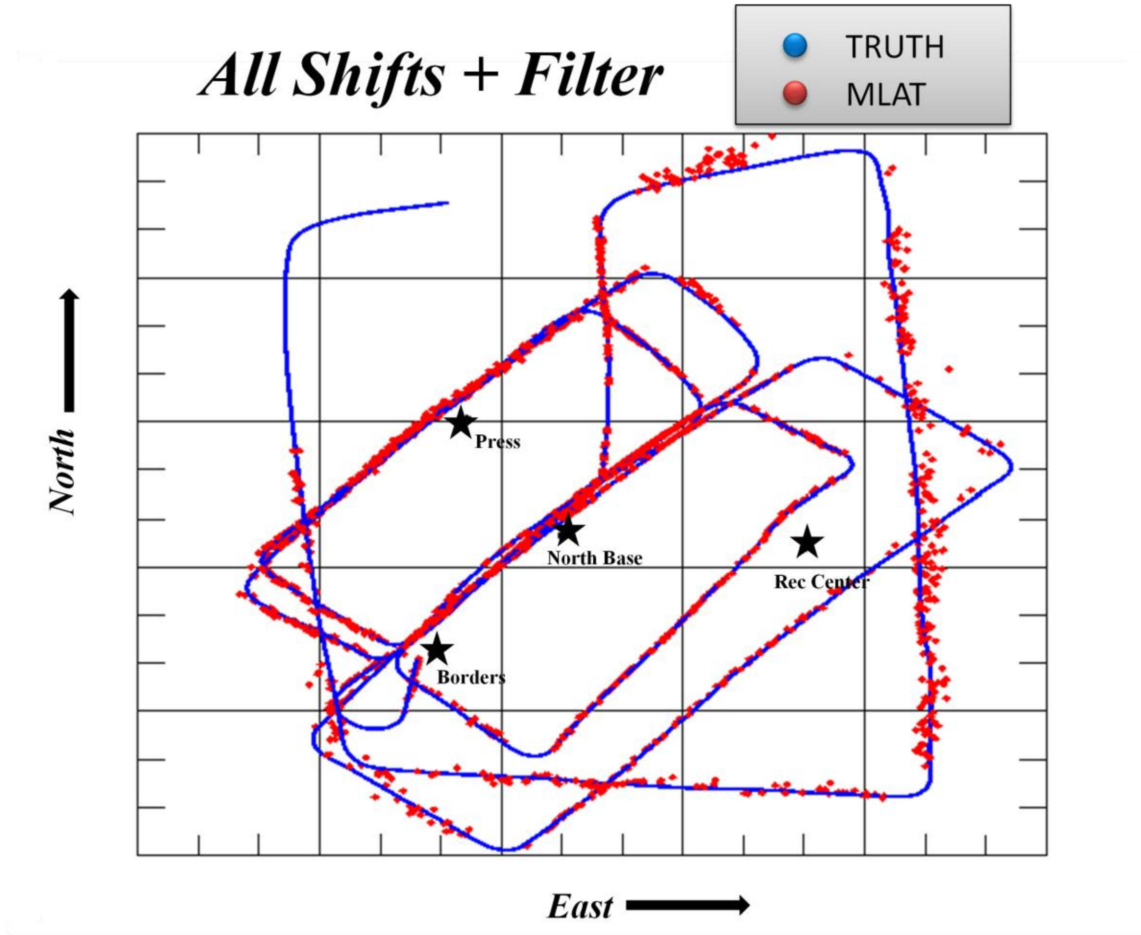

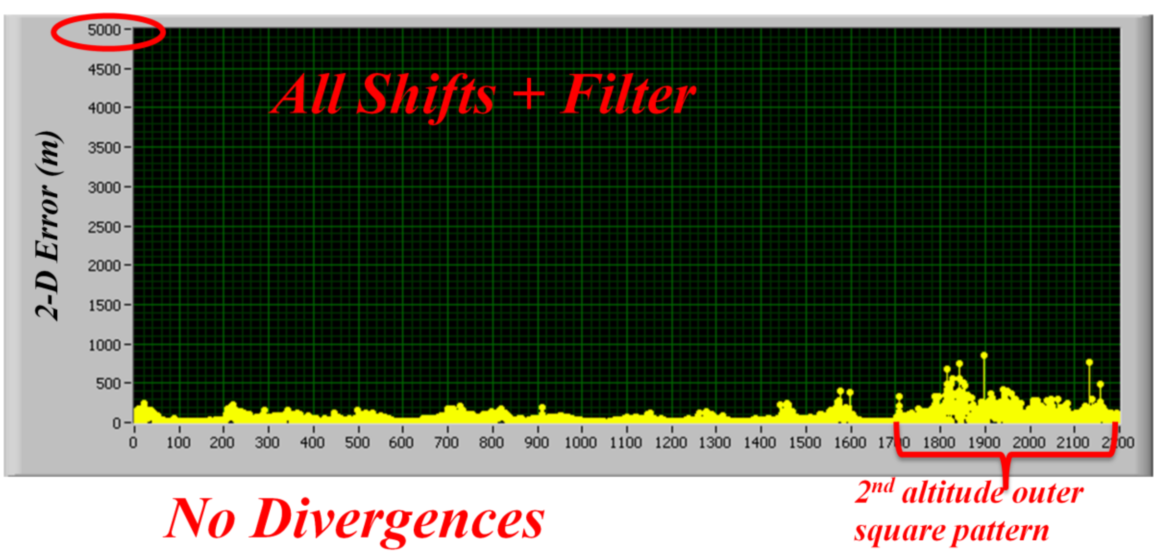

Figure 5. 12 - East-North view of MLAT vs. truth data after all rotational shifts and filter (top). 2-D error analysis (bottom).

Figure 5.13 is a magnified look at the error profile of the entire truth flight illustrating the expected fluctuations in accuracy as the aircraft flew in and out of the triangular geometry. The areas of geometry traversal show two-dimensional error with sample mean clearly less than 20 meters. Likewise, three-dimensional error has a sample mean below 50 meters at each of the traversals. At the second altitude (5500 ft MSL), the outer square pattern (indicated in Figure 5.13) is clearly where system accuracy is poorest as predicted by the GDOP analysis. With GDOP > 30 well outside of the geometry (Figure 4.26), sample mean is approximately 200 m which validates the GDOP model.

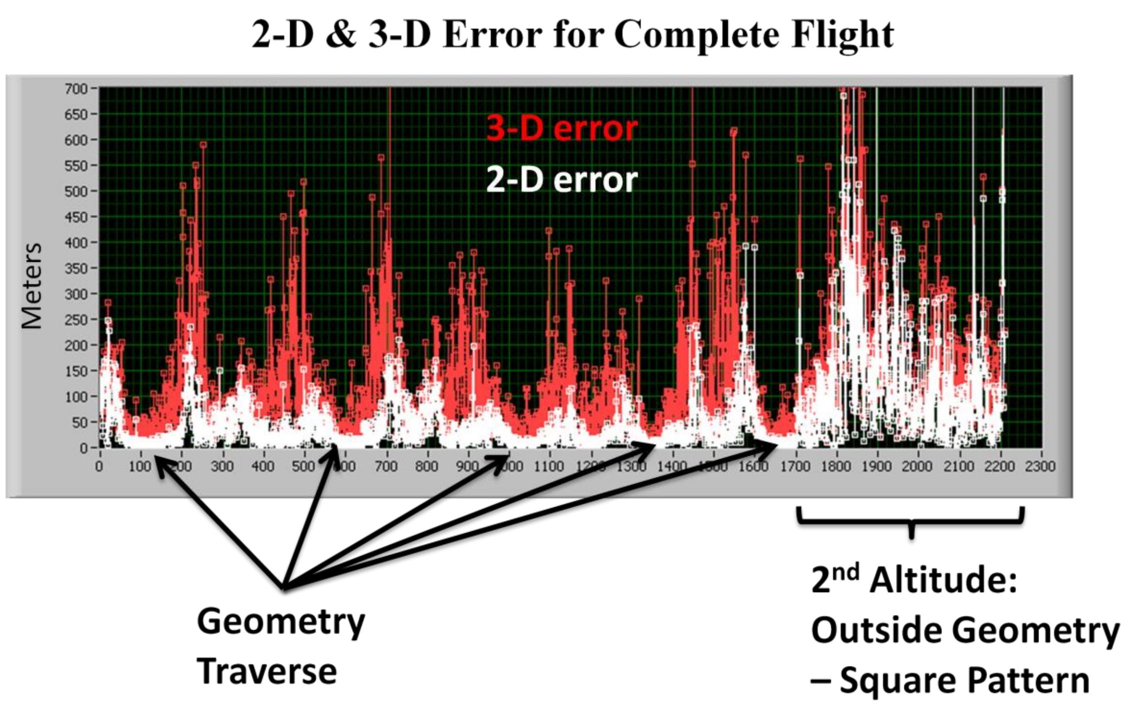

Figure 5. 13 - 2-D and 3-D error profile for entire truth flight. Error follows GDOP predictions as can be seen from tight accuracy inside the geometry.

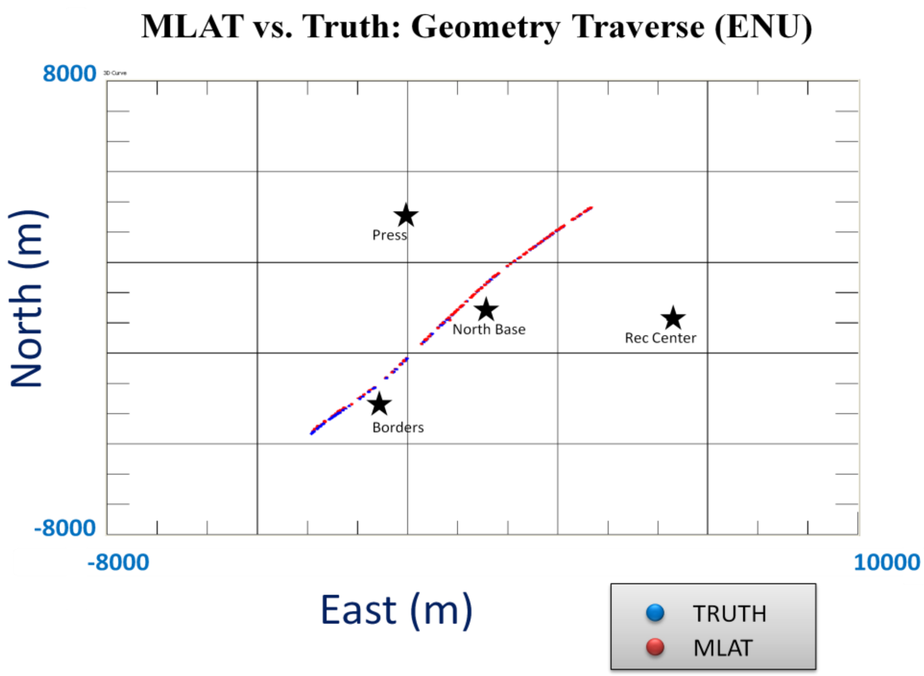

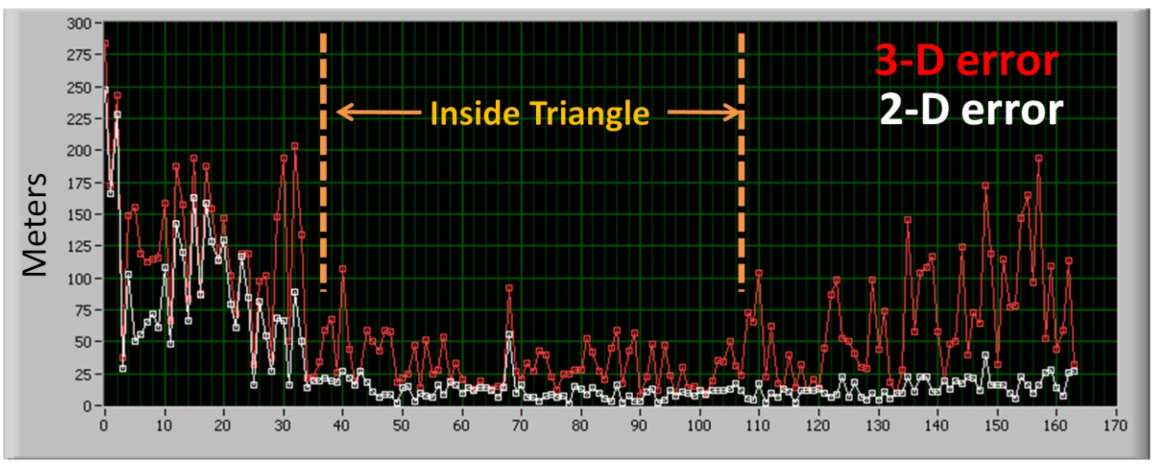

Figure 5. 14 - MLAT vs. truth during traversal of geometry.

Figure 5.14 illustrates the accuracy both inside and outside the geometry. Traveling from SW to NE thru the triangle, the error reacts as expected based on the GDOP calculations. Notice that after exiting to the NE, the 2-D error remains low even at a considerable distance outside of the triangular geometry. Altitude estimates, however, and hence 3-D error, suffers once the aircraft leaves the network of sensors.

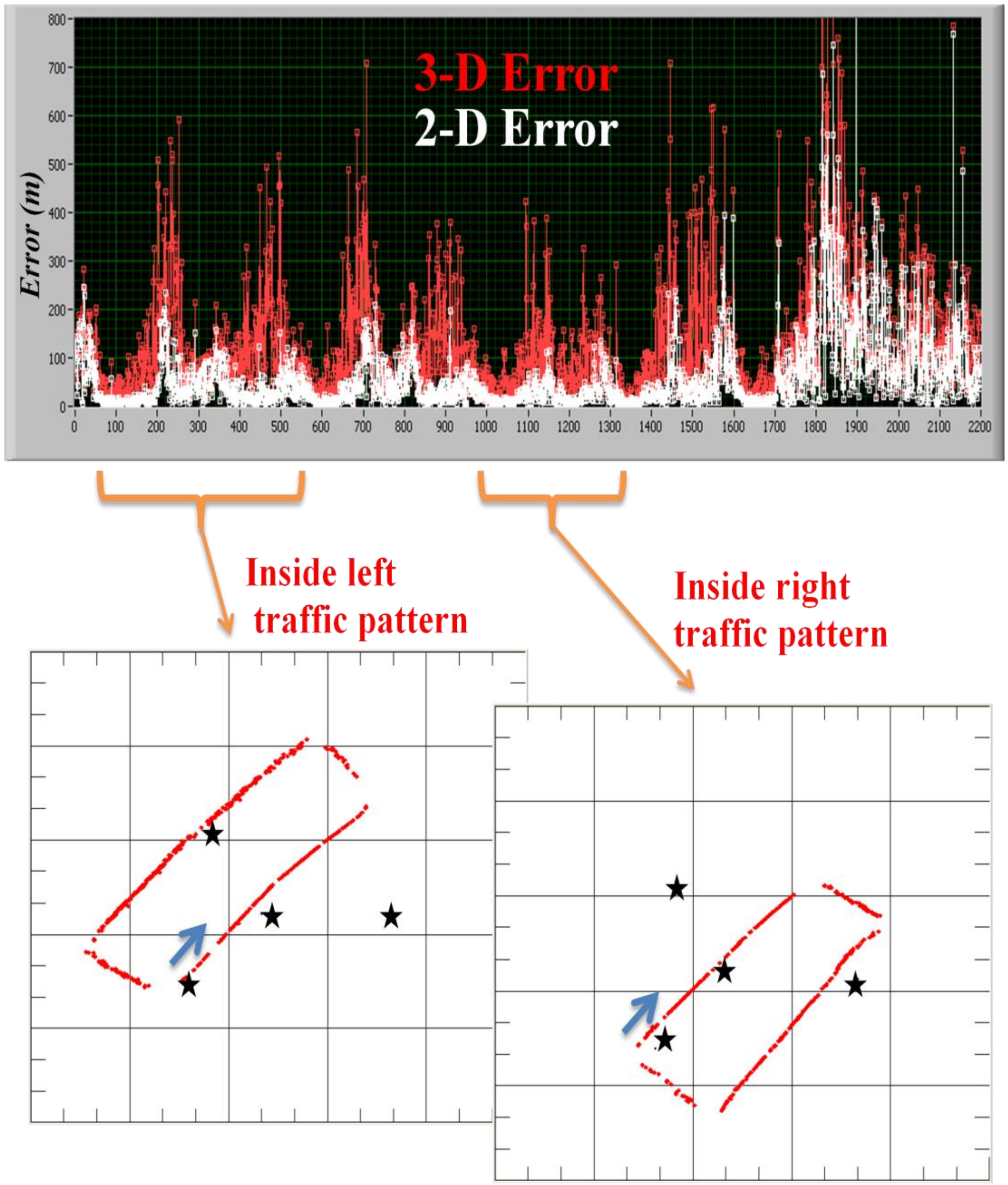

Figure 5. 15 - Inside left and right traffic patterns.

Figure 5.15 illustrates the portions of the error profile correlating to the inside left and inside right traffic patterns. The blue arrow indicates the starting point for each pattern which corresponds to the leftmost portion of its error analysis segment.

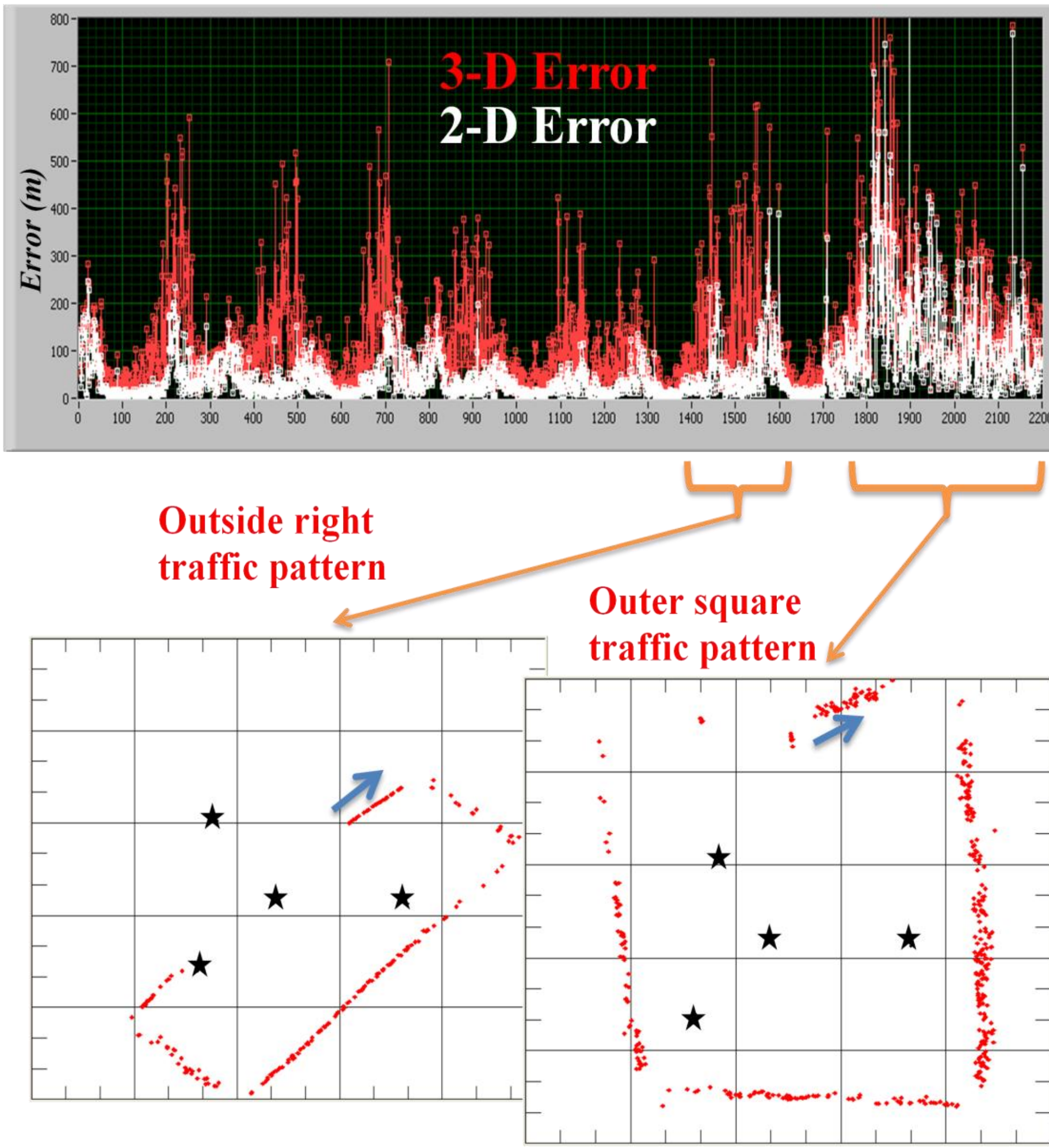

Figure 5. 16 – Outside right and outré square traffic patterns.

Figure 5.16 illustrates the portions of the error profile correlating to the outside right traffic pattern and the outer square traffic patterns. The blue arrow indicates the starting point for each pattern which corresponds to the leftmost portion of its error analysis segment. Direction of travel on both patterns is clockwise. Notice an obvious decrease in accuracy for the outer square pattern due to its distance from the geometry.

Zooming in on each of the segments from Figures 5.15 and 5.16 provides a much more detailed view of the error analysis of each segment of flight. Figures 5.17 through 5.20 are

In each of the figures, different points of each segment are denoted by a sequence of points 'A', 'B', 'C' and 'D' correlating the error profiles with the actual flight pattern locations. Using this visual correlation, the consistency of the algorithm is demonstrated with each traversal of the multilateration geometry. For example, in Figure 5.17, it can be seen that shortly after the beginning of the sequence (point 'A'), the flight enters the geometry with consistent accuracy in two and three dimensions with little variance.

As point 'B' is being approached the track remains very accurate in two dimensions even though it is well outside of the triangle, but elevation accuracy is beginning to fade. The poorest performance is between 'B' and 'C' and then again approaching 'D' which are the segments that are the furthest away from the sensor network. This confirms the GDOP analysis performed in Chapter 4.

Similar and repeatable results are illustrated in Figure 5.18 with another traversal of the geometry, this time to the right (east) instead of left. Figures 5.19 and 5.20 are patterns that are completely outside of the geometry of the sensors. Along with a decrease in accuracy, a decrease in update rate is also observed. There are two explanations for this decrease. First, the RF signal is weaker and hence, fewer valid triggers are generated based on the trigger level used for the test. Second, the solution equations are more susceptible to divergences at large distances from the sensor network. Therefore, more singularities are filtered out resulting in fewer valid data points.

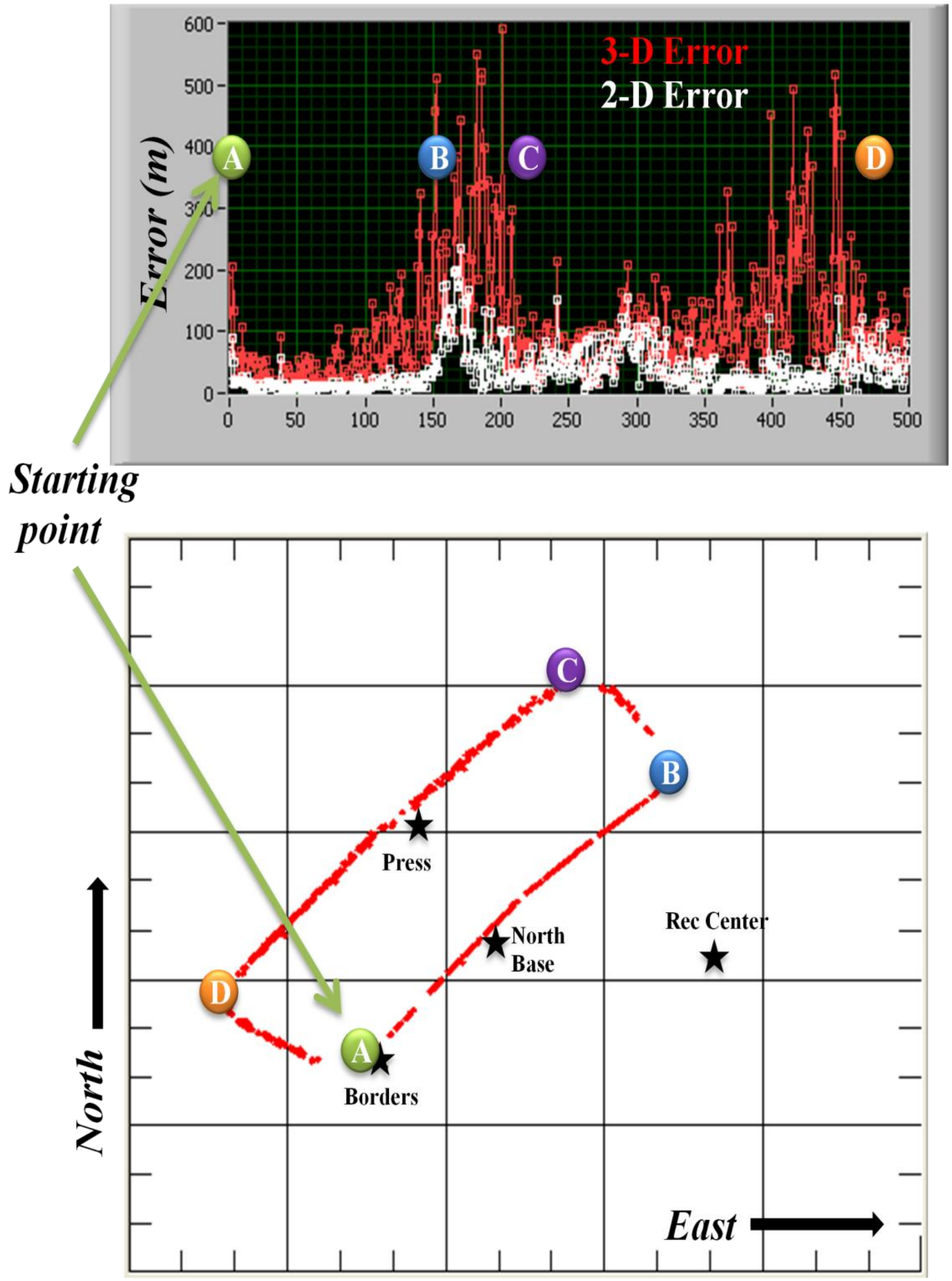

Figure 5. 17 - Error profile for inside left traffic pattern at 3500 ft MSL.

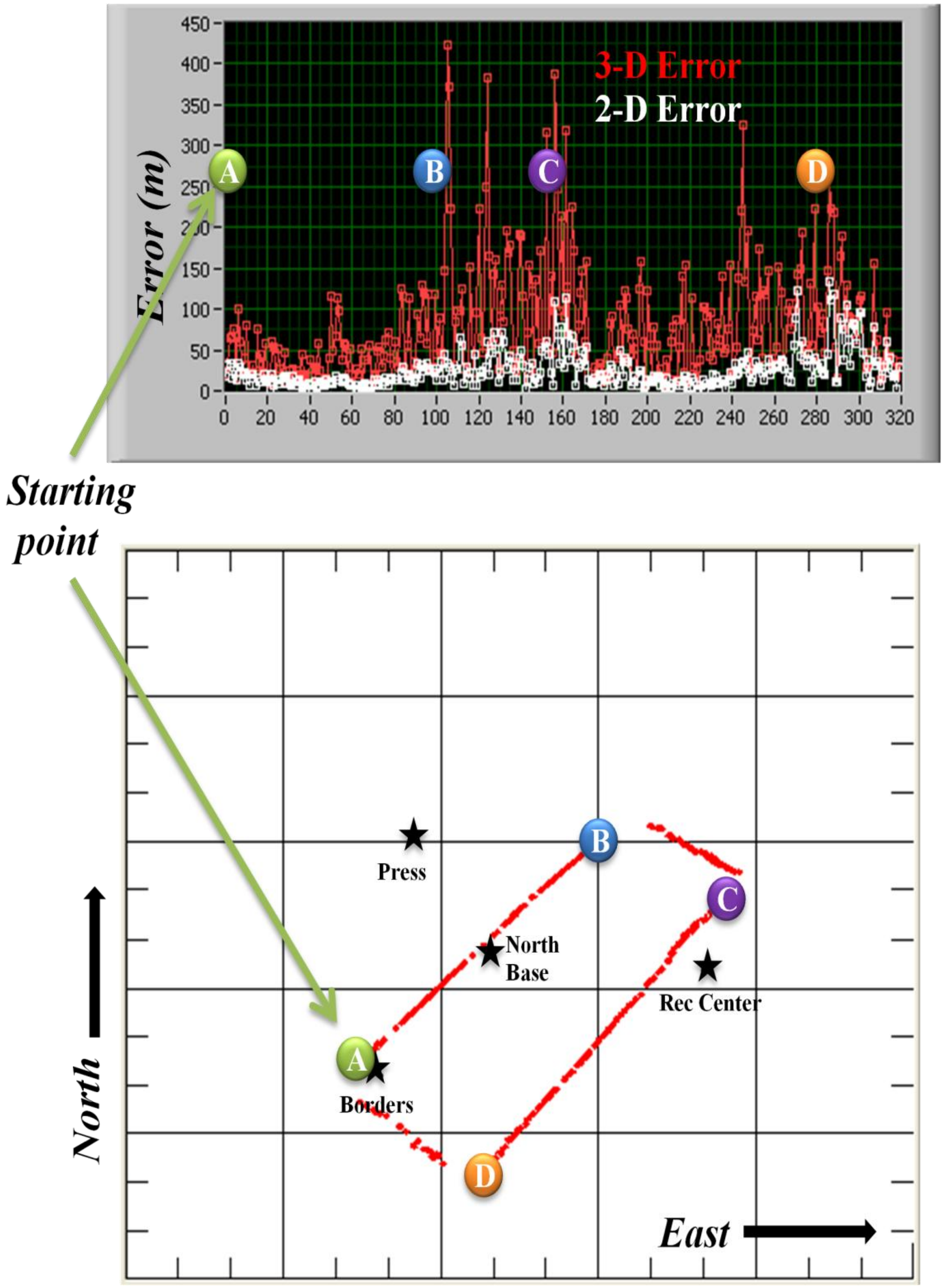

Figure 5. 18 - Error profile for inside right traffic pattern at 3500 ft MSL.

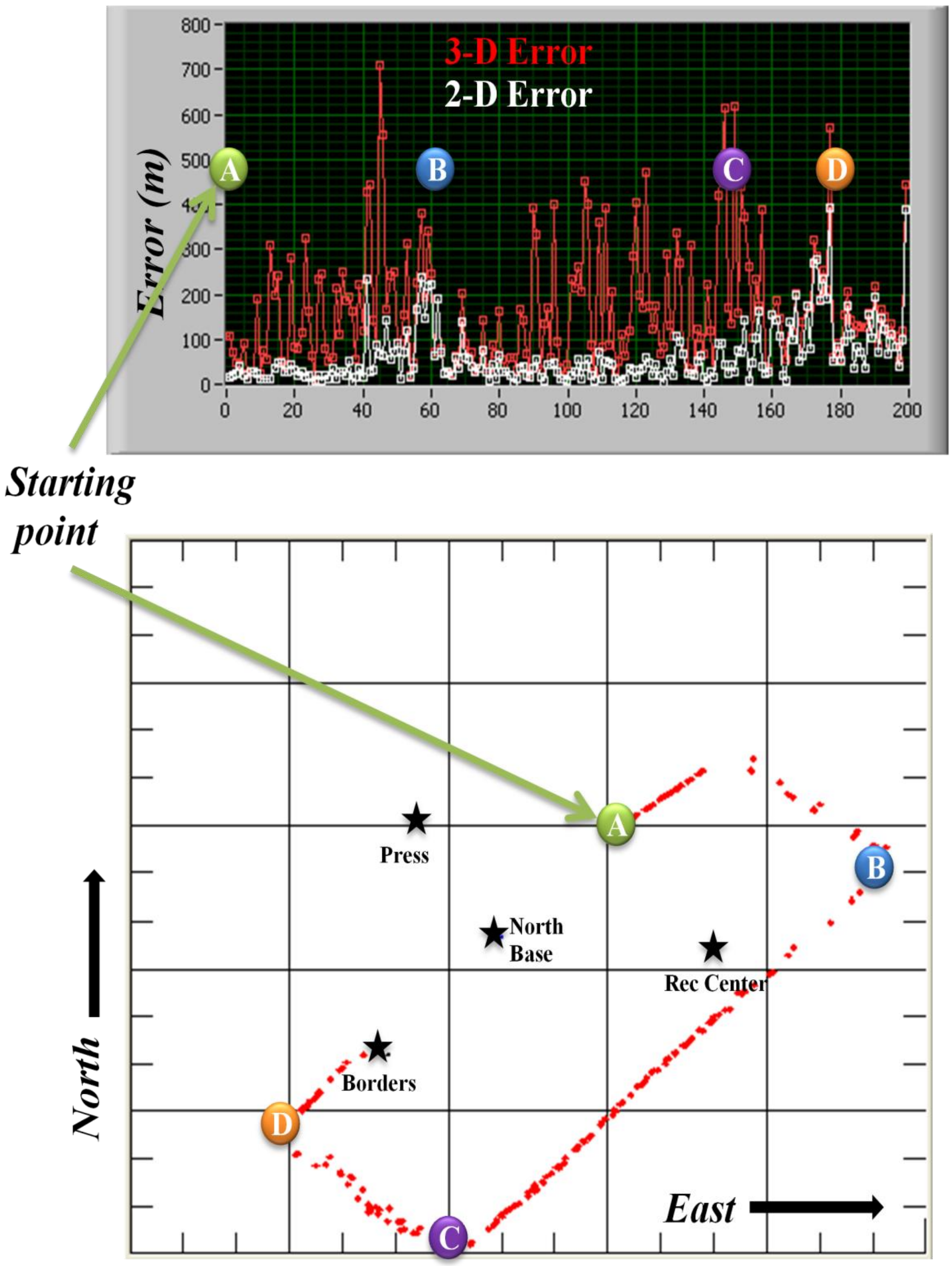

Figure 5. 19 - Error profile for outside right traffic pattern at 3500 ft MSL.

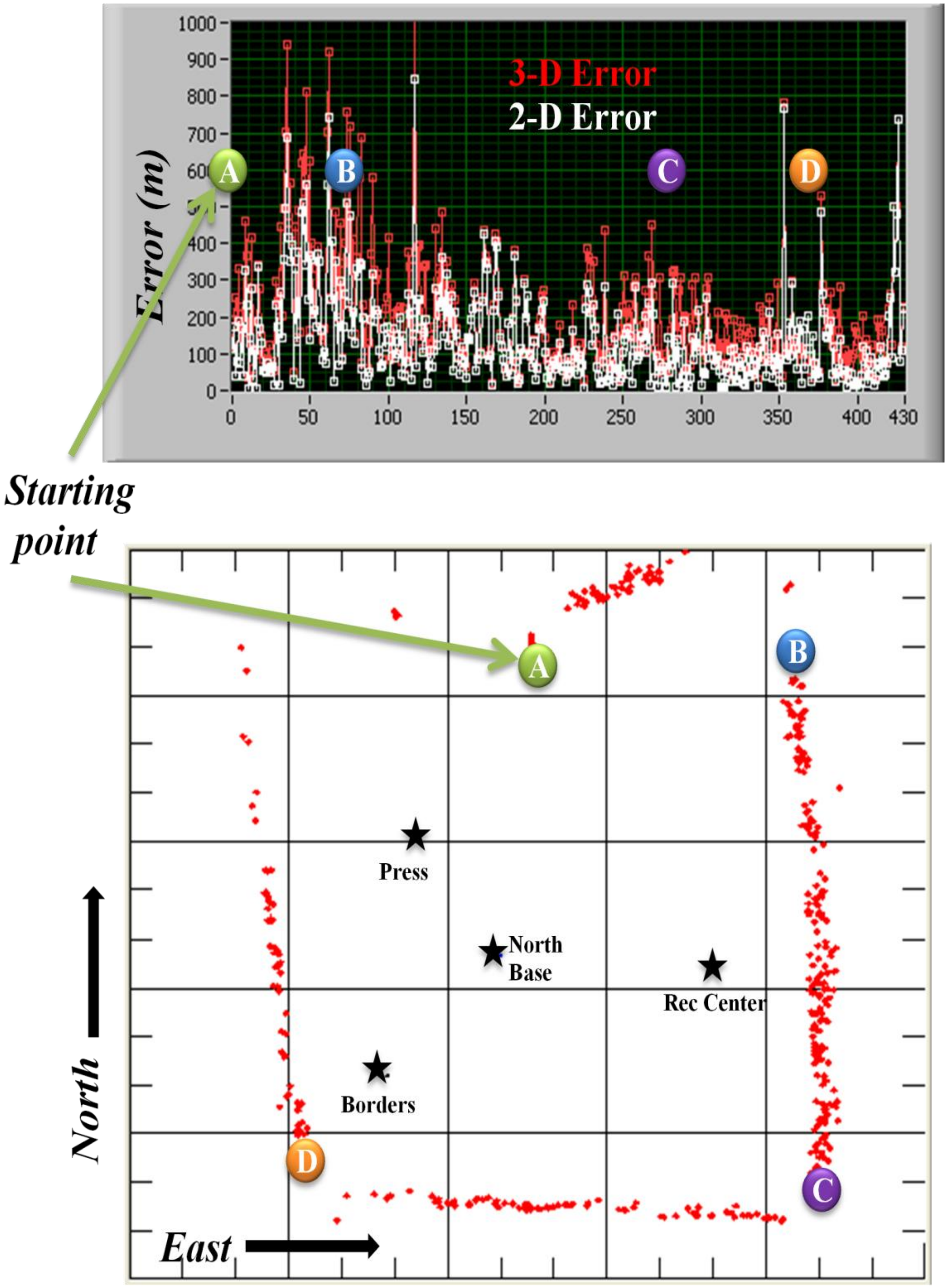

Figure 5. 20 - Error profile for outer square pattern at 5500 MSL.

Figure 5.21 (top) is an illustration of the entire position tracking performance of the multilateration system with IDENT squawks only without the truth data. During a flight time of just over 43 minutes, over 2200 valid position locations were calculated. This correlates to nearly once per second.

Since the truth flight was flown when there was very little traffic in the Max Westheimer air space, it is also reasonable to plot the solutions of all squawks (IDENT as well as altitude) and compare the results to the truth data. There is no way to verify that the altitude squawks are that of the truth flight, but the correlation to the rest of the flight path tends to agree with that of the same aircraft. This is a good indicator of the increased update rate that is promised by the multilateration system over conventional systems such as primary and secondary radar. Figure 5.21 (bottom) is an illustration of 'all' altitudes squawks and all IDENT squawks that correlated with the truth flight. Over 5000 valid position solutions were calculated over the same 43 minutes which pushed the overall update rate up to nearly 2 updates per second. The figure reflects the increased update rate by filling in the gaps that were present in the IDENT only graph.

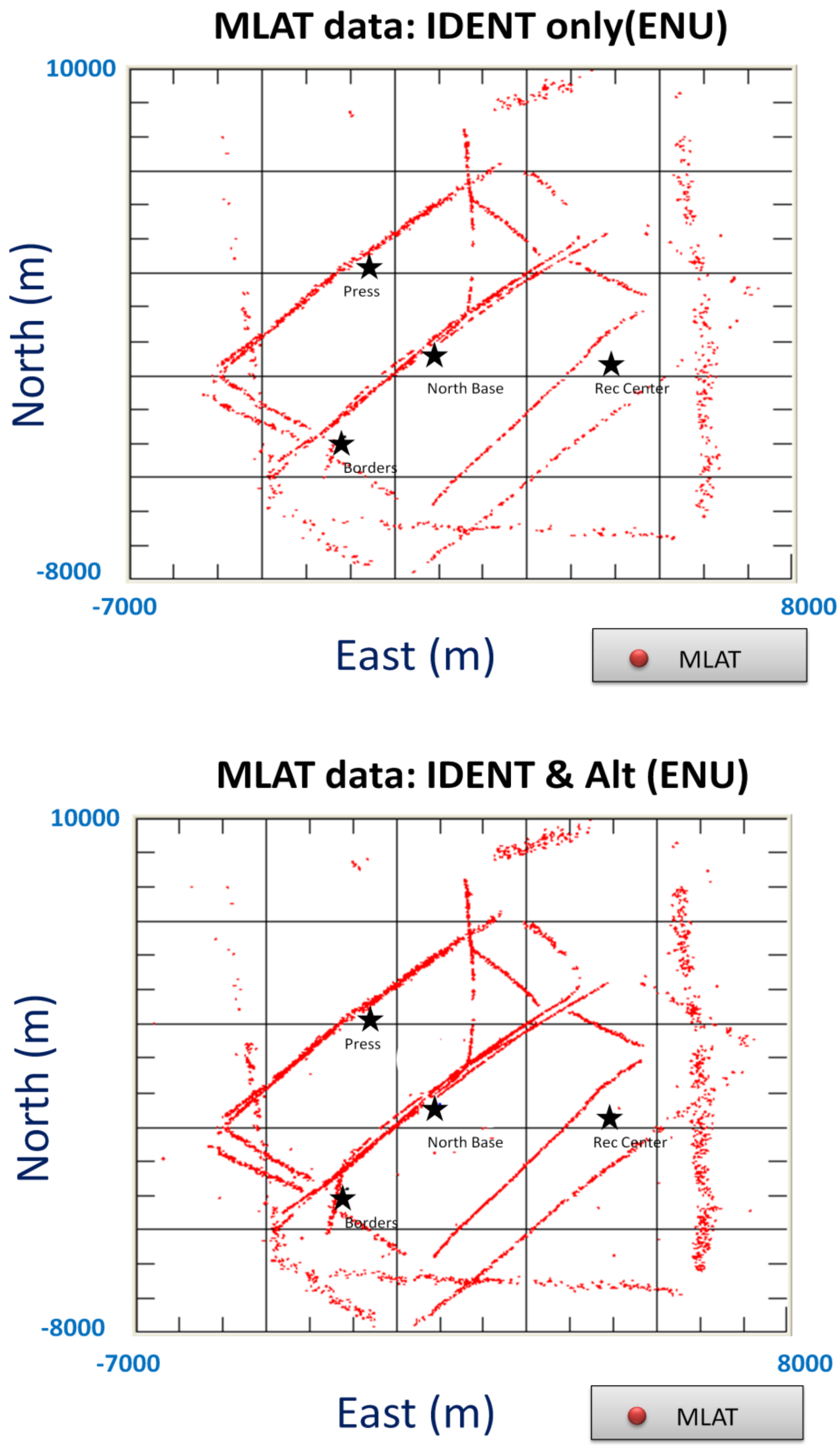

Figure 5. 21 - All IDENT squawks which produces valid position values (top). All squawks, IDENT and altitude that produces position solutions (bottom).

5.4 *Results Summary*

Statistical analysis was performed on three distinct zones of the truth flight in an attempt to characterize accuracy in different areas of the network of sensors (including zones outside of the geometry). All statistical calculations were performed on the data taken from IDENT squawks only. The classification of each zone is as follows:

1) ***Interior*** – all traffic inside the geometry (3500 ft MSL)
2) ***Exterior Near*** – the area outside the geometry for the inside left and inside right patterns (3500 ft MSL)
3) ***Outer Square*** – Outside square pattern (5500 ft MSL)

Table 5.1 contains the results of the statistical analysis of three-dimensional and two-dimensional accracy of the system in the three zones described above:

Zone	*Sample Size*	*3D Error Mean (m)*	*3D Error Stand Dev (m)*	*2D Error Mean (m)*	*2D Error Stand Dev (m)*
Interior	224	35.7	31.3	12.2	9.6
Exterior Near	690	107	94.3	36.7	33.8
Outer Square	461	198.7	158.3	137.9	126.5

Table 5. 1 - Statistical results of truth flights in three distinct geographical zones.

The data in Table 5.1 supports the theoretical advantages of multilateration over Secondary Surveillance Radar. Using multilateration to determine range, bearing and altitude, the three-dimensional error mean inside the geometry of the sensors is 35.7 meters. The two-dimensional (East-North) error mean is 12.2 meters.

SSR is dependent on the aircraft to provide altitude information, and its uncertainty in terminal area applications (30 miles) in two-dimensions is approximately 500 meters. Even when using SSR at a range of 10 miles, its uncertainty is approximately 140 meters and dependent on the aircraft for elevation (Mode C) broadcasts.

In areas outside of the multilateration geometry, the two-dimensional performance remains strong despite the loss of accuracy in resolving altitude. The East-North error mean is 36.7 meters outside of the geometry.

Overall the data proves that the new multilateration algorithms provide a better solution than PSR and SSR.

CHAPTER 6

Conclusion and Future Work

6.1 Conclusion

Realization of the proof of concept produced desired results in areas within the geometry defined by the layout of the RF sensors. The system also produced better than expected results (especially in two-dimensions) in areas well outside the boundary of the network. This was an unexpected result based on the original estimates from the initial GDOP analysis.

This successful implementation of the new model provides a solution that is very accurate in two dimensions. Both the two-dimensional and the three-dimensional accuracy inside the geometrical configuration was demonstrated as an improvement over current surveillance systems which utilize primary and secondary surveillance radar. Unlike radar, this multilateration model will actually provide results with more accurate position solutions when it is implemented over a larger geographical area. In such a deployment which assumes the same methodology, but implemented over a larger area, the significance of measurement error will be mitigated. This is due to the fact that the resolution of the event timer will be unchanged at ±30 nsec (which relates to approximately ± 30 feet). When compared to a larger sensor layout, this ± 30 feet is much less significant as a fraction of the overall area of coverage than the system which was developed for this research.

The system implemented in this research is more reliable than all multilateration designs that exist today. Autonomy is also achieved which allows the distribution of the RF sensors across a network without the limitation of line of sight from one node to the next.

The primary contribution of the research that made the implementation possible is the concept of a rotational geometry to optimize the solution equations based on the actual position of the aircraft. This methodology eliminates the need for classifying ‘no fly’ zones due to singularities in areas within the geometry – a hindrance that accompanies even most ‘surface’ tracking (2-dimensional) multilateration systems.

Additionally, challenges in the development phase uncovered other details that would be suitable for future improvements of the system. A list of these ideas along with a brief description is addressed in section 6.2.

6.2 Future Work

While the research discussed in this document was extremely successful and provided results which met the goals of its original proposal, there were many facets of the research which warrant future work in order to truly realize the potential of the multilateration system architecture. The scope of this research did not allow for the time and financial commitment to explore each of the areas discussed in this section on future work. Although there are numerous issues that arose as challenges that could not be resolved due to the time budget, only the areas which could bring about significant improvements of the system architecture will be discussed.

Real-time network/infrastructure – Going live with real-time data feed to the Central Processing Station and providing active, real-time position data. This is the obvious piece of future work which would bring the multilateration system to the point of practical use and prove its value in industry. Although technically this step would not be extremely challenging, the time and cost associated with installing the necessary networking and communications infrastructure would be significant.

Additional RF Hardware filtering/amplification – Signal/Noise is an ongoing optimization problem that always has room for improvement. While gaining ground on overall gain/bandwidth of the system is critical, there is a tradeoff associated with too much filtering and amplification because of the alteration of the actual signal which affects time of arrival and also alters the original details of the message waveforms. The rounding effect of filters causes pulse rise times to be distorted which can cause time of arrival error due to the method being used for analog triggering with the digitizer.

Antennas with Better Vertical Pattern **–** The DME antennas used for this research had poor performance for receiving signals from aircraft as they approached the airspace directly overhead. This caused a drop off of signal which eliminated the possibility of computing a solution as data from all four sensors must be received in order for the formula for plotting the solution to be used.

Sector Antennas on the Boundary Sensors – In boundary areas of the sensor geometry bandwidth is strained due to aircraft outside the geometry saturating one or possibly two of the sensors which affects the overall network sensitivity. A possible solution to this problem would be to replace the boundary area antennas (all antennas except for those interior to the geometry) with ‘sector’ antennas which look into the geometry and don’t allow the reception of signal coming from outside the geometry. This would increase overall bandwidth and system sensitivity.

Additional Digital Signal Processing on the Message – The process of decoding the binary coded pulse message that is being received at each sensor is one which has room for future work and optimization. A limited amount of signal processing was performed as part of this research, but additional digital signal processing would increase the number of valid squawks that are acquired which might otherwise be dismissed as noise. Specifically, when dealing with overlapping messages, the development of an algorithm for separation of messages of different signal strength would prevent overlapped pulses from being grouped in with the primary message being decoded.

Tracking Algorithm – The addition of a Kalman filter for the purpose of tracking the position solutions of aircraft would be an additional way to identify and filter false solutions and place an increased confidence on each position solution [21].

Vector/Velocity Calculations – A benefit that would emerge from the tracking algorithm would be the ability to calculate velocity and heading based on the presence of present and historical position data.

. ***Research on Scalability of Geometry*** – Theoretically the widening of the geometry to cover a broader area scales with predictable results. The realization of this theory might result in better resolution due to the fact that your measurement resolution in time of arrival measurements becomes less significant in relation to the overall distance between sensors. However, this might introduce more measurement error based on addition gain/bandwidth constraints.

Sensor Redundancy – For the scope of this research, only four sensors were used which is the minimum requirement to plot a three-dimensional solution. The limitation that this introduced was that if a single sensor failed to receive a transmission, then no solution could be plotted. Given a network with additional sensors in additional locations, a redundancy would be built in which would increase the update rates achieved by the multilateration system.

6.3 Summary

Like all technologies, multilateration has weaknesses (as described in chapter 2), but the advantages are extremely significant. With an update rate approximately five times better than radar and much better accuracy, multilateration is an attractive choice for the Federal Aviation Administration’s modernization of ATC. Its low cost and small size also contribute to its value. Given significant improvements, such as those proposed and validated in this research, the technology will mature enough to be considered one of the primary alternatives to radar in the future.

BIBLIOGRAPHY

[1] Trim, R. M., Mode S: An Introduction and Overview [Secondary Surveillance Radar], Electronics & Communications Engineering Journal, Volume 2, Issue 2, April 1990, pp 53-59.

[2] Federal Aviation Administration, Automatic Dependent Surveillance Broadcast (ADS-B), <http://www.faa.gov/airports_airtraffic/technology/ads-b/>

[3] Martone, P. J., Tucker, G. E., Candidate Requirements for Multilateration and ADS-B Systems to Serve as Alternatives to Secondary Radar, Digital Avionics Systems, 2001. DASC. The 20th Conference, October 2001, Volume 2, pp 7C2/1-7C2/12.

[4] Geyer, M., Daskalakis, A., Solving Passive Multilateration Equations Using Bancroft's Algorithm, Digital Avionics Systems Conference, 1998. Volume 2, 1998, pp F41/1 – F41/8.

[5] Dunstone, G., Owusu, K. Hewitt, K. (Australian Strategic Air Traffic Management Group), Comparison of Surveillance Technologies, prepared for ICAO Asia Pacific ADS-B Task Force.

[6] ATCMonitor, Air Traffic Control Radar – How It Works and Where It's Going, <http://atcmonitor.com/radar.html>.

[7] Federal Aviation Administration, Airport Surveillance Radar (ASR-11), April 2007, <http://www.faa.gov/airports_airtraffic/technology/asr-11/>.

[8] Stevens, Michael C., Secondary Surveillance Radar, ARTECH HOUSE, Inc., 1988, p. 21.

[9] Federal Aviation Administration, Department of Transportation, [Docket No. FAA-2007-29305; Notice No. 07-15], 14 CFR Part 91, RIN 2120-AI92, October 2007.

[10] Sayed, A., Yousef, N., Wireless Location, Wiley Encyclopedia of Telecommunications, Wiley & Sons, NY, 2003.

[11] Gerosa, L., Valenzise, G., Antonacci, F., Tagliasacchi, M., Sarti, A., Scream and Gunshot Detection in Noisy Environments, EURASIP European Signal Processing Conference, Poznan, Poland, September 2007.

[12] Morissey, R.P., Jarvis, S., Dimarzio, N., Ward, J., Moretti, D.J., North Atlantic Right Wale (Eubalaena glacialis) Detection & Localization in the Bay of Fundy Using Widely Spaced, Bottom Mounted Sensors, OCEANS 2006, September 2006, pp. 1-6

[13] Kaplan, Elliott D., Hegarty, Christopher J., Understanding GPS Principles and Applications – Second Edition, ARTECH HOUSE, Inc, 2006, p. 21.

[14] Bucher, R., Misra, D., A Synthesizable VHDL Model of the Exact Solution for Three-Dimensional Hyperbolic Positioning System, VLSI Design, 2002 Vol. 15 (2), pp. 507-520.

[15] Kaplan, E., Hegarty C., Understanding GPS Principles and Applications Second Edition, ARTECH HOUSE, Inc., p. 324.

[16] Dana, Peter H., Geodetic Datum Overview, <http://www.colorado.edu/geography/gcraft/notes/datum/datum.html>, 1999

[17] Grewal, Mohiner S., Weill, Lawrence R., Andrews, Angus P., Global Positioning Systems, Inertial Navigation, and Integration, John Wiley & Sons, Inc., January 2002.

[18] Phillips, Daryl, Mode A and Mode C – The Straight Scoop on How It Works, < http://www.airsport-corp.com/modec.htm>.

[19] U.S. Department of Transportation – Federal Aviation Administration FAA Academy, Air Traffic Control Beacon Interrogator (ATCBI-5) Theory of Operations – Seventh Edition, Published by Mike Monroney Aeronautical Center, Oklahoma City, August 2003.

[20] Yegnanarayana, B., Murthy, H. A., Significance of Group Delay Functions in Spectrum Estimation, Signal Processing, IEEE Transactions, Volume 40, Issue 9, September 1992.

[21] Pearson, J., Goodall, R., Eastham, M., MacLeod, C., Investigation of Kalman Filter Divergence Using Robust Stability Techniques [Combat Aircraft Tracking/Navigation System], Proceedings of the 36th IEEE Conference on Decision and Control, December 1997.

APPENDIX A – Mode C Altitude Codes

SQUAWK	*Altitude*	*SQUAWK*	*Altitude*	*SQUAWK*	*Altitude*	*SQUAWK*	*Altitude*
0040	-1200	1044	30800	0046	62800	1042	94800
0060	-1100	1064	30900	0066	62900	1062	94900
0020	-1000	1024	31000	0026	63000	1022	95000
0030	-900	1034	31100	0036	63100	1032	95100
0010	-800	1014	31200	0016	63200	1012	95200
0410	-700	1414	31300	0416	63300	1412	95300
0430	-600	1434	31400	0436	63400	1432	95400
0420	-500	1424	31500	0426	63500	1422	95500
0460	-400	1464	31600	0466	63600	1462	95600
0440	-300	1444	31700	0446	63700	1442	95700
0640	-200	1644	31800	0646	63800	1642	95800
0660	-100	1664	31900	0666	63900	1662	95900
0620	0	1624	32000	0626	64000	1622	96000
0630	100	1634	32100	0636	64100	1632	96100
0610	200	1614	32200	0616	64200	1612	96200
0210	300	1214	32300	0216	64300	1212	96300
0230	400	1234	32400	0236	64400	1232	96400
0220	500	1224	32500	0226	64500	1222	96500
0260	600	1264	32600	0266	64600	1262	96600
0240	700	1244	32700	0246	64700	1242	96700
0340	800	1344	32800	0346	64800	1342	96800
0360	900	1364	32900	0366	64900	1362	96900
0320	1000	1324	33000	0326	65000	1322	97000
0330	1100	1334	33100	0336	65100	1332	97100
0310	1200	1314	33200	0316	65200	1312	97200
0710	1300	1714	33300	0716	65300	1712	97300
0730	1400	1734	33400	0736	65400	1732	97400
0720	1500	1724	33500	0726	65500	1722	97500
0760	1600	1764	33600	0766	65600	1762	97600
0740	1700	1744	33700	0746	65700	1742	97700
0540	1800	1544	33800	0546	65800	1542	97800
0560	1900	1564	33900	0566	65900	1562	97900
0520	2000	1524	34000	0526	66000	1522	98000
0530	2100	1534	34100	0536	66100	1532	98100
0510	2200	1514	34200	0516	66200	1512	98200
0110	2300	1114	34300	0116	66300	1112	98300
0130	2400	1134	34400	0136	66400	1132	98400
0120	2500	1124	34500	0126	66500	1122	98500
0160	2600	1164	34600	0166	66600	1162	98600
0140	2700	1144	34700	0146	66700	1142	98700
4140	2800	5144	34800	4146	66800	5142	98800
4160	2900	5164	34900	4166	66900	5162	98900
4120	3000	5124	35000	4126	67000	5122	99000
4130	3100	5134	35100	4136	67100	5132	99100
4110	3200	5114	35200	4116	67200	5112	99200
4510	3300	5514	35300	4516	67300	5512	99300
4530	3400	5534	35400	4536	67400	5532	99400

SQUAWK	***Altitude***	***SQUAWK***	***Altitude***	***SQUAWK***	***Altitude***	***SQUAWK***	***Altitude***
4520	3500	5524	35500	4526	67500	5522	99500
4560	3600	5564	35600	4566	67600	5562	99600
4540	3700	5544	35700	4546	67700	5542	99700
4740	3800	5744	35800	4746	67800	5742	99800
4760	3900	5764	35900	4766	67900	5762	99900
4720	4000	5724	36000	4726	68000	5722	100000
4730	4100	5734	36100	4736	68100	5732	100100
4710	4200	5714	36200	4716	68200	5712	100200
4310	4300	5314	36300	4316	68300	5312	100300
4330	4400	5334	36400	4336	68400	5332	100400
4320	4500	5324	36500	4326	68500	5322	100500
4360	4600	5364	36600	4366	68600	5362	100600
4340	4700	5344	36700	4346	68700	5342	100700
4240	4800	5244	36800	4246	68800	5242	100800
4260	4900	5264	36900	4266	68900	5262	100900
4220	5000	5224	37000	4226	69000	5222	101000
4230	5100	5234	37100	4236	69100	5232	101100
4210	5200	5214	37200	4216	69200	5212	101200
4610	5300	5614	37300	4616	69300	5612	101300
4630	5400	5634	37400	4636	69400	5632	101400
4620	5500	5624	37500	4626	69500	5622	101500
4660	5600	5664	37600	4666	69600	5662	101600
4640	5700	5644	37700	4646	69700	5642	101700
4440	5800	5444	37800	4446	69800	5442	101800
4460	5900	5464	37900	4466	69900	5462	101900
4420	6000	5424	38000	4426	70000	5422	102000
4430	6100	5434	38100	4436	70100	5432	102100
4410	6200	5414	38200	4416	70200	5412	102200
4010	6300	5014	38300	4016	70300	5012	102300
4030	6400	5034	38400	4036	70400	5032	102400
4020	6500	5024	38500	4026	70500	5022	102500
4060	6600	5064	38600	4066	70600	5062	102600
4040	6700	5044	38700	4046	70700	5042	102700
6040	6800	7044	38800	6046	70800	7042	102800
6060	6900	7064	38900	6066	70900	7062	102900
6020	7000	7024	39000	6026	71000	7022	103000
6030	7100	7034	39100	6036	71100	7032	103100
6010	7200	7014	39200	6016	71200	7012	103200
6410	7300	7414	39300	6416	71300	7412	103300
6430	7400	7434	39400	6436	71400	7432	103400
6420	7500	7424	39500	6426	71500	7422	103500
6460	7600	7464	39600	6466	71600	7462	103600
6440	7700	7444	39700	6446	71700	7442	103700
6640	7800	7644	39800	6646	71800	7642	103800
6660	7900	7664	39900	6666	71900	7662	103900
6620	8000	7624	40000	6626	72000	7622	104000
6630	8100	7634	40100	6636	72100	7632	104100
6610	8200	7614	40200	6616	72200	7612	104200
6210	8300	7214	40300	6216	72300	7212	104300

SQUAWK	***Altitude***	***SQUAWK***	***Altitude***	***SQUAWK***	***Altitude***	***SQUAWK***	***Altitude***
6230	8400	7234	40400	6236	72400	7232	104400
6220	8500	7224	40500	6226	72500	7222	104500
6260	8600	7264	40600	6266	72600	7262	104600
6240	8700	7244	40700	6246	72700	7242	104700
6340	8800	7344	40800	6346	72800	7342	104800
6360	8900	7364	40900	6366	72900	7362	104900
6320	9000	7324	41000	6326	73000	7322	105000
6330	9100	7334	41100	6336	73100	7332	105100
6310	9200	7314	41200	6316	73200	7312	105200
6710	9300	7714	41300	6716	73300	7712	105300
6730	9400	7734	41400	6736	73400	7732	105400
6720	9500	7724	41500	6726	73500	7722	105500
6760	9600	7764	41600	6766	73600	7762	105600
6740	9700	7744	41700	6746	73700	7742	105700
6540	9800	7544	41800	6546	73800	7542	105800
6560	9900	7564	41900	6566	73900	7562	105900
6520	10000	7524	42000	6526	74000	7522	106000
6530	10100	7534	42100	6536	74100	7532	106100
6510	10200	7514	42200	6516	74200	7512	106200
6110	10300	7114	42300	6116	74300	7112	106300
6130	10400	7134	42400	6136	74400	7132	106400
6120	10500	7124	42500	6126	74500	7122	106500
6160	10600	7164	42600	6166	74600	7162	106600
6140	10700	7144	42700	6146	74700	7142	106700
2140	10800	3144	42800	2146	74800	3142	106800
2160	10900	3164	42900	2166	74900	3162	106900
2120	11000	3124	43000	2126	75000	3122	107000
2130	11100	3134	43100	2136	75100	3132	107100
2110	11200	3114	43200	2116	75200	3112	107200
2510	11300	3514	43300	2516	75300	3512	107300
2530	11400	3534	43400	2536	75400	3532	107400
2520	11500	3524	43500	2526	75500	3522	107500
2560	11600	3564	43600	2566	75600	3562	107600
2540	11700	3544	43700	2546	75700	3542	107700
2740	11800	3744	43800	2746	75800	3742	107800
2760	11900	3764	43900	2766	75900	3762	107900
2720	12000	3724	44000	2726	76000	3722	108000
2730	12100	3734	44100	2736	76100	3732	108100
2710	12200	3714	44200	2716	76200	3712	108200
2310	12300	3314	44300	2316	76300	3312	108300
2330	12400	3334	44400	2336	76400	3332	108400
2320	12500	3324	44500	2326	76500	3322	108500
2360	12600	3364	44600	2366	76600	3362	108600
2340	12700	3344	44700	2346	76700	3342	108700
2240	12800	3244	44800	2246	76800	3242	108800
2260	12900	3264	44900	2266	76900	3262	108900
2220	13000	3224	45000	2226	77000	3222	109000
2230	13100	3234	45100	2236	77100	3232	109100
2210	13200	3214	45200	2216	77200	3212	109200

SQUAWK	Altitude	SQUAWK	Altitude	SQUAWK	Altitude	SQUAWK	Altitude
2610	13300	3614	45300	2616	77300	3612	109300
2630	13400	3634	45400	2636	77400	3632	109400
2620	13500	3624	45500	2626	77500	3622	109500
2660	13600	3664	45600	2666	77600	3662	109600
2640	13700	3644	45700	2646	77700	3642	109700
2440	13800	3444	45800	2446	77800	3442	109800
2460	13900	3464	45900	2466	77900	3462	109900
2420	14000	3424	46000	2426	78000	3422	110000
2430	14100	3434	46100	2436	78100	3432	110100
2410	14200	3414	46200	2416	78200	3412	110200
2010	14300	3014	46300	2016	78300	3012	110300
2030	14400	3034	46400	2036	78400	3032	110400
2020	14500	3024	46500	2026	78500	3022	110500
2060	14600	3064	46600	2066	78600	3062	110600
2040	14700	3044	46700	2046	78700	3042	110700
3040	14800	2044	46800	3046	78800	2042	110800
3060	14900	2064	46900	3066	78900	2062	110900
3020	15000	2024	47000	3026	79000	2022	111000
3030	15100	2034	47100	3036	79100	2032	111100
3010	15200	2014	47200	3016	79200	2012	111200
3410	15300	2414	47300	3416	79300	2412	111300
3430	15400	2434	47400	3436	79400	2432	111400
3420	15500	2424	47500	3426	79500	2422	111500
3460	15600	2464	47600	3466	79600	2462	111600
3440	15700	2444	47700	3446	79700	2442	111700
3640	15800	2644	47800	3646	79800	2642	111800
3660	15900	2664	47900	3666	79900	2662	111900
3620	16000	2624	48000	3626	80000	2622	112000
3630	16100	2634	48100	3636	80100	2632	112100
3610	16200	2614	48200	3616	80200	2612	112200
3210	16300	2214	48300	3216	80300	2212	112300
3230	16400	2234	48400	3236	80400	2232	112400
3220	16500	2224	48500	3226	80500	2222	112500
3260	16600	2264	48600	3266	80600	2262	112600
3240	16700	2244	48700	3246	80700	2242	112700
3340	16800	2344	48800	3346	80800	2342	112800
3360	16900	2364	48900	3366	80900	2362	112900
3320	17000	2324	49000	3326	81000	2322	113000
3330	17100	2334	49100	3336	81100	2332	113100
3310	17200	2314	49200	3316	81200	2312	113200
3710	17300	2714	49300	3716	81300	2712	113300
3730	17400	2734	49400	3736	81400	2732	113400
3720	17500	2724	49500	3726	81500	2722	113500
3760	17600	2764	49600	3766	81600	2762	113600
3740	17700	2744	49700	3746	81700	2742	113700
3540	17800	2544	49800	3546	81800	2542	113800
3560	17900	2564	49900	3566	81900	2562	113900
3520	18000	2524	50000	3526	82000	2522	114000
3530	18100	2534	50100	3536	82100	2532	114100

SQUAWK	Altitude	SQUAWK	Altitude	SQUAWK	Altitude	SQUAWK	Altitude
3510	18200	2514	50200	3516	82200	2512	114200
3110	18300	2114	50300	3116	82300	2112	114300
3130	18400	2134	50400	3136	82400	2132	114400
3120	18500	2124	50500	3126	82500	2122	114500
3160	18600	2164	50600	3166	82600	2162	114600
3140	18700	2144	50700	3146	82700	2142	114700
7140	18800	6144	50800	7146	82800	6142	114800
7160	18900	6164	50900	7166	82900	6162	114900
7120	19000	6124	51000	7126	83000	6122	115000
7130	19100	6134	51100	7136	83100	6132	115100
7110	19200	6114	51200	7116	83200	6112	115200
7510	19300	6514	51300	7516	83300	6512	115300
7530	19400	6534	51400	7536	83400	6532	115400
7520	19500	6524	51500	7526	83500	6522	115500
7560	19600	6564	51600	7566	83600	6562	115600
7540	19700	6544	51700	7546	83700	6542	115700
7740	19800	6744	51800	7746	83800	6742	115800
7760	19900	6764	51900	7766	83900	6762	115900
7720	20000	6724	52000	7726	84000	6722	116000
7730	20100	6734	52100	7736	84100	6732	116100
7710	20200	6714	52200	7716	84200	6712	116200
7310	20300	6314	52300	7316	84300	6312	116300
7330	20400	6334	52400	7336	84400	6332	116400
7320	20500	6324	52500	7326	84500	6322	116500
7360	20600	6364	52600	7366	84600	6362	116600
7340	20700	6344	52700	7346	84700	6342	116700
7240	20800	6244	52800	7246	84800	6242	116800
7260	20900	6264	52900	7266	84900	6262	116900
7220	21000	6224	53000	7226	85000	6222	117000
7230	21100	6234	53100	7236	85100	6232	117100
7210	21200	6214	53200	7216	85200	6212	117200
7610	21300	6614	53300	7616	85300	6612	117300
7630	21400	6634	53400	7636	85400	6632	117400
7620	21500	6624	53500	7626	85500	6622	117500
7660	21600	6664	53600	7666	85600	6662	117600
7640	21700	6644	53700	7646	85700	6642	117700
7440	21800	6444	53800	7446	85800	6442	117800
7460	21900	6464	53900	7466	85900	6462	117900
7420	22000	6424	54000	7426	86000	6422	118000
7430	22100	6434	54100	7436	86100	6432	118100
7410	22200	6414	54200	7416	86200	6412	118200
7010	22300	6014	54300	7016	86300	6012	118300
7030	22400	6034	54400	7036	86400	6032	118400
7020	22500	6024	54500	7026	86500	6022	118500
7060	22600	6064	54600	7066	86600	6062	118600
7040	22700	6044	54700	7046	86700	6042	118700
5040	22800	4044	54800	5046	86800	4042	118800
5060	22900	4064	54900	5066	86900	4062	118900
5020	23000	4024	55000	5026	87000	4022	119000

SQUAWK	*Altitude*	*SQUAWK*	*Altitude*	*SQUAWK*	*Altitude*	*SQUAWK*	*Altitude*
5030	23100	4034	55100	5036	87100	4032	119100
5010	23200	4014	55200	5016	87200	4012	119200
5410	23300	4414	55300	5416	87300	4412	119300
5430	23400	4434	55400	5436	87400	4432	119400
5420	23500	4424	55500	5426	87500	4422	119500
5460	23600	4464	55600	5466	87600	4462	119600
5440	23700	4444	55700	5446	87700	4442	119700
5640	23800	4644	55800	5646	87800	4642	119800
5660	23900	4664	55900	5666	87900	4662	119900
5620	24000	4624	56000	5626	88000	4622	120000
5630	24100	4634	56100	5636	88100	4632	120100
5610	24200	4614	56200	5616	88200	4612	120200
5210	24300	4214	56300	5216	88300	4212	120300
5230	24400	4234	56400	5236	88400	4232	120400
5220	24500	4224	56500	5226	88500	4222	120500
5260	24600	4264	56600	5266	88600	4262	120600
5240	24700	4244	56700	5246	88700	4242	120700
5340	24800	4344	56800	5346	88800	4342	120800
5360	24900	4364	56900	5366	88900	4362	120900
5320	25000	4324	57000	5326	89000	4322	121000
5330	25100	4334	57100	5336	89100	4332	121100
5310	25200	4314	57200	5316	89200	4312	121200
5710	25300	4714	57300	5716	89300	4712	121300
5730	25400	4734	57400	5736	89400	4732	121400
5720	25500	4724	57500	5726	89500	4722	121500
5760	25600	4764	57600	5766	89600	4762	121600
5740	25700	4744	57700	5746	89700	4742	121700
5540	25800	4544	57800	5546	89800	4542	121800
5560	25900	4564	57900	5566	89900	4562	121900
5520	26000	4524	58000	5526	90000	4522	122000
5530	26100	4534	58100	5536	90100	4532	122100
5510	26200	4514	58200	5516	90200	4512	122200
5110	26300	4114	58300	5116	90300	4112	122300
5130	26400	4134	58400	5136	90400	4132	122400
5120	26500	4124	58500	5126	90500	4122	122500
5160	26600	4164	58600	5166	90600	4162	122600
5140	26700	4144	58700	5146	90700	4142	122700
1140	26800	0144	58800	1146	90800	0142	122800
1160	26900	0164	58900	1166	90900	0162	122900
1120	27000	0124	59000	1126	91000	0122	123000
1130	27100	0134	59100	1136	91100	0132	123100
1110	27200	0114	59200	1116	91200	0112	123200
1510	27300	0514	59300	1516	91300	0512	123300
1530	27400	0534	59400	1536	91400	0532	123400
1520	27500	0524	59500	1526	91500	0522	123500
1560	27600	0564	59600	1566	91600	0562	123600
1540	27700	0544	59700	1546	91700	0542	123700
1740	27800	0744	59800	1746	91800	0742	123800
1760	27900	0764	59900	1766	91900	0762	123900

SQUAWK	Altitude	SQUAWK	Altitude	SQUAWK	Altitude	SQUAWK	Altitude
1720	28000	0724	60000	1726	92000	0722	124000
1730	28100	0734	60100	1736	92100	0732	124100
1710	28200	0714	60200	1716	92200	0712	124200
1310	28300	0314	60300	1316	92300	0312	124300
1330	28400	0334	60400	1336	92400	0332	124400
1320	28500	0324	60500	1326	92500	0322	124500
1360	28600	0364	60600	1366	92600	0362	124600
1340	28700	0344	60700	1346	92700	0342	124700
1240	28800	0244	60800	1246	92800	0242	124800
1260	28900	0264	60900	1266	92900	0262	124900
1220	29000	0224	61000	1226	93000	0222	125000
1230	29100	0234	61100	1236	93100	0232	125100
1210	29200	0214	61200	1216	93200	0212	125200
1610	29300	0614	61300	1616	93300	0612	125300
1630	29400	0634	61400	1636	93400	0632	125400
1620	29500	0624	61500	1626	93500	0622	125500
1660	29600	0664	61600	1666	93600	0662	125600
1640	29700	0644	61700	1646	93700	0642	125700
1440	29800	0444	61800	1446	93800	0442	125800
1460	29900	0464	61900	1466	93900	0462	125900
1420	30000	0424	62000	1426	94000	0422	126000
1430	30100	0434	62100	1436	94100	0432	126100
1410	30200	0414	62200	1416	94200	0412	126200
1010	30300	0014	62300	1016	94300	0012	126300
1030	30400	0034	62400	1036	94400	0032	126400
1020	30500	0024	62500	1026	94500	0022	126500
1060	30600	0064	62600	1066	94600	0062	126600
1040	30700	0044	62700	1046	94700	0042	126700